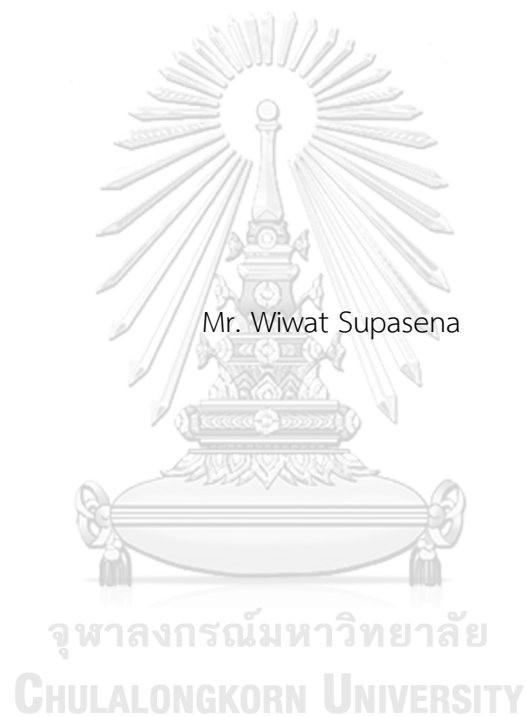SYNTHESIS AND CHARACTERIZATION OF POLYETHYLENE GLYCOL-DOXORUBICIN
CONJUGATES CONTAINING β-THIOPROPANAMIDE LINKERS FOR ENHANCED SELECTIVE
CYTOTOXICITY AGAINST BREAST CANCER CELLS

Mr. Wiwat Supasena

A Dissertation Submitted in Partial Fulfillment of the Requirements

for the Degree of Doctor of Philosophy in Pharmaceutical Technology

Department of Pharmaceutics and Industrial Pharmacy

FACULTY OF PHARMACEUTICAL SCIENCES

Chulalongkorn University

Academic Year 2019

Copyright of Chulalongkorn University

การสังเคราะห์และการบรรยายลักษณะของโพลีเอทิลีนไกลคอล-ดอกโซรูบิซินคอนจูเกตส์ซึ่งมีตัวเชื่อม
เบต้าไทโอโพรพานาไมด์เพื่อเพิ่มความจำเพาะของความเป็นพิษต่อเซลล์มะเร็งเต้านม

นายวิวัฒน์ ศุภเสนา

วิทยานิพนธ์นี้เป็นส่วนหนึ่งของการศึกษาตามหลักสูตรปริญญาวิทยาศาสตรดุษฎีบัณฑิต
สาขาวิชาเทคโนโลยีเภสัชกรรม ภาควิชาวิทยาการเภสัชกรรมและเภสัชอุตสาหกรรม
คณะเภสัชศาสตร์ จุฬาลงกรณ์มหาวิทยาลัย
ปีการศึกษา 2562

Thesis Title	SYNTHESIS AND CHARACTERIZATION OF POLYETHYLENE GLYCOL-DOXORUBICIN CONJUGATES CONTAINING β-THIOPROPANAMIDE LINKERS FOR ENHANCED SELECTIVE CYTOTOXICITY AGAINST BREAST CANCER CELLS
By	Mr. Wiwat Supasena
Field of Study	Pharmaceutical Technology
Thesis Advisor	Associate Professor Pornchai Rojsitthisak, Ph.D.
Thesis Co Advisor	Assistant Professor Jittima Luckanagul, Ph.D.

Accepted by the FACULTY OF PHARMACEUTICAL SCIENCES, Chulalongkorn University in Partial Fulfillment of the Requirement for the Doctor of Philosophy

--- Dean of the FACULTY OF PHARMACEUTICAL SCIENCES

(Assistant Professor RUNGPETCH SAKULBUMRUNGSIL, Ph.D.)

DISSERTATION COMMITTEE

--- Chairman

(Associate Professor PARKPOOM TENGAMNUAY, Ph.D.)

--- Thesis Advisor

(Associate Professor Pornchai Rojsitthisak, Ph.D.)

--- Thesis Co-Advisor

(Assistant Professor Jittima Luckanagul, Ph.D.)

--- Examiner

(Assistant Professor WALAISIRI MUANGSIRI, Ph.D.)

--- Examiner

(Associate Professor PAITOON RASHATASAKHON, Ph.D.)

--- External Examiner

(Assistant Professor Sathit Niratisai, Ph.D.)

วิวัฒน์ ศุภเสนา : การสังเคราะห์และการบรรยายลักษณะของโพลีเอทิลีนไกลคอล-ดอกโซรูบิซินคอนจูเกตส์ ซึ่งมีตัวเชื่อมเบต้าไทโอโพรพานาไมด์เพื่อเพิ่มความจำเพาะของความเป็นพิษต่อเซลล์มะเร็งเต้านม. (SYNTHESIS AND CHARACTERIZATION OF POLYETHYLENE GLYCOL-DOXORUBICIN CONJUGATES CONTAINING β-THIOPROPANAMIDE LINKERS FOR ENHANCED SELECTIVE CYTOTOXICITY AGAINST BREAST CANCER CELLS) อ.ที่ปรึกษาหลัก : รศ. ภก. ดร.พรชัย โรจน์สิทธิ ศักดิ์, อ.ที่ปรึกษาร่วม : ผศ. ภญ. ดร.จิตติมา ลัคนากุล

ดอกโซรูบิซิน (DOX) เป็นยาเคมีบำบัดชนิดหนึ่งซึ่งมีข้อจำกัดในการใช้รักษาโรคมะเร็งเนื่องจากมีฤทธิ์ไม่พึงประสงค์คือ การฆ่าเซลล์แบบไม่จำเพาะเจาะจง งานวิจัยนี้มุ่งออกแบบตัวเชื่อมเบต้าไทโอโพรพานาไมด์ (-S-CH$_2$-C(R)H-CONH-) สำหรับการ คอนจูเกต DOX เพื่อช่วยเพิ่มความจำเพาะและฤทธิ์การฆ่าเซลล์มะเร็ง DOX คอนจูเกต 2 ชุด ซึ่งประกอบด้วยตัวเชื่อมเบต้าไทโอโพ รพานาไมด์หลายชนิดถูกสังเคราะห์และประเมินความจำเพาะต่อการฆ่าเซลล์มะเร็ง DOX คอนจูเกตชุดแรกประกอบด้วย DOX อนาล็อก 7 ชนิดซึ่งมีตัวเชื่อมเบต้าไทโอโพรพานาไมด์ที่แตกต่างกัน DOX อนาล็อกถูกสังเคราะห์โดยใช้เอทิลไทโอไกลโคเลตและ อนาล็อกของกรดอะคริลิคเพื่อสร้างตัวเชื่อมเบต้าไทโอโพรพานาไมด์ที่แตกต่างกัน ซึ่งตัวเชื่อมเหล่านี้จะถูกนำไปใช้ในการทำพอลิ เมอร์-DOX คอนจูเกต DOX คอนจูเกตชุดหลังประกอบด้วยพอลิเมอร์-DOX คอนจูเกตซึ่งมีตัวเชื่อมเบต้าไทโอโพรพานาไมด์ชนิดไม่มี หมู่แทนที่ (-S-CH$_2$-CH$_2$-CONH-, A) ทำหน้าที่เชื่อม DOX กับเมทอกซีโพลีเอทิลีนไกลคอล (mPEG) เพื่อชะลอการปลดปล่อยยาใน ระบบหมุนเวียนโลหิต เพิ่มการตอบสนองของสารคอนจูเกตต่อตัวกระตุ้นและเพิ่มความจำเพาะต่อเซลล์มะเร็ง mPEG-DOX คอนจู เกต mPEG-DOX คอนจูเกตที่มีตัวเชื่อมเบต้าไทโอโพรพานาไมด์ชนิดไม่มีหมู่แทนที่ (P-A-DOX) ถูกสังเคราะห์จากเมทอกซีโพลีเอ ทิลีนไกลคอลที่มีหมู่ไทออลและกรดอะคริลิคเพื่อสร้างตัวเชื่อมเบต้าไทโอโพรพานาไมด์กับ DOX โดยมี mPEG-DOX คอนจูเกตที่ไม่มี ตัวเชื่อม (P-DOX) เป็นตัวควบคุม DOX อนาล็อกและคอนจูเกตทั้งหมดถูกตรวจสอบโครงสร้างเคมีด้วยเทคนิคนิวเคลียร์แมกเนติกเร โซแนนซ์สเปกโทรสโกปีและวิธีวิเคราะห์ทางเคมี การศึกษาความคงตัวในหลอดทดลองโดยปัจจัยค่าพีเอชและการทดสอบฤทธิ์การฆ่า เซลล์ต่อเซลล์มะเร็งเต้านมชนิด MDA-MB-231, MCF-7 และเซลล์เต้านมชนิด MCF-10A ได้ถูกดำเนินการ ผลการทดลองแสดงให้ เห็นว่า DOX อนาล็อก (3a) ที่มีตัวเชื่อมเบต้าไทโอโพรพานาไมด์ (หมู่ R = H) เพิ่มความคงตัวของยาขณะที่ P-A-DOX และ P-DOX คอนจูเกตสามารถชะลอการปลดปล่อยยาภายใต้ค่าฟิสิโอโลจิคอลพีเอช นอกจากนี้ยังพบว่า DOX อนาล็อก 3a และ P-A-DOX สามารถจับกับบริเวณเร่งของเอนไซม์คาเทปซินแอลได้กว่า P-DOX ซึ่งคาเทปซินแอลเป็นเอนไซม์ของเซลล์มะเร็งที่ทำหน้าที่ตัด พันธะเอไมด์และทำให้เกิดการปลดปล่อยยา จากผลการทดลองจึงสรุปอันดับของฤทธิ์การฆ่าเซลล์มะเร็งความจำเพาะต่อเซลล์มะเร็ง ของดังนี้ P-A-DOX > P-DOX > DOX. P-A-DOX พวกเราให้ความเห็นว่า P-A-DOX ซึ่งมีตัวเชื่อมเบต้าไทโอโพรพานาไมด์ชนิดไม่มี หมู่แทนที่สามารถใช้สำหรับระบบนำส่ง DOX ที่มีความจำเพาะในการรักษาโรคมะเร็งเต้านมได้

สาขาวิชา	เทคโนโลยีเภสัชกรรม	ลายมือชื่อนิสิต ....
ปีการศึกษา	2562	ลายมือชื่อ อ.ที่ปรึกษาหลัก ....
		ลายมือชื่อ อ.ที่ปรึกษาร่วม ....

5776558533 : MAJOR PHARMACEUTICAL TECHNOLOGY

KEYWORD: beta-thiopropanamide; Breast cancer; Cathepsin L; Doxorubicin; Cytotoxicity; Selectivity index

Wiwat Supasena : SYNTHESIS AND CHARACTERIZATION OF POLYETHYLENE GLYCOL-DOXORUBICIN CONJUGATES CONTAINING β-THIOPROPANAMIDE LINKERS FOR ENHANCED SELECTIVE CYTOTOXICITY AGAINST BREAST CANCER CELLS. Advisor: Assoc. Prof. Pornchai Rojsitthisak, Ph.D. Co-advisor: Asst. Prof. Jittima Luckanagul, Ph.D.

Doxorubicin (DOX) is a chemotherapeutic agent that suffers from its severe adverse effects due to non-selective cytotoxicity. This study aims to design novel *beta*-thiopropanamide linkers ($-S-CH_2-C(R)H-CONH-$) for DOX conjugation to promote cancer cell selectivity and cytotoxicity. Two series of DOX conjugates with various *beta*-thiopropanamide linkers were synthesized and evaluated for their cytotoxic selectivity. The first series contains 7 DOX analogues with different *beta*-thiopropanamide linkers. The DOX analogues were synthesized using ethyl thioglycolate and acrylic acid analogues to establish a series of *beta*-thiopropanamide linkages with DOX, and the potential linkers were intended to be incorporated in polymer-DOX conjugates. The other series contains a polymer-DOX conjugate, in which the unsubstituted thiopropanamide ($-S-CH_2-CH_2-CONH-$, A) is selected as the linker, which conjugates DOX with methoxypolyethylene glycol (mPEG) to sustain systemic drug release, and to promote stimuli responsiveness and cancer cell selectivity. The mPEG-DOX conjugate with the unsubstituted *beta*-thiopropanamide linker (P-A-DOX) was synthesized using thiol-functionalized methoxypolyethylene glycol and acrylic acid to establish the *beta*-thiopropanamide linkage with DOX, using the mPEG-DOX (P-DOX) conjugate as the control. All DOX analogues and conjugates were structurally characterized by NMR and chemical assay. The *in vitro* hydrolytic stability as a function of pH and cytotoxicity tests (MDA-MB-231 and MCF-7 breast cancer cells vs MCF-10A noncancerous cells) were performed. The DOX analogue (3a) with the *beta*-thiopropanamide linker (where R = H) improved physicochemical stability while the P-A-DOX and P-DOX conjugates additionally exhibited sustained drug release under physiological pH conditions. Both 3a and P-A-DOX were docked in the active site of cathepsin L closer than P-DOX, which cathepsin L is a cancer enzyme that has a preference to cleave the amide bond to initiate intracellular drug release. 3a was found to enhance cancer cell selectivity. However, P-A-DOX enhanced both cancer cell cytotoxicity and selectivity and the summative effects were translated to enhance cancer cell cytotoxicity and selectivity in the following order: P-A-DOX > P-DOX > DOX. We suggest that the mPEG-DOX conjugate with the unsubstituted *beta*-thiopropanamide linker can serve as a selective DOX delivery system for breast cancer treatment.

Field of Study: Pharmaceutical Technology   Student's Signature ....

Academic Year: 2019   Advisor's Signature ....

    Co-advisor's Signature ....

ACKNOWLEDGEMENTS

TABLE OF CONTENTS

Page

จุฬาลงกรณ์มหาวิทยาลัย

CHULALONGKORN UNIVERSITY

LIST OF TABLES

จุฬาลงกรณ์มหาวิทยาลัย

CHULALONGKORN UNIVERSITY

LIST OF FIGURES

LIST OF ABBREVIATION

Å	Angstrom
ASP	Aspartic acid
ATCC	American Type Culture Collection
CYS	Cysteine
DOX	Doxorubicin
DMEM	Dulbecco's modified Eagle's medium
DMPP	Dimethylphenylphosphine
DMSO	Dimethyl sulfoxide
°C	Degree Celcius
DMAP	4-Dimethylaminopyridine
DMF	Dimethylformamide
EDC	1-Ethyl-3-(3-dimethylaminopropyl)carbodiimide
g	Gram
GLY	Glycine
h	Hour
IC$_{50}$	Half maximal inhibitory concentration
HPLC	High-performance liquid chromatography
HOBt	1-Hydroxybenzotriazole
kcal	Kilocalorie
kDa	Kilodalton
LEU	Leucine
LGA	Lamarckian genetic algorithm
m/z	Mass-to-charge ratio
MW	Molecular weight
µg	Microgram
µL	Microliter
µM	Micromolar

mg	Milligram
mL	Milliliter
mm	Millimeter
mM	Millimolar
mol	Mole
mmol	Millimole
min	Minute
mPEG	Methoxypolyethylene glycol
MS	Mass spectrometry
N	Normality
NHS	*N*-Hydroxysuccinimide
nm	Nanometer
NMM	*N*-methylmorpholine
NMR	Nuclear Magnetic Resonance Spectroscopy
NOE	Nuclear Overhauser effect
PDB	Protein Data Bank
PEG	Polyethylene glycol
PEO	Polyethylene oxide
PHE	Phenylalanine
POE	Polyoxyethylene
R (chemical configuration)	Rectus
S (chemical configuration)	Sinister
THF	Tetrahydrofuran
UCSF	University of California, San Francisco
v/v	Volume-by-volume
w/w	Weight-by-weight

CHAPTER 1

INTRODUCTION

Doxorubicin (DOX), the anticancer drugs for various type of cancers, is usually given in combination with other chemotherapeutic drugs. It can stop the growth or kill breast cancer cells by inhibiting topoisomerase II which is responsible for DNA replication thus stopping the reproduction of cancer cells (Pommier et al. 2010). DOX cannot be used as a free drug for cancer treatment because of its non-selective toxicity limiting its anticancer applications (Tacar et al. 2013). Moreover, the poor stability of DOX in physiological pH condition (Beijnen et al. 1986; Janssen et al. 1985) also compromises its efficacy resulting in the use of higher doses of this drug that may cause potential side effects such as cardiotoxicity (Hershman et al. 2008; Volkova and Russell 2011). Over the past decades, numerous researches were focused on the development of a new delivery system to enhance its cancer selectivity by exploiting the difference on characteristics between cancer and normal cells, including dysregulated pH (White et al. 2017) and enzyme overexpression (Sreedhar and Zhao 2018). There had been numerous publications on polymer-DOX conjugate with a stimuli-responsive effect for DOX delivery with good selectivity and safety (N. Li et al. 2014; C. Y. Sun et al. 2014; Yang et al. 2013).

The stimuli-responsive drug delivery system has received an extensive application for anticancer drug delivery in recent years. Its drug release is triggered by suitable external stimuli such as dysregulated pH or overexpressed enzymes found in cancer cells, which are different from those of normal cells. With reference to pH-responsive system, the drug delivery system can exploit the acidic environment of cancer cells to release the covalently conjugated drug from an acid-labile linker. Several acid-labile linkers such as, hydrazone (Lu et al. 2009), acetal (Tomlinson et al. 2003), cis-aconityl (Kakinoki et al. 2008), imine (J. Li et al. 2016) and beta-thiopropionate (Oishi et al. 2003) linkers have been used to introduce the pH-

responsive function and enhance the anticancer drug delivery specificity. In the case of enzyme-responsive system, the drug delivery relies on the overexpressed enzyme of cancer cells to free the covalently conjugated drug. Enzyme-responsive linkers such as a small peptide GFLG linker (Wei et al. 2016) that is cleaved by cathepsin B, have been employed to develop enzyme-responsive drug delivery system.

Utilization of sulphur containing linker to provide stimuli-responsive effects has received a considerable attention (Oishi et al. 2003; Oishi et al. 2005). The *beta*-thiopropionate linker ($-S-CH_2-CH_2-COO-$) that incorporates a *beta* position sulfur atom next to a carbonyl ester functional group exhibits an increase in the hydrolytic reaction under acidic conditions (Schoenmakers et al. 2004). This is partly due to the electron inductive effect of sulfur atom that can generate a partial positive charge on the ester carbonyl carbon and promote its interaction with aqueous medium. The sulphur containing linker is able to aid to sustain the drug release in a non-acidic medium and release the drug in response to the acidic milieu (Pramanik et al. 2016; Liang Qiu et al. 2016; L. Qiu et al. 2017). The *beta*-thiopropionate linker however has been reported to be susceptible to enzymatic/chemical hydrolysis in the systemic circulation due to the abundance of the esterase enzyme (Ratnatilaka Na Bhuket et al. 2019; Rudakova et al. 2011). Instead of conventional ester linkage, the amide bond has been proposed in the development of a slow-release drug delivery system where drug conjugate or prodrug is designed (Chhikara et al. 2011). The amide bond is relatively resistant to esterase action. It undergoes a fast cleavage in response to specific protease enzymes such as cysteine proteases and metalloproteinases found in the cancer cells (Mahesh et al. 2018).

With reference to polymer-drug conjugates, PEGylation provides a stealth property to a drug and enables prolonged drug circulation due to the polyethylene glycol (PEG) is able to suppress non-specific protein adsorption onto the conjugate and its uptake by the reticuloendothelial system (Schöttler et al. 2016). PEG can

increase the cellular drug uptake via its P-glycoprotein inhibitory action that negates drug efflux from cancer cells (Hodaei et al. 2015; Hugger et al. 2002). PEG is biocompatible, water-soluble, and non-toxic (Lutz and Hoth 2006). The high-molecular weight PEG (≥ 10,000 Da) is preferable for use in drug conjugation because it provides an extended plasma half-life of conjugate in the systemic circulation and is not immunogenic (Nie et al. 2017).

From the literature reviews, we have decided to synthesize a series of DOX analogues with several *beta*-thiopropanamide substituents containing *beta*-thiopropanamide linkers with and without substitution on the nitrogen of daunosamine sugar of DOX (Figure 1) to discover a stimuli-responsive linker for selective polymer-DOX conjugate to cancer cells. The *in vitro* release in buffer solution with different pH was studied to confirm the hydrolytic property of the new DOX analogues. Finally, *in vitro* cytotoxicity studies in MDA-MB-231 and MCF-7 breast cancer cells were performed along with MCF-10A normal breast cells to determine their cytotoxicity and selectivity.
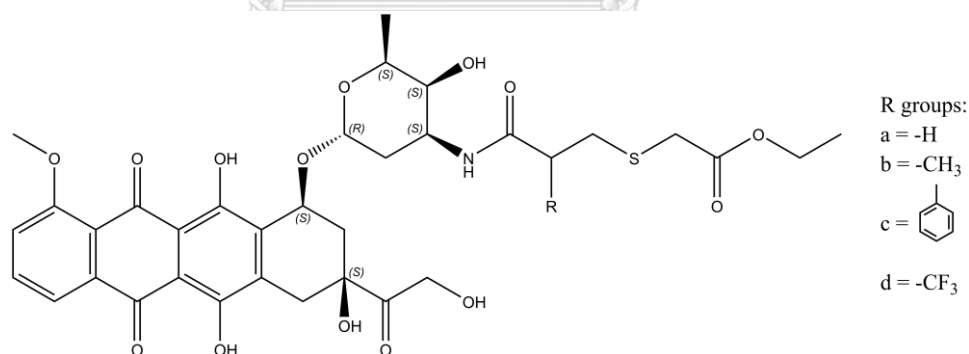
Figure 1 *Structure of DOX analogues with several beta-thiopropanamide substituents on the nitrogen.*

After a potential linker was found, we continued to develope a polymer-drug conjugate with this novel linker for doxorubicin delivery (Figure 2). For the polymer carrier, an FDA approved methoxypolyethylene glycol (mPEG) was chosen because of its biocompatibility, water-solubility, non-toxicity (Lutz and Hoth 2006) and its

suppression ability to non-specific protein adsorption (Schöttler et al. 2016). Methoxypolyethylene glycol with high molecular weight of 10,000 Da was selected for our conjugations as it was known to increase the half-life of the conjugate in the systemic circulation (Nie et al. 2017). The release study was conducted to assess whether our newly designed linker can improve the selectivity of the conjugate by pH stimulatory effect while the cytotoxicity study was performed to determine its selectivity against breast cancer cells.
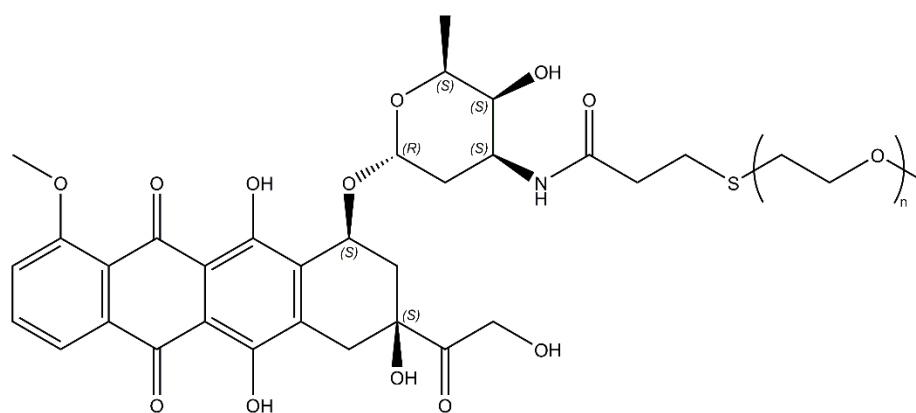
Figure 2 *Structure of methoxypolyethylene glycol-doxorubicin conjugates containing beta-thiopropanamide linker.*

The main objectives of this research study are as follows:

1. To synthesize and elucidate structures of DOX analogues containing:

    a. *Beta*-thiopropanamide linker

    b. Methyl-substituted *beta*-thiopropanamide linker

    c. Phenyl-substituted *beta*-thiopropanamide linker

    d. Trifluoromethyl-substituted *beta*-thiopropanamide linker

2. To evaluate the chemical hydrolysis and cytotoxicity of DOX analogues containing different linkers

3. To synthesize and elucidate structures of methoxy polyethylene glycol-doxorubicin conjugates containing novel linkers

4. To evaluate the chemical hydrolysis and cytotoxicity of methoxy polyethylene glycol-doxorubicin conjugates containing novel linkers in MDA-MB-231, MCF-7 breast cancer cells and MCF-10A normal cells.

CHAPTER 2

LITERATURE REVIEW

2.1. Cancer

Cancer is a cell or a group of cells that growing abnormally and losing their ability to stop growing. The normal cells can transform to cancerous cell by various factors such as chemicals, radiation, infection or even hormones. The evolution of cancerous cells causes by the errors during DNA replication. The cell replication is normally prevented by the intact genome, but the mechanism fails to stop if the impair genome presents. This leads to the neoplasm or even malignant tumor. These cancerous cells without an apoptosis ability will result in an uncontrolled cell growth, cell invasion and eventually the widespread of these cancerous cells throughout the body or metastasis. Most cancers present in the form of solid tumors or carcinomas, which normally initiate from epithelial cells, but they may present in other forms like liquid tumor in body fluids such as myeloma, lymphoma and leukemia which are originated from the bone marrow, the lymph system and the blood respectively.

The prevalence of cancer tends to increase in the future suggested by a number of people having a history of cancer are around 15.5 million in USA and expected to reach 20.3 million in 2026. The breast cancer is the most prevalent cancer among female (3,560,570), which 75% of the population are ages 60 years or older and 7% are younger than 50 years. This information indicates that recent therapies are not efficient enough for breast cancer treatment and are still needed (development of the anticancer agents) along with other efficient treatment programs.

2.2. Cancer treatment by chemotherapy and its problems

Chemotherapy is a common method taken in the hospital by applying anticancer drugs for cancer treatment. It is often used along with other methods such as radiation. The most native properties of these anticancer agents are the

action on the cell proliferation by DNA destruction or replication or inhibition of some synthesis pathways of the intracellular products. Unfortunately, chemotherapy still faces some burden and leads to unsatisfying therapeutic outcomes such as serious side effects from anticancer drugs. These may include damage to the heart, lungs, nerve endings, kidneys, or reproductive organs. It is obvious that the poor selectivity of these drugs leads to the difficulty of treatment. Doxorubicin, an RNA synthesis inhibitor, causes the cardiotoxicity that limits its efficacy (Y. Chen et al. 2011). Moreover, most anticancer drugs are poorly water-soluble resulting low bioavailability.

On the other hand, the impedance possibly comes from the multi-drug resistance cancer cells that develop from the most cancer cells resulting in the unsuccessful treatment. For all problems in chemotherapy, the selective and effective drug delivery system should be an alternative way for cancer therapy.

2.3. Doxorubicin

Doxorubicin is an anthracycline drug discovered in the 1970's from *Streptomyces peucetius var. caesius*. Its mechanism of actions was proposed to two pathways; (i) doxorubicin intercalates into DNA and inhibits topoisomerase-II enzyme responsible for DNA double strand breaking during transcription and (ii) doxorubicin generates free radicals form its iron complex with regard to cell damage (Hrdina et al. 2000). Undoubtedly, doxorubicin has the classic problem of chemotherapeutic agents that mainly causes cardiotoxicity due to not targeting the tumor. The patients who receive doxorubicin undergo depressed immune system, microbial infections and fatigue. This leads to the dose-limiting treatment to reduce adverse reactions.

The effort to improve the specificity of doxorubicin is evidenced by DOXIL®, a liposomal drug delivery system. This liposomal drug has been formulated and expected to reduce off-target release by encapsulation and prolong circulation of doxorubicin by evading the immune system caused from pegylated surface. It targets

tumor by enhanced permeability and retention effect. The released doxorubicin is believed to come from the high concentration of ammonia at the tumor site by glutaminolysis (Silverman and Barenholz 2015).

2.4. Controlled-drug release system

One strategy used for delivering DOX is formulating the controlled-drug release system. The system should be able to minimize the drug release during the delivery and efficiently release drug at the desired sites. Several controlled-drug release systems were employed to DOX for example, polymer conjugation (Kakinoki et al. 2008; Wei et al. 2016) and nanoparticles (Rao et al. 2017; Yu et al. 2015). In these systems, the sustained release behaviour is usually achieved to reduce the toxicity of DOX. The stimuli-responsive system based on the distinctive environment of tumor or cancer cells including dysregulated pH or enzyme overexpression is used to produce the rapid release of DOX at the tumor or cancer cells.

The chemical linkage plays a major role in the stimuli-responsive system. It can render an effect under chemical or enzymatic process depending on its chemical compositions for example, the ester linkage that can be hydrolysed under acidic condition or the GLY-PHE-LEU-GLY linkage that can be cleaved by an enzyme. However, it needs to balance these stimuli-responsive properties with the overall release behavior in order to produce an efficient and safely DOX delivery system.

2.5. Stimuli-responsive system

The stimuli-responsive system can be categorized into several types for example, pH, enzyme, reduction, etc. With reference to pH-responsive system, the drug delivery system can exploit the acidic environment of cancer cells to release the covalently conjugated drug from an acid-labile linker. Several acid-labile linkers such as, hydrazone (Lu et al. 2009), acetal (Tomlinson et al. 2003), cis-aconityl (Kakinoki et al. 2008), imine (J. Li et al. 2016) and *beta*-thiopropionate (Oishi et al. 2003) linkers have been used to introduce the pH-responsive function and enhance

the anticancer drug delivery specificity. In the case of enzyme-responsive system, the drug delivery relies on the overexpressed enzyme of cancer cells to free the covalently conjugated drug. Enzyme-responsive linkers, such as disulfide which is cleaved by glutathione enzyme (Lv et al. 2014) and small peptide GLY-PHE-LEU-GLY linker (Wei et al. 2016) that is cleaved by cathepsin B, have been employed to develop enzyme-responsive drug delivery system.

2.6. Amide-based linkers

Doxorubicin can be chemically modified by amide conjugation at the amino group of daunosamine sugar moiety. It is known that an amide bond is versatile in hydrolytic condition especially physiological environment as well as the enzymatic tolerance in blood circulation because the low abundance of proteases enzyme in the blood. However, it may not provide sufficient drug release in cancer cells since it is stable in mild acid. To gain an advantage of the amide bond for anticancer drug delivery, it needs to develop a new amide-based linker with some modifications for example, an amide-carboxylic acid system that takes an advantage of the five-membered intermediate formed by the adjacent carboxylic acid group with the carbonyl carbon of amide bond, which the intermediate is labile in acidic buffer (Kluger and Lam 1978). This mechanism also presents in a cis-aconityl linker (Dillman et al. 1988) that is occasionally utilized in pH-responsive anticancer drug delivery. Nevertheless, the amide bond can be used to generate an enzyme-responsive effect which it can be cleaved by an overexpressed enzyme in cancer cells. Many publications used some small peptide linkers to gain the enzyme responsiveness in their formulations (Lee et al. 2015; N. Li et al. 2014; Wei et al. 2016).

2.7. *Beta*-thiopropionate linker

The *beta*-thiopropionate linker (Figure 3) is the interesting chemical bond often applied in several pH-responsive drug delivery systems for examples, polymeric micelles (Lv et al. 2014), dendrimer (K. Chen et al. 2016), polymer-drug conjugate

(Liang Qiu et al. 2016) and inorganic nanoparticles (L. Qiu et al. 2017). In term of the synthesis, this linker can be simply synthesized by a simple ester-coupling procedure and Michael addition reaction for establishing ester and thioether moieties.
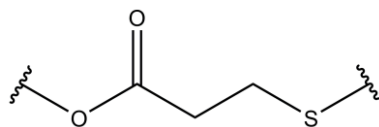
Figure 3 *The Beta-thiopropionate linker.*

The hydrolytic mechanism of the *beta*-thiopropionate linker happens by induction of the sulfur atom at the *beta* position to the carbonyl carbon of ester bond that generate a partial positive effect (Schoenmakers et al. 2004). From this investigation, it is clearly that the carbonyl carbon will be partially positive and it will be more positive when the distance of the sulfur atom is reduced (Figure 4). This partially positive charge affects the drug release profile (13 and 4 days at 50% release for 4-sulfanylpropionate and 3-sulfanylpropionate respectively). From this insight, it is possible that the carbonyl carbon might become more positive charge if some nucleophiles present in the alkyl chain to generate an electron withdrawing effect on the carbonyl carbon of amide bond resulting a susceptible spot in hydrolytic cleavage. The hydrolysis rate is even greater when the *beta*-thiopropionate linker is in the acidic condition (Oishi et al. 2003). The *beta*-thiopropionate linker, however, contained an ester bond which has been reported to be susceptible to enzymatic hydrolysis in the systemic circulation due to the abundance of the esterase enzyme (Ratnatilaka Na Bhuket et al. 2019; Rudakova et al. 2011). Instead of conventional ester linkage, the amide bond has been proposed in the development of a slow-release drug delivery system due to its high stability in plasma (Gao et al. 2012). The amide bond is relatively resistant to esterase action. It undergoes a fast cleavage in response to specific protease enzymes such as cysteine proteases and metalloproteinases found in the cancer cells (Mahesh et al. 2018).

Therefore, the incorporation of an amide bond and a beta-sulfur atom should be useful to establish a sustained-drug delivery system with the pH- and enzyme-responsive effects.

+0.822   +0.808   +0.793
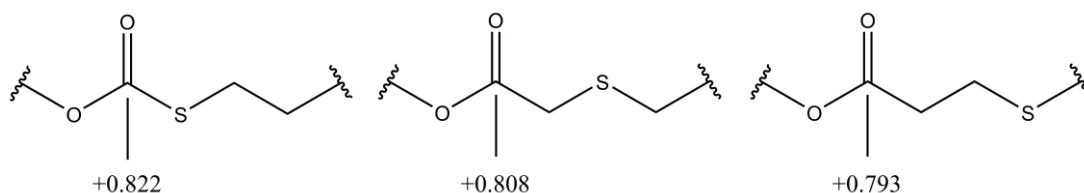
Figure 4 *Different inductive effect from left to right: 2-sulfanylpropionate, 3-sulfanylpropionate and 4-sulfanylpropionate respectively.*

2.8. Polymer-drug conjugate

For the solid tumors, the vasculatures at the tumors are leaky due to the fast growth of tumors. These impaired vasculatures provide the occasion to deliver macromolecules or nano-size materials to the tumor tissues (Matsumura and Maeda 1986). Therefore, many drug delivery systems are exploited for delivering drug to the tumor for example, micelles, nanoparticles, dendrimers and drug conjugates.

It is known that doxorubicin has poor specificity to cancer cells. Therefore, the design of drug delivery system is crucial for a potential doxorubicin delivery. The polymer-drug conjugation is one of several methods for selectivity enhancement to cancer cells. It produces the enhanced permeability and retention effect that increase accumulation of drug at the tumor sites. Generally, the polymer-drug conjugate consists of the hydrophilic polymer with or without the modified linker and the therapeutic agents (Figure 5). It is made not only for achieving water-soluble and sustain release properties due to the slow degradation of the covalent bond, but they also provide safety, biocompatibility or biodegradability. Although, these properties are suitable for the anticancer drug delivery since it could minimize the drug release in systemic circulation, some modifications are still needed to gain the selective drug release at the tumors and sufficient release of a therapeutic agent.

Figure 5 *Common structure of polymer-drug conjugate.*

On the other hand, a polymer-drug conjugate can behave as a prodrug during systemic circulation, thus it can reduce toxicity of doxorubicin during delivery. When the conjugate enters the tumor or cells, this conjugated prodrug subsequently releases and becomes an active form after chemical or enzymatic hydrolysis. This idea can be applied for doxorubicin delivery which correspond to the use of polymer-drug conjugate as it can minimize the premature drug release before reaching the target.

Noteworthy, the conjugated polymer extremely influences the physicochemical properties and pharmacokinetics of the polymer-drug conjugates. The use of water-soluble polymer could increase the drug solubility with regard to the drug bioavailability. Nevertheless, the kind of polymer is an important factor that should be concerned since it plays a role in the selectivity to cancer cells.

2.9. Polyethylene glycol

Polyethylene glycol (PEG) is a water soluble and biocompatible polymer consisting of repeating units of polyethylene oxide (PEO) or polyoxyethylene (POE) (Figure 6). The proposal of the conjugation of PEG to other therapeutic agents or molecules (i.e., PEGylation) is to make the water-soluble products and to protect the therapeutic agent from the mononuclear phagocyte system resulting long circulation half-life and good stability (Abuchowski et al. 1977; van Vlerken et al. 2007) which increase the occasion of drug accumulation in tumors. PEG is suitable for establishing the polymer-drug conjugate because it is not immunogenic, and it can be excreted by urinary system.
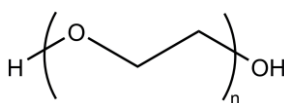
Figure 6 Polyethylene glycol.

In term of drug delivery, the selection of PEG molecular weight should not be overlooked because it impacts on drug release as well as drug accumulation at the tumor site. Several studies demonstrated that the conjugation of high molecular weight polymer resulted in long circulation half-life of the conjugate which is evident by pharmacokinetic studies of PEG-Ara-C (1-β-D arabinofuranosilcytosyne) conjugate in mice (Schiavon et al. 2004). The half-life of the PEG-Ara-C conjugate with mPEG 20 kDa showed around three-fold longer than the PEG-Ara-C conjugate with mPEG 5 kDa. Another pharmacokinetic studies showed the decrease in blood clearance of PEG by administrating ^{125}I-labeled PEG in mice. The urinary clearance decreased when the PEG molecular weight increased from 6 kDa to 170 kDa suggesting the low renal glomerular permeability of high molecular weight PEG (Yamaoka et al. 1994). On the other hand, the use of PEG with molecular weight more than 1 kDa was not feasible for oral administration due to low oral bioavailability and subjected to intravenous injection. A research group found the oral bioavailability around 57% for PEG500 and 9.8% for PEG1000 (Shaffer et al. 1950). In addition, the mPEG with molecular weight 20kDa showed immunogenicity that the IgG antibody was found after administering mPEG 20 kDa-mmTRAIL, which is the PEGylated cytotoxic protein, to rhesus monkeys (Nie et al. 2017). The study also showed that the mPEG 10 kDa-mmTRAIL had no immunogenicity and long serum half-life as well as the mPEG 20 kDa-mmTRAIL. From these reviews, the appropriate molecular weight of PEG for potential conjugation should be 10kDa for safety and retention effect. The use of high molecular weight (>40 kDa) will undergo the difficulties in term of the synthesis that will face the difficulty in term of synthesis and characterization because of the low percentage of conjugated drug from the steric hindrance of polymer and low

instrument signal of the conjugated drug during identification. These evidences indicate that PEG with molecular weight 10kDa may suitable to make a polymer conjugation for injection of doxorubicin.

In the view of synthesis, the functionalized PEGs are needed to construct the polymer-drug conjugate in order to create the bond between the linker and the drug. The selection of the functionalized PEGs should be based on the conjugation feasibility and the chemical bond in the PEG chain. Several functionalized PEGs contain the labile chemical bonds for example an ester bond which might affect the pharmacokinetic properties of the synthesized conjugates. In this work, we selected the thiol-functionalized PEG in order to synthesize the mPEG-doxorubicin conjugate containing a novel linker with an amide bond between the linker and doxorubicin.

2.10. The design of the novel linkers

It is highly required a linker that can improve the selectivity of the polymer-doxorubicin conjugate for anticancer delivery. The conjugate should be selectively hydrolyzed by chemical or enzymatic process, and it should have good stability in the physiological pH of blood circulation. In addition, the available functional group of the anticancer drug is important for linker design.

According to the review, designing a new linker with electron deficiency on carbonyl carbon is important for elevating its selectivity towards acidic tumors or cancer cells. This can provide by high electronegative atoms or moieties. Because of the similarity of hydrolysis pathway of the ester and amide bond, it will be able to introduce the same idea to increase the positive state of carbonyl carbon of amide bond. This suggests us to create new linkers that contain of high electronegative atoms or moieties adjacent to amide bond. The chemical moieties incorporated in the linkers include acrylic acid, methacrylic acid, atropic acid, and 2-(trifluoromethyl) acrylic acid to produce the effect on electronegative atoms or moieties differentiating by sulfur, methyl, phenyl and fluorine (Figure 7).

R groups:

a = -H

b = -CH$_3$

c =

d = -CF$_3$
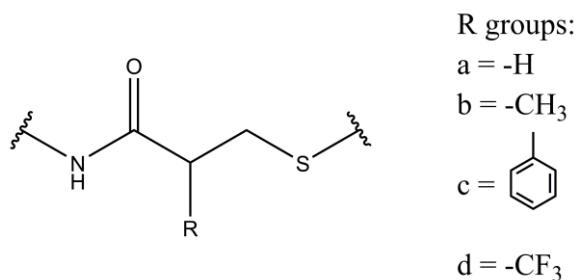
Figure 7 New linkers from different compounds a) a linker from acrylic acid b) a linker from methacrylic acid c) a linker from atropic acid and d) a linker from 2-(trifluoromethyl) acrylic acid.

These designed linkers will be used to synthesize small conjugates of doxorubicin by conjugating to doxorubicin at amine group of daunosamine sugar moiety. The other side of the linker will be capped by ethyl thioglycolate to create a thioether moiety. Moreover, to see the effect of the new linkers on doxorubicin delivery system, the new linker obtained from the best selective small conjugate for cancer cells will be used to create a simple polymer-drug conjugate. To exploit the sustained release property and avoid the immunogenicity, the methoxy polyethylene glycol (mPEG) with molecular weight 10 kDa will be used for conjugating with doxorubicin (DOX) via a novel linkage to produce an mPEG-DOX conjugate containing a novel linker. The synthesized conjugate will be evaluated the cytotoxicity and selectivity in breast cancer cells.

CHAPTER 3

RESEARCH METHODOLOGY

3.1. Chemicals, cell lines, media and equipments

1) Doxorubicin hydrochloride (DOX), Energy Chemical, China

2) 1-Ethyl-3-(3-dimethylaminopropyl) carbodiimide hydrochloride (EDC.HCl), Energy Chemical, China

3) Hydroxybenzotriazole (HOBt), Energy Chemical, China

4) Acrylic acid, Tokyo Chemical Industry Co., Ltd., Japan

5) Methacrylic acid, Tokyo Chemical Industry Co., Ltd., Japan

6) Atropic Acid, Tokyo Chemical Industry Co., Ltd., Japan

7) 2-(Trifluoromethyl) acrylic acid, Energy Chemical, China

8) 4-Methylmorpholine (NMM), Energy Chemical, China

9) Ethyl thioglycolate, Energy Chemical, China

10) Dimethylphenylphosphine (DMPP), Alfa Aesar, USA

11) Tetrahydrofuran (THF), Merck KGaA, Darmstadt, Germany

12) Dimethylformamide (DMF), Merck KGaA, Darmstadt, Germany

13) Acetonitrile, Honeywell Burdick & Jackson, USA

14) Methanol, Honeywell Burdick & Jackson, USA

15) Potassium dihydrogen phosphate, Merck KGaA, Darmstadt, Germany

16) Sodium acetate trihydrate, Merck KGaA, Darmstadt, Germany

17) Glacial acetic acid, Sigma-Aldrich, USA

18) Sodium dihydrogen phosphate, Merck KGaA, Darmstadt, Germany

19) 37% Hydrochloric acid, Merck KGaA, Darmstadt, Germany

20) Sodium hydroxide, Merck KGaA, Darmstadt, Germany

21) Sodium chloride, Sigma-Aldrich, USA

22) Sodium bicarbonate, Sigma-Aldrich, USA

23) Thiol-functionalized methoxypolyethylene glycol (mPEG-SH) with MW. 10,000, Laysan Bio, Inc., USA

24) Methoxypolyethylene glycol succinimidyl propionate (mPEG-NHS) with MW. 10,000, Jenkem Technology USA, USA

25) 4-Dimethyl aminopyridine (DMAP), Sigma Aldrich, USA

26) Amicon® Ultra-15 centrifugal filter MWCO 3 kDa, Merck KGaA, Darmstadt, Germany

27) Human breast adenocarcinoma (MDA-MB-231, ATCC No. HTB-26), USA

28) Human breast adenocarcinoma (MCF-7, ATCC No. HTB-22), USA

29) Human fibrocystic breast (MCF-10A, ATCC No. CRL-10317), USA

30) Dulbecco's Modified Eagle Medium (DMEM), Invitrogen, NY, USA

31) Ham's F-12 Nutrient Mixture, Invitrogen, NY, USA

32) Fetal bovine serum (FBS), Merck-Millipore, Massachusetts, USA

33) Horse serum, Lonza, Basel, Switzerland

34) Epidermal growth factor, Lonza, Basel, Switzerland

35) Insulin, Lonza, Basel, Switzerland

36) Hydrocortisone, Lonza, Basel, Switzerland

37) Penicilin-Streptomycin, Invitrogen, NY, USA

38) Laminar flow hood, Model: BV-126 (Thermo Scientific), USA

39) CO2 Incubator for cell culture (Thermo Scientific), USA

40) Vortex mixer, Model: Vortex-Genie 2, Scientific Industries, USA

41) pH meter, Model: SevenEasy™, METTLER TOLEDO, Italy

42) Centrifuge, Hettich instrument 1706-01 Rotina 380R Benchtop, USA

43) Microplate reader, CLARIOstar, BMG LABTECH, Germany

44) 96 well plates for cell culture, Corning, USA

45) 75 T-flask for cell culture, Corning, USA

46) Heating block, Stuart, SBH 130D, UK

47) Varian 400 MR 400 MHz nuclear magnetic resonance spectrometer, Varian, Palo Alto, USA

48) Bruker AVANCE III HD/OXFORD 500 MHz nuclear magnetic resonance spectrometer, Bruker, USA

49) Bruker micrOTOF Q-II mass spectrometer, Bruker, USA

50) Shimadzu Prominence HPLC System coupled with RF-20Axs Fluorescence Detector, Shimadzu, Japan

Methodology of study

The methodology of this study is show in Figure 8.
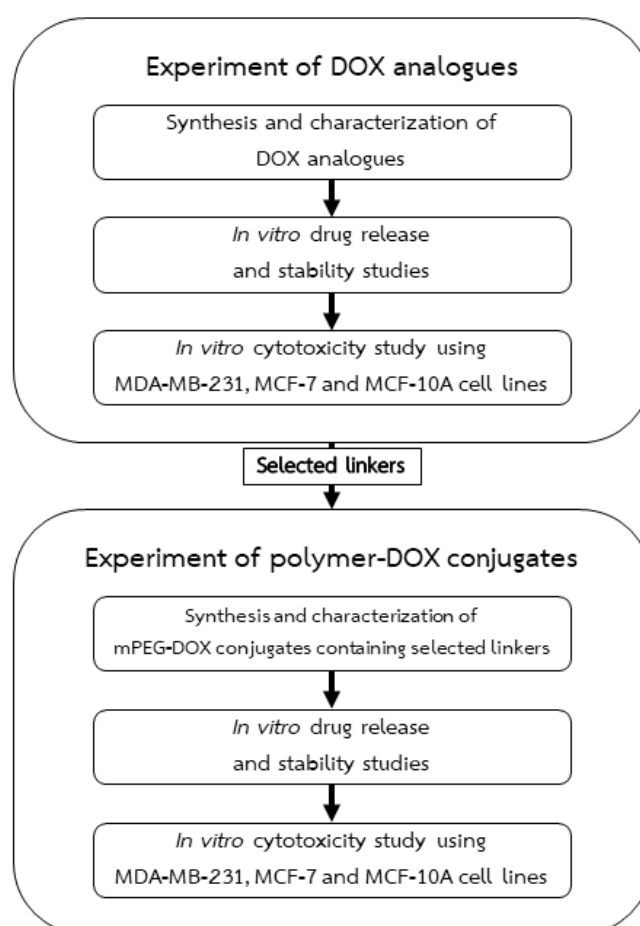
Figure 8 *Methodology of study.*

3.2. Experiments for DOX analogues

3.2.1 General synthesis procedure of the *beta*-thiopropanoic acid substituents

Four *beta*-thiopropanoic acid substituents were synthesized via Thiol Michael addition reaction (Figure 9). Briefly, ethyl thioglycolate (2 equivalents) and four alkenyl carboxylic acids including acrylic acid (1a), methacrylic acid (1b), atropic acid (1c), and 2-(trifluoromethyl)acrylic acid (1d) (1 equivalent) were dissolved in 5 mL THF and the solution was stirred at 25 ± 1°C. Subsequently, DMPP (0.2 equivalent) was added to the solution and continuously stirred for 24 h. The solution mixture was evaporated under vacuum (<10 mbar). The residue was collected and purified using column chromatography with dichloromethane: methanol as the mobile phase. The eluate was monitored by thin layer chromatography (TLC) (silica gel 60 F_{254}, 0.25mm thickness) with dichloromethane: methanol as the mobile phase.
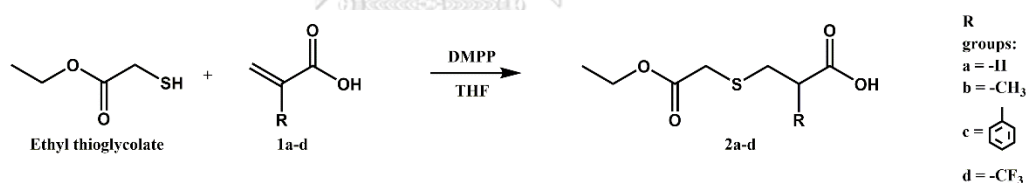
Figure 9 *Reaction scheme for the synthesis of four beta-thiopropanoic acid substituents.*

3.2.1.1. 3-((2-ethoxy-2-oxoethyl)thio)propanoic acid (2a)

The compound 2a was synthesized from ethyl thioglycolate (110 μL, 1 mmol) and acrylic acid (1a) (35 μL, 0.5 mmol). The residue from the general procedure was collected and purified using column chromatography with dichloromethane: methanol (9.5:0.5) as the mobile phase.

3.2.1.2.   3-((2-ethoxy-2-oxoethyl)thio)-2-methylpropanoic acid (2b)

The compound 2b was synthesized from ethyl thioglycolate (110 µL, 1 mmol) and methacrylic acid (1b) (43 µL, 0.5 mmol). The residue from the general procedure was collected and purified using column chromatography with petroleum ether: ethyl acetate (4:6) as the mobile phase.

3.2.1.3.   3-((2-ethoxy-2-oxoethyl)thio)-2-phenylpropanoic acid (2c)

The compound 2c was synthesized from ethyl thioglycolate (110 µL, 1 mmol) and atropic acid (1c) (74.1 mg, 0.5 mmol). The residue from the general procedure was collected and purified using column chromatography with dichloromethane: methanol (9.6:0.4) as the mobile phase.

3.2.1.4.   2-(((2-ethoxy-2-oxoethyl)thio)methyl)-3,3,3-trifluoropropanoic acid (2d)

The compound 2d was synthesized from ethyl thioglycolate (330 µL, 3 mmol) and 2-(trifluoromethyl)acrylic acid (1d) (210.1 mg, 1.5 mmol). The residue from the general procedure was collected and purified using column chromatography with petroleum ether: ethyl acetate (8:2) as the mobile phase.

3.2.2 General synthesis procedure of the DOX analogues

Seven *DOX* analogues were synthesized by conjugating an amino group with four carboxylic acid substituents from section 2.2 (Figure 10). Each of 4 *beta*-thiopropanoic acid substituents (2a-d) (1.2 equivalents) was transferred to a round-bottom flask and dissolved in 5 mL DMF. In a separate flask, EDC.HCl (1.2 equivalents) and HOBt (1.2 equivalents) were dissolved in 2 mL DMF. Both solutions were mixed under continuous magnetic stirring in an ice bath for 30

min. DOX (1 equivalent) was dissolved in 10 mL DMF with stirring and added with 4-methylmorpholine (1.2 equivalents) to increase its solution pH to 11 and to facilitate the amide coupling reaction. The activated carboxylic acid solution was added dropwise into the DOX solution and continuously stirred for 4 h at $25 \pm 1°C$. The reaction mixture was then filtered and evaporated under vacuum (<10 mbar). The residue was collected and initially purified using column chromatography followed by preparative thin layer chromatography with dichloromethane: methanol as the mobile phase. The eluate was monitored by thin layer chromatography (TLC) (silica gel 60 F_{254}, 0.25mm thickness) with dichloromethane: methanol as the mobile phase.
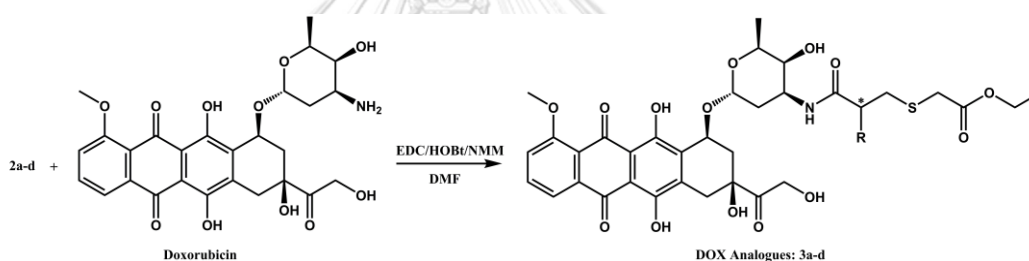
Figure 10 *Reaction scheme for the synthesis of 7 DOX analogues based on different beta-thiopropanamide substituents.*

3.2.2.1. DOX-analogue 3a

The DOX analogue 3a was synthesized from compound 2a (76.3 mg, 0.39 mmol) and DOX (191.4 mg, 0.33 mmol). The residue from the general procedure was collected and purified using column chromatography with dichloromethane: methanol (9.5:0.5) as the mobile phase.

3.2.2.2. DOX analogue 3b-1

The DOX analogue 3b-1 was separated from the residue yielded from the amide coupling reaction of the compound 2b (49.4 mg, 0.24

mmol) and DOX (116 mg, 0.2 mmol). The residue from the general procedure was collected and purified using column chromatography with dichloromethane: methanol (9.5:0.5) as the mobile phase. The first collected fraction from the column chromatography was the DOX analogue 3b-1.

3.2.2.3. DOX analogue 3b-2

The DOX analogue 3b-2 was separated from the same residue as in the section 3.2.2.2. The residue from the general procedure was collected and purified using column chromatography with dichloromethane: methanol (9.5:0.5) as the mobile phase. The second collected fraction from the column chromatography was the DOX analogue 3b-2.

3.2.2.4. DOX analogue 3c-1

The DOX analogue 3c-1 was separated from the residue yielded from the amide coupling reaction of the compound 2c (97.2 mg, 0.36 mmol) and DOX (174.6 mg, 0.3 mmol). The residue from the general procedure was collected and purified using column chromatography with dichloromethane: methanol (9:0.5) as the mobile phase. After finishing the column chromatography, the mixture collected from the column chromatography was further separated using preparative thin layer chromatography with dichloromethane: methanol (9.8:0.2) as the mobile phase. The first collected fraction from the preparative thin layer chromatography was the DOX analogue 3c-1.

3.2.2.5. DOX analogue 3c-2

The DOX analogue 3c-2 was separated from the residue yielded from the same residue as in the section 3.2.2.4. The residue from the

general procedure was collected and purified using column chromatography with dichloromethane: methanol (9:0.5) as the mobile phase. After finishing the column chromatography, the mixture collected from the column chromatography was further separated using preparative thin layer chromatography with dichloromethane: methanol (9.8:0.2) as the mobile phase. The second collected fraction from the preparative thin layer chromatography was the DOX analogue 3c-2.

3.2.2.6. DOX analogue 3d-1

The DOX analogue 3d-1 was separated from the residue yielded from the amide coupling reaction of the compound 2d (224.8 mg, 0.86 mmol) and DOX (417 mg, 0.72 mmol). The residue from the general procedure was collected and purified using column chromatography with dichloromethane: methanol (9.5:0.5) as the mobile phase. After finishing the column chromatography, the mixture collected from the column chromatography was further separated using preparative thin layer chromatography with dichloromethane: methanol (9.8:0.2) as the mobile phase. The first collected fraction from the preparative thin layer chromatography was the DOX analogue 3d-1.

3.2.2.7. DOX analogue 3d-2

The DOX analogue 3d-2 was separated from the residue yielded from the same residue as in the section 3.2.2.6. The residue from the general procedure was collected and purified using column chromatography with dichloromethane: methanol (9.5:0.5) as the mobile phase. After finishing the column chromatography, the mixture collected from the column chromatography was further separated using preparative thin layer chromatography with dichloromethane: methanol (9.8:0.2) as

the mobile phase. The second collected fraction from the preparative thin layer chromatography was the DOX analogue 3d-2.

3.2.3 Determination of absolute configuration of diastereomeric products by Nuclear Overhauser effect difference

The absolute configuration of all diastereomers obtained from the syntheses was determined by one dimensional NMR using Nuclear Overhauser effect (NOE) difference experiment. The absolute configuration of the alpha substituent was investigated by checking the undergoing cross-relaxation of the neighbor protons when the 6″ proton of DOX analogues (2.53, 2.55, 3.88, 3.81, 3.72 and 3.72 ppm for 3b-1, 3b-2, 3c-1, 3c-2, 3d-1 and 3d-2, respectively) was saturated by the radio frequency irradiation. If the neighbor protons present a NOE in the spectrum (positive), it means that those neighbor protons are close to the 6″ proton in space, thus giving a similar configuration.

To measure the distance between the 6″ proton and the neighbor protons with an appeared NOE signal, the three-dimensional structures of all DOX analogues were established by Chem3D software version 18.1.0.535, and all structure were optimized using MM2 force field to gain the lowest energy state. The measured distance was compared to the NOE signal in the respective ^{1}H NMR spectrum to determine the chiral configuration of the alpha substituent of the DOX analogue.

3.2.4 *In vitro* drug release and stability

The *in vitro* stability and DOX release of seven DOX analogues (3a-d) in acetate buffer pH 4.0, phosphate buffer pH 5.5, and phosphate buffer pH 7.4 were evaluated. Each DOX analogue were dissolved separately in methanol at a concentration of 0.2 mg/mL as stock solution. One hundred μL of the DOX analogue stock solutions were diluted with 400 μL buffer solution to obtain a

final concentration of 0.04 mg/mL (~50 µM). The solution was vortex-mixed and incubated at 37°C. Aliquots were withdrawn from the solution at specific time intervals (0, 24, 48, 72, 144, 192 and 240 h), except the aliquots of DOX analogue 3c-1 and 3c-2 were withdrawn from the solution at 0, 1, 2, 4, 6 and 8h. All aliquots were added with 20 % methanol at 1:20 dilution (~2.5 µM). The diluted sample was analysed by high-performance liquid chromatography (Shimadzu Prominence HPLC System, Shimadzu Corporation, Japan) using Halo C8 column (4.6 x 50 mm, 2.7 µm particle size; Advanced Materials Technology Inc., USA). The mobile phase was constituted of eluents A (acetonitrile) and B (20 mM sodium dihydrogen phosphate pH 2.0) as organic and aqueous phases, respectively. The elution program was as follows: initial 0–0.5 min, isocratic elution A–B (80:20, v/v); 0.5–3.5 min, linear change to A–B (45:55, v/v); 3.5–5.5 min, isocratic elution A–B (45:55, v/v); 5.5–6 min, linear change to A–B (80:20, v/v); 6–13 min, isocratic elution A–B (80:20, v/v). The injection volume was 10 µL. The fluorescence detector (Shimadzu RF-20Axs, Shimadzu Corporation, Japan) was set with excitation and emission wavelengths at 480 and 590 nm, respectively. The typical chromatograms of DOX, doxorubicinone, 3a, 3b-1, 3b-2, 3c-1, 3c-2, 3d-1, and 3d-2 were characterized by retention times of 2.8, 5.6, 6.8, 6.9, 7.0, 7.8, 7.9, 7.7 and 7.6 min, respectively. The DOX concentration was calculated against the DOX standard plot (0.0001-0.0075 mg/mL). The concentration of each DOX analogue was normalized against the original concentration of the corresponding conjugate or DOX at time = 0 h. All experiments were performed in triplicate. The drug release profile was characterized by the percentage of DOX release against the incubation time. The stability profiles of the DOX analogues were characterized by the remaining concentration of conjugates against the incubation time, with the stability kinetic parameters including kinetic constant (k_{obs}) and half-life ($t_{1/2}$) being

calculated using the pseudo-first order kinetic model. The stability profile of free DOX was similarly assessed with reference to the incubation intervals of 0, 24, 48, 96, 168, 216 and 264 h.

3.2.5 Cytotoxicity

Two human breast cancer cell lines (MDA-MB-231; ATCC No. HTB-26 and MCF-7; ATCC No. HTB-22) and the human breast normal epithelial cell line (MCF-10A; ATCC No. CRL-10317) were obtained from American Type Culture Collection (ATTC), USA. The MDA-MB-231 and MCF-7 cells were grown in complete medium, comprising of Dulbecco's modified Eagle's Medium (DMEM; Invitrogen, USA) supplemented with 10% (v/v) heat-inactivated fetal bovine serum (FBS; Merck-Millipore, USA) and 1% (v/v) 100 U/ mL penicillin and 100 µg/mL streptomycin (Invitrogen, USA), while the MCF-10A cells were cultured in Dulbecco's modified Eagle's Medium/Ham's F12 Medium ((Invitrogen, USA) supplemented with 5% horse serum, 20 ng/mL epidermal growth factor, 0.01 mg/mL insulin, 500 ng/mL hydrocortisone (Lonza, Basel, Switzerland) and 1% (v/v) 100 U/mL penicillin and 100 µg/mL streptomycin.

3.2.5.1. 3-(4,5-dimethylthiazol-2-yl)-2,5-diphenyltetrazolium bromide (MTT) assay

The cytotoxicity of DOX analogues or free DOX was evaluated by *in vitro* colorimetric 3-(4,5-dimethylthiazol-2-yl)-2,5-diphenyltetrazolium bromide assay. The MDA-MB-231, MCF-7 and MCF-10A cells were cultured in 96 well plate with a density of 10,000, 20,000 and 30,000 cells/well, respectively. The plates were incubated at 37°C with 5% carbon dioxide/95% air for 24 h. The cells were then washed with serum-free medium and were re-incubated with DOX analogues that were diluted in serum-free medium in five concentrations (0.01, 0.1, 1, 5 and 10 µM DOX

equivalent). Dimethyl sulfoxide (DMSO) in serum free medium with a final concentration of 0.5% (v/v) was used as a control following incubation for 24 h, all cells were washed with phosphate buffer saline pH 7.2. The MTT solution (0.5 mg/ml in phosphate buffer saline pH 7.2) was added and the cells were re-incubated for another 4 h. These cells were then washed with phosphate buffer saline and DMSO was added to dissolve the formazan crystals. The optical density at 540 nm was measured using a microplate reader (CLARIOstar, BMG Labtech, Germany). The experiments were performed in four replicates and the results were presented as % cell viability against the control. The selectivity index of DOX analogues and DOX for cancer cells was determined using the following equation (Oliveira et al. 2015):

Selectivity index = IC_{50} of the sample in MCF-10A/IC_{50} of the sample in MCF-7 or MDA-MB-231 [1]

3.2.6 Molecular docking

Molecular docking was conducted to assess the affinity of specific cancer enzymes for the DOX analogue 3a. Several cathepsins found overexpressed in MDA-MB-231 and MCF-7 cell lines (Ishibashi et al. 1999; Lah et al. 2000; Laurent-Matha et al. 1998; Radenkovic et al. 2017) including cathepsin B, D and L (PDB code 1HUC, 1LYB and 3HHA) were adopted in molecular docking using AutoDock version 4.2.6 running under AutoDockTools version 1.5.6 Sep_17_14 (The Scripps Research Institute, USA). All bonds of the DOX analogue 3a were set as rotatable, except ring and amide bonds, and the enzyme was kept rigid. Docking was carried out using Lamarckian genetic algorithm (LGA) with a number of individuals in population of 150, a maximum number of energy evaluations of 2500000, a maximum number of generations of 27000, a rate of

gene mutation of 0.02, a rate of crossover of 0.8, a number of top individuals to survive to next generation of 1, a genetic algorithm's selection window of 10, a maximum number of local search iterations of 300 and a grid point spacing of 0.375 Å. All binding conformations were depicted in UCSF Chimera version 1.14 (build 42094).

3.2.7 Statistical analysis

Statistical analysis was performed using IBM SPSS Statistics software version 22. One-way ANOVA with the Scheffe test was used to assess the statistical significance. All data are presented as mean ± SD, with p values of <0.01 indicating statistical significance.

3.3. Experiments for polymer-DOX conjugates

3.3.1 Synthesis of the mPEG-S-acrylic acid conjugate

The mPEG-S-acrylic acid conjugate was synthesized via Thiol-Michael addition reaction (Figure 11). Briefly, the mPEG-SH (600 mg, 0.06 mmol) and acrylic acid (81 µL, 1.2 mmol) were dissolved in 10 mL THF and the resulting solution was magnetically stirred at 25 ± 1°C. DMPP (18 µL, 0.12 mmol) was added to the solution and continuously stirred for 24 h. The solution mixture was evaporated under vacuum (<10 mbar) and the residue was re-dissolved in 1 mL dichloromethane. Subsequently, 200 mL diethyl ether was added to the solution and the white precipitate of mPEG-S-acrylic acid conjugate was collected by filtration (Whatman® qualitative grade 1 filter paper, GE Healthcare Life Sciences, USA).

mPEG-SH   Acrylic acid   mPEG-S-acrylic acid (1)
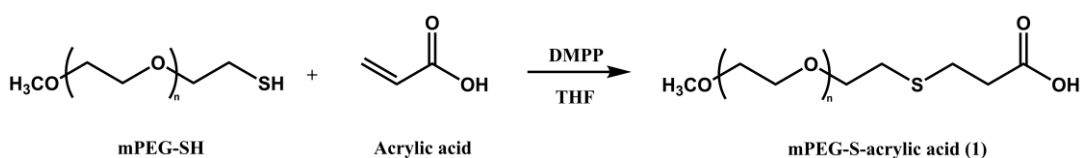
Figure 11 Reaction scheme for the synthesis of mPEG-S-acrylic acid conjugate.

3.3.2 Synthesis of the mPEG-doxorubicin conjugate with acrylic acid linker (P-A-DOX)

The P-A-DOX was synthesized via amide bond formation between the amino group of DOX and the carboxylic acid group of the mPEG-S-acrylic acid conjugate (Figure 12). The mPEG-S-acrylic acid conjugate (200 mg, 0.02 mmol) was transferred into a round-bottom flask and dissolved in 5 mL DMF. EDC (77 mg, 0.4 mmol) and HOBt (54 mg, 0.4 mmol) were dissolved in 2 mL DMF in a separate flask. Both solutions were mixed under continuous magnetic stirring in an ice bath for 30 min. DOX HCl (232 mg, 0.4 mmol) was dissolved in 10 mL DMF with stirring and added with 4-methylmorpholine (44 µL, 0.4 mmol) to increase its solution pH to 11 to facilitate the amide coupling reaction. The activated mPEG-S-acrylic acid conjugate solution was added dropwise into the DOX solution and continuously stirred for 4 h at 25 ± 1°C. The reaction mixture was then filtered and evaporated under vacuum. The filtered residue was re-dissolved in 1 mL dichloromethane. Subsequently, 200 mL diethyl ether was added to the solution and a red precipitate was formed. The precipitate was harvested and re-dissolved in purified water, and further purified using Amicon® Ultra-15 centrifugal filter to isolate the red P-A-DOX conjugate.
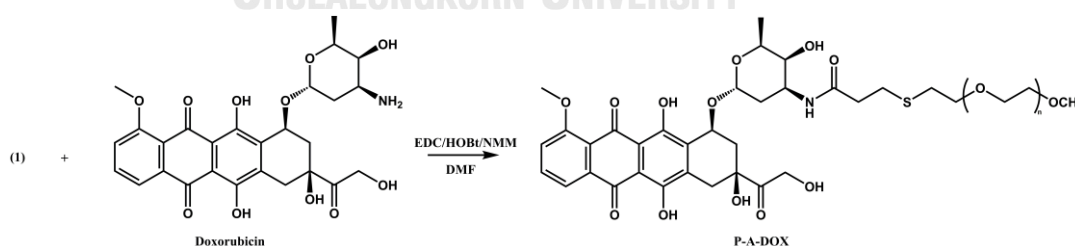
Figure 12 Reaction scheme for the synthesis of the P-A-DOX conjugate.

3.3.3 Synthesis of the mPEG-doxorubicin conjugate (P-DOX)

The P-DOX conjugate was synthesized by direct amide bond formation between the amino group of DOX and the activated carboxylate group of mPEG-NHS without the introduction of a linker (Figure 13). mPEG-NHS (200 mg,

0.02 mmol) and DOX HCl (232 mg, 0.4 mmol) were dissolved in 5 mL DMF under continuous magnetic stirring. DMAP (49 mg, 0.4 mmol), previously dissolved in 1 mL DMF, was added to the solution of mPEG-NHS and DOX. The mixture was allowed to react under stirring at 25 ±1°C for 5 h. The reaction mixture was filtered, and the filtrate was evaporated under vacuum. The residue was re-dissolved in 1 mL dichloromethane. Subsequently, 200 mL diethyl ether was added to the solution and a red precipitate was formed. The precipitate was re-dissolved in purified water and further purified by means of Amicon® Ultra-15 centrifugal filtration.
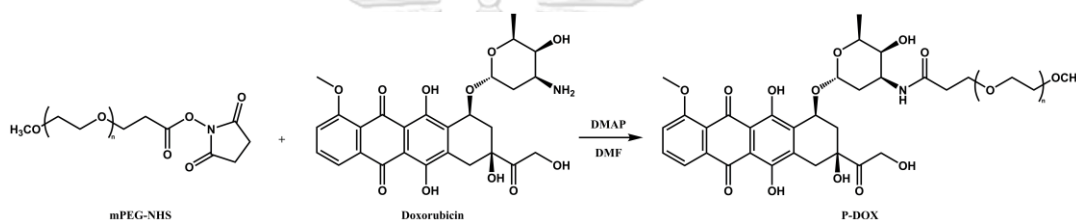
Figure 13 *Reaction scheme for the synthesis of the P-DOX conjugate.*

3.3.4 DOX content

The DOX content of the P-A-DOX and P-DOX conjugates was determined by an acidic hydrolysis approach. The P-A-DOX and P-DOX conjugates were separately dissolved in 1 mL of 1N hydrochloric acid solution at a final concentration of 2 mg/mL. The solution was incubated at 37°C for 1 h and the hydrolytic product, doxorubicinone (Figure 14), was analysed by high-performance liquid chromatography (Shimadzu Prominence HPLC System, Shimadzu corporation, Japan) using Halo C8 column (4.6 x 50 mm, 2.7 μm particle size; Advanced Materials Technology Inc., USA). The mobile phase was constituted of eluents A (acetonitrile) and B (20 mM sodium dihydrogen phosphate pH 2.0) as organic and aqueous phases, respectively. The elution program was as follows: initial 0–0.5 min, isocratic elution A–B (80:20, v/v); 0.5–3.5 min, linear change to A–B (45:55, v/v); 3.5–5.5 min, isocratic elution A–B

(45:55, v/v); 5.5–6 min, linear change to A–B (80:20, v/v); 6–13 min, isocratic elution A–B (80:20, v/v). The injection volume was 10 µL. The fluorescence detector (Shimadzu RF-20Axs, Shimadzu Corporation, Japan) was set with excitation and emission wavelengths at 480 and 590 nm, respectively, for doxorubicinone detection. All experiments were performed in triplicate. The doxorubicinone content of P-A-DOX and P-DOX conjugates was calculated against a doxorubicinone standard plot (0.0007-0.0071 mg/mL). The DOX content (%w/w) was calculated using the following equation:

Drug content (% w/w) = [(amount of doxorubicinone × DOX molecular weight/ doxorubicinone molecular weight)/conjugate weight] × 100   [2]
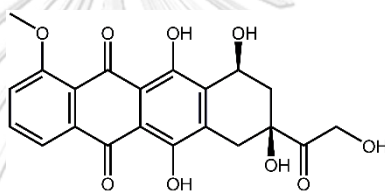
Figure 14 *The structure of Doxorubicinone*

3.3.5 *In vitro* drug release and stability

The *in vitro* drug release and stability of the P-A-DOX and P-DOX conjugates in acetate buffer at pH 4.0 and phosphate buffer at pH 7.4 were evaluated. The P-A-DOX and P-DOX conjugates were dissolved separately in 20% methanol at a concentration of 40 mg/mL as stock solutions. One hundred µL of the P-A-DOX or P-DOX stock solution were diluted with 400 µL buffer solution to obtain a final conjugate concentration of 8 mg/mL (~173 and 670 µM of DOX equivalent concentration for P-A-DOX and P-DOX, respectively). The solution was vortex-mixed and incubated at 37°C. Aliquots were withdrawn from the solution at specific time intervals (0, 2, 4, 6, 8, 12, 24, 48, 96, 168, 216 and 264 h) and subsequently added with 20% methanol at 1:20 dilution (~8.6 and 8.4 µM of DOX equivalent concentration for P-A-DOX and P-DOX, respectively). The diluted sample was subjected to HPLC analysis for the

remaining conjugate and the released DOX using the similar condition as described in section 3.3.4. The typical chromatograms of DOX, doxorubicinone, P-DOX and P-A-DOX were characterized by retention times of 2.8, 5.6, 6.7 and 6.6 min, respectively. The DOX concentration was calculated against the DOX standard curve (0.0001-0.0075 mg/mL). The concentration of each conjugate or DOX was normalized against the original concentration of the corresponding conjugate or DOX at time = 0 h. All experiments were performed in triplicate. The drug release profile was characterized by the percentage of DOX release against the incubation time. The stability profile of the P-A-DOX and P-DOX conjugates was characterized by the remaining concentration of conjugates against the incubation time, with the stability kinetic parameters including kinetic constant (k_{obs}) and half-life ($t_{1/2}$) being calculated using the pseudo-first order kinetic model. The stability profile of DOX was similarly assessed with reference to the incubation intervals of 0, 24, 48, 96, 168, 216 and 264 h.

3.3.6 Cytotoxicity

Two human breast cancer cell lines (MDA-MB-231; ATCC No. HTB-26 and MCF-7; ATCC No. HTB-22) and the human breast normal epithelial cell line (MCF-10A; ATCC No. CRL-10317) were obtained from American Type Culture Collection (ATTC), USA. The MDA-MB-231 and MCF-7 cells were grown in complete medium, comprising of Dulbecco's modified Eagle's Medium (DMEM; Invitrogen, USA) supplemented with 10% (v/v) heat-inactivated fetal bovine serum (FBS; Merck-Millipore, USA) and 1% (v/v) 100 U/ mL penicillin and 100 µg/mL streptomycin (Invitrogen, USA), while the MCF-10A cells were cultured in Dulbecco's modified Eagle's Medium/Ham's F12 Medium ((Invitrogen, USA) supplemented with 5% horse serum, 20 ng/mL epidermal growth factor, 0.01

mg/mL insulin, 500 ng/mL hydrocortisone (Lonza, Basel, Switzerland) and 1% (v/v) 100 U/mL penicillin and 100 µg/mL streptomycin.

3.3.6.1. *3-(4,5-dimethylthiazol-2-yl)-2,5-diphenyltetrazolium bromide (MTT) assay*

The cytotoxicity of P-A-DOX, mPEG-S-acrylic acid, P-DOX or DOX was evaluated by *in vitro* colorimetric MTT assay. The MDA-MB-231 cells were cultured in 96 well plate with a density of 15,000 cells/well, whereas the MCF-7 and MCF-10A cells were cultured in 96-well plates with a density of 30,000 cells/well. The plates were incubated at 37°C with 5% carbon dioxide/95% air for 24 h. The cells were then washed with serum-free medium and re-incubated with P-A-DOX, mPEG-S-acrylic acid, P-DOX or DOX that were previously diluted in serum-free medium at the final concentrations of 0.001, 0.01, 0.1, 0.5 and 1 µM DOX equivalent. Dimethyl sulfoxide (DMSO) in serum-free medium with a final concentration of 0.5% (v/v) was used as a control. Following incubation for 72 h, the cells were washed with phosphate buffer saline pH 7.2. Then, the cells were added with the MTT solution (0.5 mg/ml in phosphate buffer saline pH 7.2) and further incubated for 4 h. After incubation, the cells were washed with phosphate buffer saline and DMSO was then added to dissolve the formazan crystals. The optical density at 540 nm was recorded using a microplate reader (CLARIOstar, BMG Labtech, Germany). The experiments were performed in four replicates and the results were presented as % cell viability against the control. The selectivity index of P-A-DOX, P-DOX and DOX for cancer cells was determined using the equation [1].

3.3.7 Molecular docking

Molecular docking was conducted to assess the affinity of specific cancer enzymes for the P-DOX and P-A-DOX conjugates. Several cathepsins found in breast cancer cells including cathepsin B, D and L (PDB code 1HUC, 1LYB and 3HHA, respectively) were adopted in molecular docking using AutoDock version 4.2.6 running under AutoDockTools version 1.5.6 Sep_17_14 (The Scripps Research Institute, USA). The conjugate with five ethylene glycol units was used in the docking study in order to meet the molecular torsion limit of AutoDOCK program. All bonds of the conjugate were set as rotatable excepting rings and amide bonds, and the enzyme was kept rigid. Docking was carried out using Lamarckian genetic algorithm (LGA) with a number of individuals in population of 150, a maximum number of energy evaluations of 2500000, a maximum number of generations of 27000, a rate of gene mutation of 0.02, a rate of crossover of 0.8, a number of top individuals to survive to next generation of 1, a genetic algorithm's selection window of 10, a maximum number of local search iterations of 300 and a grid point spacing of 0.375 Å. All binding conformations were depicted in UCSF Chimera version 1.14 (build 42094).

3.3.8 Statistical analysis

Statistical analysis was performed using IBM SPSS Statistics software version 22. One-way ANOVA with the Scheffe test was used to assess the statistical significance. All data are presented as mean ± SD, with p values of <0.01 indicating statistical significance.

CHAPTER 4

RESULTS

4.1. Experimental results of DOX analogues

4.1.1 Synthesis of the *beta*-thiopropanoic acid substituents

Four *beta*-thiopropanoic acid substituents were successfully synthesized by Thiol Michael addition reaction to arrange the sulfur atom at two carbon atoms away from the carbonyl carbon of the acid (Figure 9). All ^{1}H NMR and ^{13}C NMR spectra are shown in Appendix A. In this synthesis, ethyl thioglycolate was used because of its fast kinetic reactions and complete thiol conversion (Chan et al. 2010). The resulting reaction was catalysed by DMPP yielding a phosphine-enolate zwitter ion (Chan et al. 2010). In this case, DMPP reacted with an alkene of the carboxylic acid compound generating a phosphine-enolate zwitter ion that further abstracted a proton from the thiol group of ethyl thioglycolate. These reactions were an initiation step. The propagation step began at the deprotonated thiol or thiolate anion of ethyl thioglycolate that continued to attack the unsaturated alkene of the carboxylic acid compound producing an enolate anion. Finally, the enolate anion abstracted a proton from ethyl thioglycolate in the reaction to the alpha-carbon position and ended up as thioether compound (Figure 15). Remarkably, the thioether compound generated from the enolate anion can be considered as enantiomers if the alkenyl carboxylic acid compound has a chiral carbon atom resulted from the different configuration of the abstracted proton at the alpha-carbon position. This reveals that the compounds 1b, 1c and 1d gave enantiomer products as 2b, 2c and 2d, respectively. The enantiomers were difficult to separate so we decided to use them as racemates for the next reaction.
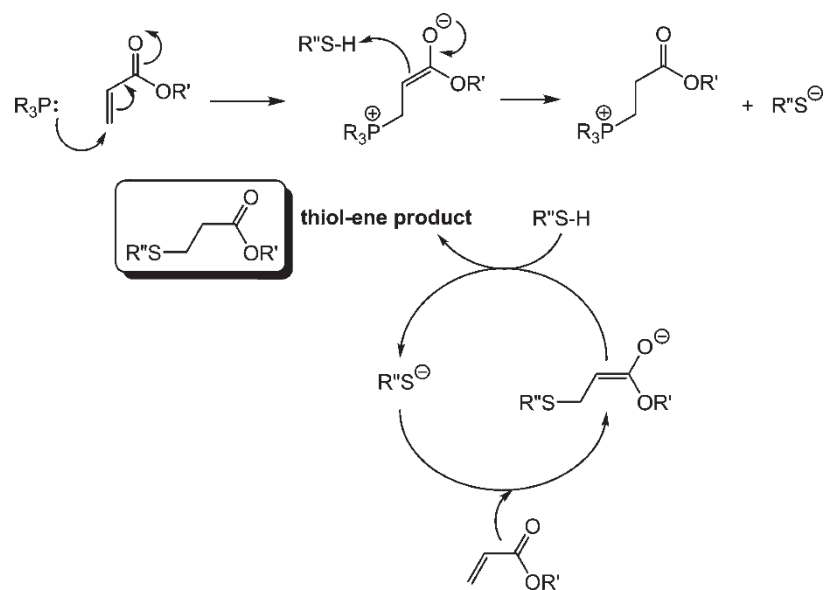
Figure 15 *Proposed reaction mechanism via nucleophilic Initiation for the phosphine-mediated Thiol-Michael reaction with an acrylic substrate (Chan et al. 2010).*

4.1.1.1.   3-((2-ethoxy-2-oxoethyl)thio)propanoic acid (2a)

The final product was obtained as colourless liquid with 74% yield (70.9 mg). ^{1}H NMR (400 MHz, CDCl$_3$) (Appendix A; Figure 37) was assigned as follows: δ 8.97 (s, 1H), 4.15 (q, *J* = 7.1 Hz, 2H), 3.20 (s, 2H), 2.86 (t, *J* = 7.1 Hz, 2H), 2.66 (t, *J* = 7.2 Hz, 2H), 1.24 (t, *J* = 7.1 Hz, 3H). ^{13}C NMR (101 MHz, CDCl$_3$) (Appendix A; Figure 37) was assigned as follows: δ 177.32 (d, *J* = 1.9 Hz), 170.47, 61.55, 34.06, 33.66, 27.14, 14.08. HRMS (ESI-TOF) (Appendix A; Figure 49): m/z 215.0363. Calculated for C$_7$H$_{12}$O$_4$SNa: 215.0349 [M+Na]$^+$.

4.1.1.2.   3-((2-ethoxy-2-oxoethyl)thio)-2-methylpropanoic acid (2b)

The final product was obtained as colourless liquid with 48% yield (49.4 mg). ^{1}H NMR (400 MHz, CDCl$_3$) (Appendix A; Figure 38) was assigned as follows: δ 9.29 (s, 2H), 4.15 (q, *J* = 7.1 Hz, 2H), 3.20 (s, 2H), 2.92 (t, *J* = 6.4 Hz, 1H), 2.77 − 2.65 (m, 2H), 1.27 − 1.22 (m, 6H). ^{13}C NMR (101 MHz, CDCl$_3$) (Appendix A; Figure 38) was assigned as follows: δ 180.68,

170.43, 61.49, 39.62, 35.35, 34.00, 16.65, 14.09. HRMS (ESI-TOF) (Appendix A; Figure 50): m/z 229.0524. Calculated for $C_8H_{14}O_4SNa$: 229.0505 $[M+Na]^+$.

4.1.1.3.   3-((2-ethoxy-2-oxoethyl)thio)-2-phenylpropanoic acid (2c)

The final product was obtained as colourless liquid with 73% yield (97.2 mg). ^1H NMR (400 MHz, CDCl$_3$) (Appendix A; Figure 39) was assigned as follows: δ 10.04 (s, 1H), 7.37 – 7.25 (m, 5H), 4.17 (q, *J* = 7.1 Hz, 2H), 3.89 (dd, *J* = 9.2, 6.3 Hz, 1H), 3.29 (dd, *J* = 13.5, 9.2 Hz, 1H), 3.19 (s, 2H), 3.00 (dd, *J* = 13.5, 6.2 Hz, 1H), 1.25 (t, *J* = 7.1 Hz, 3H). ^{13}C NMR (101 MHz, CDCl$_3$) (Appendix A; Figure 39) was assigned as follows: δ 178.23, 170.41, 136.86, 128.92, 128.10, 127.94, 61.56, 51.64, 35.06, 33.95, 14.12. HRMS (ESI-TOF) (Appendix A; Figure 51): m/z 291.0676. Calculated for $C_{13}H_{16}O_4SNa$: 291.0662 $[M+Na]^+$.

4.1.1.4.   2-(((2-ethoxy-2-oxoethyl)thio)methyl)-3,3,3-trifluoropropanoic acid (2d)

The final product was obtained as colourless liquid with 53% yield (204.9 mg). ^1H NMR (400 MHz, CDCl$_3$) (Appendix A; Figure 40) was assigned as follows: δ 9.91 (s, 2H), 4.20 (q, *J* = 7.1 Hz, 2H), 3.61 – 3.47 (m, 1H), 3.27 (dd, *J* = 15.0 Hz, 2H), 3.15 – 3.04 (m, 2H), 1.28 (t, *J* = 7.1 Hz, 3H). ^{13}C NMR (101 MHz, CDCl$_3$) (Appendix A; Figure 40) was assigned as follows: δ 170.75, 170.28, 128.34 – 118.57 (m), 61.95, 50.65 (q, *J* = 27.7 Hz), 33.90, 28.04 (q, *J* = 2.6 Hz), 13.98. HRMS (ESI-TOF) (Appendix A; Figure 52): m/z 283.0239. Calculated for $C_8H_{11}O_4F_3SNa$: 283.0222 $[M+Na]^+$.

4.1.2 Synthesis of the DOX analogues

According to the second reaction (Figure 10), 4 DOX analogues were expected from the syntheses. However, 7 analogues were generated, of which the extra analogues were derived from compound 2b, 2c and 2d. The resulting

products were further separated using preparative thin layer chromatography to yield 3b-1, 3b-2, 3c-1, 3c-2, 3d-1 and 3d-2, which were confirmed as diastereomers by their ^{1}H NMR, ^{13}C NMR spectra (Appendix A; Figure 42-47) and NOE difference spectra (Appendix A; Figure 48). The stereoisomer configuration of all diastereomers are shown in Table 1. The key reason for the occurrence of these diastereomeric products is that their reactions were conducted using an enantiomerically pure DOX (only one configuration produced from a biosynthesis by *Streptomyces peucetius* (Lomovskaya et al. 1999)), while the *beta*-thiopropanoic acid substituents (2b, 2c and 2d) were the racemates. There was no stereoisomers for the DOX analogue 3a since there was only one configuration available for 2a. After the reaction, the product resulted into two different stereoisomers that are not mirror images of each other with the yield ratio of 1:1, hence are diastereomers. These diastereomers can be separated by a partition chromatography technique without a chiral separation ability.

Table 1 *Stereoisomer configuration, NOE protons and calculated distance between 6″ proton and NOE proton (Chem3D) of all diastereomers.*

Compound	Absolute configuration (R group)	Correlated protons with 6″ proton	Distance (Chem3D) (Å)	NOE signal
3b-1	R	2′	7.274	No
		2′-CH$_3$	4.690, 5.959, 6.452	No
		4″	3.952, 4.671	Yes
		2″	7.108, 7.826	No
3b-2	S	2′	5.979	Yes
		2′-CH$_3$	3.023, 4.381, 4.668	Yes
		4″	4.443, 5.600	Yes
		2″	5.835, 6.968	Yes
3c-1	S	9	5.946	Yes
		2′-CH$_3$	2.922, 4.325, 4.528	Yes
3c-2	R	9	7.901	No
		2′-CH$_3$	4.323, 5.309, 6.104	No
3d-1	S	9	5.916	Yes
3d-2	R	9	6.440	No

The success of the syntheses of DOX analogues were confirmed by the change of chemical shift of methine protons at 4′ position in ^{1}H-NMR spectra that was changed to downfield at around 4.0 ppm compared to that of DOX at 3.3 ppm (Appendix A; Figure 36). Furthermore, the methylene protons of the linker at 2″, 3″, and 4″ positions appeared in their spectra. The NOE difference spectra (Appendix A; Figure 48) indicated the NOE between a proton at 6″ positions and the neighbor protons which it appeared positive when they were in the same configuration. The stereoisomer configurations of all diastereomers were considered along with their three-dimensional structures, which they were

optimized using MM2 force field model to acquire the most stable conformation. The distance between the NOE proton and the 6″ proton were measured and compared to their NOE difference spectra. The results were shown in Table 1.

4.1.2.1. DOX-analogue 3a

The final *product* was obtained as red powder with 62% yield (152.4 mg). ^{1}H NMR (400 MHz, DMSO-d_6) (Appendix A; Figure 41) was assigned as follows: δ 13.90 (s, 1H), 13.14 (s, 1H), 7.79 (t, J = 7.9 Hz, 1H), 7.75 (s, 1H), 7.63 (d, J = 8.2 Hz, 1H), 7.52 (dd, J = 8.4, 1.6 Hz, 1H), 5.37 (s, 1H), 5.18 (d, J = 4.0 Hz, 1H), 4.84 (dd, J = 5.4, 3.3 Hz, 1H), 4.74 (s, 1H), 4.56 (s, 2H), 4.15 (q, J = 6.5 Hz, 1H), 4.02 (q, J = 7.1 Hz, 2H), 3.98 − 3.95 (m, 1H), 3.91 (s, 3H), 3.40 − 3.33 (m, 1H), 3.26 (s, 2H), 2.84 (dd, J = 18.1 Hz, 2H), 2.66 (t, J = 7.4 Hz, 2H), 2.41 − 2.24 (m, 2H), 2.18 (d, J = 13.5 Hz, 1H), 2.04 (dd, J = 14.4, 5.8 Hz, 1H), 1.82 (td, J = 12.8, 4.0 Hz, 1H), 1.41 (dd, J = 12.3, 4.8 Hz, 1H), 1.17 − 1.08 (m, 6H). ^{13}C NMR (101 MHz, DMSO-d_6) (Appendix A; Figure 41) was assigned as follows: δ 214.37, 186.69, 186.57, 170.53, 169.98, 161.10, 156.51, 154.91, 136.52, 135.78, 134.85, 134.37, 120.17, 119.99, 119.29, 111.02, 110.89, 100.92, 75.33, 70.33, 68.50, 67.10, 64.19, 61.05, 56.92, 45.45, 36.85, 35.42, 33.12, 32.41, 30.17, 28.17, 17.46, 14.43. HRMS (ESI-TOF) (Appendix A; Figure 53): m/z 740.1983. Calculated for $C_{34}H_{39}O_{14}NSNa$: 740.1983 [M+Na]$^+$.

4.1.2.2. DOX-analogue 3b-1

The final product was obtained as red powder with 33.7% yield (49.3 mg). ^{1}H NMR (400 MHz, DMSO-d_6) (Appendix A; Figure 42) was assigned as follows: δ 13.20 (s, 1H), 7.84 (d, J = 6.9 Hz, 2H), 7.67 − 7.51 (m, 2H), 5.39 (s, 1H), 5.21 (d, J = 3.6 Hz, 1H), 4.89 (s, 1H), 4.83 (t, J = 5.9 Hz,

1H), 4.67 (d, J = 6.0 Hz, 1H), 4.57 (d, J = 5.9 Hz, 2H), 4.16 (q, J = 6.6 Hz, 1H), 4.07 (q, J = 7.1 Hz, 2H), 3.99 (dd, J = 8.0, 3.2 Hz, 1H), 3.94 (s, 3H), 3.38 (dd, J = 6.4, 2.6 Hz, 1H), 3.29 (dd, J = 15.4, 3.3 Hz, 2H), 2.91 (dd, J = 60.1, 23.7 Hz, 2H), 2.71 (dd, J = 12.3, 7.3 Hz, 1H), 2.56 – 2.51 (m, 1H), 2.45 (dd, J = 12.4, 6.6 Hz, 1H), 2.19 (d, J = 13.6 Hz, 1H), 2.08 (dd, J = 14.1, 5.4 Hz, 1H), 1.83 (td, J = 12.9, 3.8 Hz, 1H), 1.42 (dd, J = 12.4, 4.5 Hz, 1H), 1.19 – 1.11 (m, 6H), 0.95 (d, J = 6.6 Hz, 3H). ^{13}C NMR (101 MHz, DMSO-d_6) (Appendix A; Figure 42) was assigned as follows: δ 214.43, 186.50, 186.35, 173.78, 170.53, 161.00, 156.47, 154.87, 136.42, 135.66, 134.67, 134.26, 119.99, 119.86, 119.19, 110.88, 110.76, 100.99, 75.31, 70.28, 68.78, 67.19, 64.24, 61.08, 56.84, 45.30, 39.65, 36.71, 35.88, 33.50, 32.34, 30.18, 17.92, 17.45, 14.46. HRMS (ESI-TOF) (Appendix A; Figure 54): m/z 754.2157. Calculated for $C_{35}H_{41}O_{14}NSNa$: 754.2140 [M+Na]$^+$.

4.1.2.3. *DOX-analogue 3b-2*

The final product was obtained as red powder with 30% yield (44.6 mg). ^{1}H NMR (400 MHz, DMSO-d_6) (Appendix A; Figure 43) was assigned as follows: δ 13.98 (d, J = 2.1 Hz, 1H), 13.21 (d, J = 2.2 Hz, 1H), 7.89 – 7.81 (m, 2H), 7.59 (d, J = 8.0 Hz, 2H), 5.40 (d, J = 1.4 Hz, 1H), 5.21 (d, J = 3.6 Hz, 1H), 4.90 (t, J = 4.6 Hz, 1H), 4.83 (t, J = 5.9 Hz, 1H), 4.75 (d, J = 6.1 Hz, 1H), 4.57 (d, J = 5.2 Hz, 2H), 4.15 (q, J = 6.5 Hz, 1H), 4.03 (q, J = 7.1 Hz, 2H), 3.99 – 3.96 (m, 1H), 3.95 (s, 3H), 3.40 – 3.36 (m, 1H), 3.28 – 3.21 (m, 2H), 2.93 (dd, J = 55.9, 18.7 Hz, 2H), 2.62 (dd, J = 12.2, 8.1 Hz, 1H), 2.55 (dd, J = 13.4, 7.0 Hz, 1H), 2.43 (dd, J = 12.2, 5.6 Hz, 1H), 2.19 (dd, J = 14.7, 2.4 Hz, 1H), 2.09 (dd, J = 14.3, 5.7 Hz, 1H), 1.84 (td, J = 12.9, 3.9 Hz, 1H), 1.42 (dd, J = 12.6, 4.6 Hz, 1H), 1.15 – 1.09 (m, 6H), 0.99 (d, J = 6.6 Hz, 3H). ^{13}C NMR (101 MHz, DMSO-d_6) (Appendix A; Figure 43) was assigned as

follows: δ 214.40, 186.53, 186.40, 173.71, 170.48, 161.02, 156.47, 154.90, 136.45, 135.65, 134.70, 134.30, 120.02, 119.87, 119.20, 110.92, 110.80, 100.98, 75.32, 70.29, 68.51, 67.15, 64.22, 61.00, 56.86, 45.31, 39.44, 36.74, 35.89, 33.23, 32.36, 30.24, 17.95, 17.45, 14.40. HRMS (ESI-TOF) (Appendix A; Figure 55): m/z 754.2145. Calculated for $C_{35}H_{41}O_{14}NSNa$: 754.2140 $[M+Na]^{+}$.

4.1.2.4.   DOX-analogue 3c-1

The final product was obtained as red powder with 23% yield (54.7 mg). ^{1}H NMR (400 MHz, DMSO-d_{6}) (Appendix A; Figure 44) was assigned as follows: δ 14.00 (d, J = 1.3 Hz, 1H), 13.23 (d, J = 1.4 Hz, 1H), 7.91 − 7.82 (m, 3H), 7.63 − 7.58 (m, 1H), 7.34 − 7.23 (m, 4H), 7.23 − 7.18 (m, 1H), 5.39 (s, 1H), 5.23 (d, J = 3.7 Hz, 1H), 4.91 (t, J = 4.4 Hz, 1H), 4.83 (t, J = 6.0 Hz, 1H), 4.74 (d, J = 6.2 Hz, 1H), 4.57 (d, J = 5.3 Hz, 2H), 4.12 (q, J = 6.6 Hz, 1H), 4.03 (q, J = 7.1 Hz, 3H), 3.97 (s, 3H), 3.88 (dd, J = 9.7, 5.5 Hz, 1H), 3.31 (dd, J = 43.9, 14.2 Hz, 2H), 3.23 (dd, J = 6.8, 2.7 Hz, 1H), 3.03 (dd, J = 13.1, 9.8 Hz, 1H), 2.91 (dd, J = 56.2, 19.7 Hz, 2H), 2.74 (dd, J = 13.0, 5.5 Hz, 1H), 2.19 (d, J = 14.4 Hz, 1H), 2.10 (dd, J = 14.4, 5.7 Hz, 1H), 1.86 (td, J = 12.9, 3.9 Hz, 1H), 1.50 (dd, J = 12.5, 4.6 Hz, 1H), 1.14 − 1.06 (m, 6H). ^{13}C NMR (126 MHz, DMSO-d_{6}) (Appendix A; Figure 44) was assigned as follows: δ 213.82, 186.33, 186.25, 170.44, 169.90, 160.69, 156.04, 154.49, 139.78, 136.09, 135.35, 134.49, 133.95, 128.19, 127.58, 126.81, 119.83, 119.59, 118.87, 110.68, 110.53, 100.40, 74.93, 69.86, 68.18, 66.81, 63.69, 60.56, 56.50, 49.91, 44.90, 36.48, 34.86, 32.47, 32.02, 30.04, 16.87, 13.94. HRMS (ESI-TOF) (Appendix A; Figure 56): m/z 816.2270. Calculated for $C_{40}H_{43}O_{14}NSNa$: 816.2296 $[M+Na]^{+}$.

4.1.2.5.   DOX-analogue 3c-2

The final product was obtained as red powder with 25% yield (58.3 mg). ^{1}H NMR (400 MHz, DMSO-d_6) (Appendix A; Figure 45) was assigned as follows: δ 13.90 (d, *J* = 1.9 Hz, 1H), 13.20 (d, *J* = 2.5 Hz, 1H), 7.89 – 7.79 (m, 3H), 7.57 (d, *J* = 6.4 Hz, 1H), 7.28 – 7.16 (m, 4H), 7.17 – 7.08 (m, 1H), 5.37 (s, 1H), 5.16 (d, *J* = 3.6 Hz, 1H), 4.86 (t, *J* = 4.2 Hz, 1H), 4.82 (t, *J* = 5.6 Hz, 1H), 4.73 (d, *J* = 6.1 Hz, 1H), 4.56 (d, *J* = 4.7 Hz, 2H), 4.16 (q, *J* = 6.5 Hz, 1H), 4.06 (q, *J* = 7.1 Hz, 2H), 3.99 – 3.95 (m, 1H), 3.93 (s, 3H), 3.81 (dd, *J* = 8.9, 6.3 Hz, 1H), 3.45 – 3.40 (m, 1H), 3.30 (dd, *J* = 14.8, 9.6 Hz, 2H), 3.09 (dd, *J* = 13.0, 8.9 Hz, 1H), 2.91 (dd, *J* = 56.4, 19.9 Hz, 2H), 2.80 (dd, *J* = 13.0, 6.3 Hz, 1H), 2.17 (d, *J* = 16.0 Hz, 1H), 2.07 (dd, *J* = 14.4, 5.6 Hz, 1H), 1.75 (td, *J* = 12.9, 3.9 Hz, 1H), 1.25 (dd, *J* = 12.7, 4.4 Hz, 1H), 1.14 (q, *J* = 6.6, 6.1 Hz, 6H). ^{13}C NMR (126 MHz, DMSO-d_6) (Appendix A; Figure 45) was assigned as follows: δ 213.84, 186.30, 186.15, 170.55, 169.96, 160.62, 155.94, 154.43, 139.64, 136.01, 135.26, 134.43, 133.84, 128.15, 127.46, 126.78, 119.79, 119.52, 118.81, 110.64, 110.48, 100.29, 74.89, 69.77, 68.34, 66.73, 63.71, 60.62, 56.44, 50.24, 45.07, 36.41, 34.54, 32.82, 31.96, 29.53, 16.95, 13.99. HRMS (ESI-TOF) (Appendix A; Figure 57): m/z 816.2275. Calculated for $C_{40}H_{43}O_{14}NSNa$: 816.2296 [M+Na]$^+$.

4.1.2.6.   DOX-analogue 3d-1

The final product was obtained as red powder with 17% yield (93.7 mg). ^{1}H NMR (500 MHz, DMSO-d_6) (Appendix A; Figure 46) was assigned as follows: δ 13.93 (d, *J* = 2.1 Hz, 1H), 13.17 (d, *J* = 2.1 Hz, 1H), 8.27 (d, *J* = 8.5 Hz, 1H), 7.81 (dd, *J* = 9.9, 7.7 Hz, 2H), 7.54 (dt, *J* = 8.3, 2.0 Hz, 1H), 5.38 (s, 1H), 5.22 (d, *J* = 3.7 Hz, 1H), 4.87 (t, *J* = 4.2 Hz, 2H), 4.58 (s, 2H), 4.19 (q, *J* = 6.5 Hz, 1H), 4.08 (q, *J* = 7.0 Hz, 2H), 4.13 – 4.02 (m, 1H), 3.93 (s, 3H), 3.72 (tq, *J* = 8.4, 4.2, 3.3 Hz, 1H), 3.39 (d, *J* = 2.9 Hz, 1H), 3.38

(dd, *J* = 55.4, 24.9 Hz, 2H), 2.96 (d, *J* = 18.2 Hz, 1H), 2.91 – 2.83 (m, 2H), 2.83 (d, *J* = 17.7 Hz, 1H), 2.19 (d, *J* = 14.2 Hz, 1H), 2.07 (dd, *J* = 14.4, 5.6 Hz, 1H), 1.84 (td, *J* = 12.8, 3.9 Hz, 1H), 1.45 (dd, *J* = 12.3, 4.6 Hz, 1H), 1.16 (dt, *J* = 14.0, 7.0 Hz, 6H). ^{13}C NMR (126 MHz, DMSO-d_6) (Appendix A; Figure 46) was assigned as follows: δ 213.90, 186.32, 186.20, 169.61, 163.62, 160.67, 156.02, 154.46, 136.04, 135.30, 134.45, 133.90, 128.70 – 125.31 (m), 119.83, 119.56, 118.84, 110.66, 110.50, 100.23, 74.86, 69.85, 68.20, 66.70, 63.72, 60.79, 56.46, 48.35 (q, *J* = 25.5, 23.6 Hz), 45.38, 36.42, 32.41, 31.97, 29.68, 26.89, 16.90, 13.95. HRMS (ESI-TOF) (Appendix A; Figure 58): m/z 808.1844. Calculated for $C_{35}H_{38}O_{14}F_3NSNa$: 808.1857 $[M+Na]^+$.

4.1.2.7. DOX-analogue 3d-2

The final product was obtained as red powder with 18% yield (99.6 mg). ^{1}H NMR (500 MHz, DMSO-d_6) (Appendix A; Figure 47) was assigned as follows: δ 13.98 (s, 1H), 13.21 (s, 1H), 8.27 (d, *J* = 8.6 Hz, 1H), 7.88 – 7.82 (m, 2H), 7.59 (dd, *J* = 7.3, 2.4 Hz, 1H), 5.40 (s, 1H), 5.23 (d, *J* = 3.8 Hz, 1H), 4.90 (dd, *J* = 5.7, 3.4 Hz, 2H), 4.57 (s, 2H), 4.17 (q, *J* = 6.5 Hz, 1H), 4.13 – 3.98 (m, 1H), 4.04 (q, *J* = 7.1 Hz, 2H), 3.95 (s, 3H), 3.72 (q, *J* = 8.1 Hz, 1H), 3.37 (d, *J* = 2.5 Hz, 1H), 3.36 (dd, *J* = 65.8, 35.7 Hz, 2H), 2.97 (d, *J* = 18.1 Hz, 1H), 2.87 (d, *J* = 18.1 Hz, 1H), 2.84 (d, *J* = 7.9 Hz, 2H), 2.18 (dd, *J* = 16.6, 2.5 Hz, 1H), 2.10 (dd, *J* = 14.3, 5.7 Hz, 1H), 1.84 (td, *J* = 12.8, 3.9 Hz, 1H), 1.46 (dd, *J* = 12.5, 4.7 Hz, 1H), 1.12 (t, *J* = 7.2 Hz, 6H). ^{13}C NMR (126 MHz, DMSO-d_6) (Appendix A; Figure 47) was assigned as follows: δ 213.83, 186.42, 186.35, 169.53, 163.49, 160.72, 156.04, 154.50, 136.13, 135.38, 134.56, 134.02, 128.48 – 125.53 (m), 119.90, 119.63, 118.92, 110.72, 110.57, 100.19, 74.90, 69.88, 68.16, 66.74, 63.68, 60.72, 56.51, 48.06 (q, *J* = 25.8, 25.4 Hz), 45.26, 36.53, 32.04, 29.80, 26.84, 16.88, 13.88. HRMS (ESI-

TOF) (Appendix A; Figure 59): m/z 808.1838. Calculated for $C_{35}H_{38}O_{14}F_3NSNa$: 808.1857 $[M+Na]^+$.

4.1.3 *In vitro* drug release and stability

There were no DOX released in pH 4.0, 5.5 and 7.4 medium at any incubation time. Conversely, doxorubicinone was present during the incubation as shown in the chromatogram of DOX analogues (Appendix B; Figure 62-68). This result suggested that DOX analogue and released DOX may be hydrolysed at its glycosidic bond. The unstable glycosidic bond of DOX can be degraded under thermal, mild acidic (pH5.5) and neutral conditions (pH 7.4) resulting to the release of doxorubicinone (Kaushik and Bansal 2015). The degradation may be occurred from the DOX analogue or the released DOX in the solution (Figure 16). This brings the difficulty to assess the pH-responsiveness of the DOX analogue. Therefore, the degradation profile was used to explain the pH-responsive behaviour.
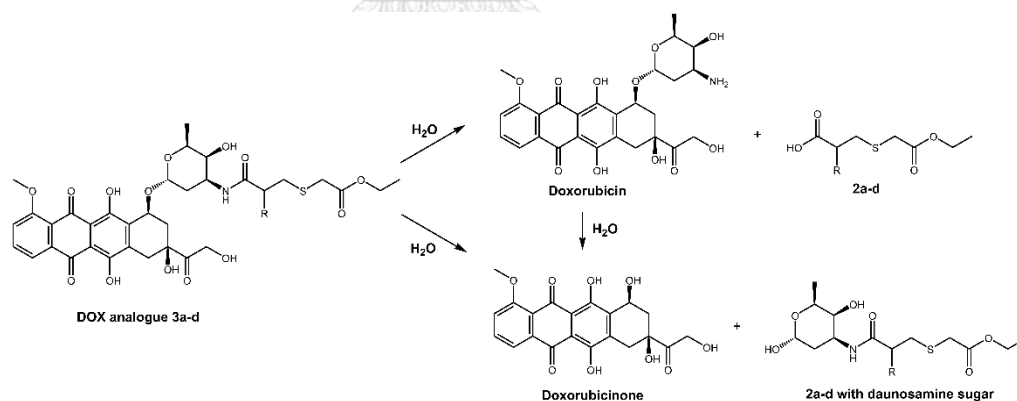
Figure 16 Proposed degradation mechanism of DOX analogues

The degradation of DOX analogues and DOX into doxorubicinone followed pseudo first-order kinetics ($r^2 > 0.9$; Figure 3). The kinetic constant (k_{obs}) and half-life ($t_{1/2}$) of all compounds were calculated and summarized in Table 2. The half-life ($t_{1/2}$) of DOX were significantly different (one-way ANOVA; $p < 0.01$, Appendix D) as compared to all DOX analogues in all pHs. This means

that all kinds of *beta*-thiopropanamide linkers except DOX analogue 3c-1 and 3c-2 can increase the stability of DOX in all pHs. The poor stability of DOX analogue 3c-1 and 3c-2 suggested that the substituted phenyl group may be an electron withdrawing group when coupled with an amide bond. This phenyl group may subsequently cause the electron deficiency to the carbonyl carbon of amide bond, and the DOX release occurred. In addition, the phenyl group may also cause the electron deficiency to the carbon at the *O*-glycosidic bond, which is also an acetal bond (Figure 17). The hydrolysis rate of an acetal bond is greatly reduced by the phenyl substituent (Liu and Thayumanavan 2017). At pH 4.0 and 5.5, the $t_{1/2}$ values of the DOX analogue 3d-1 showed significantly lower stability (one-way ANOVA; $p < 0.01$, Appendix D) as compared to other analogues. At 7.4, the low k_{obs} and high $t_{1/2}$ values of the DOX analogue 3b-2 showed significantly higher stability (one-way ANOVA; $p < 0.01$, Appendix D) as compared to other analogues. The DOX analogue 3d-1 exhibited the good pH-resonsiveness, however, it was degraded faster than the DOX analogue 3b-2 in physiological pH. In conclusion, the DOX analogue 3b-2 was an appropriate analogue for establishing the pH-responsive effect for DOX delivery because of its moderately good hydrolysis at pH 4.0 and its high stability at pH 7.4.
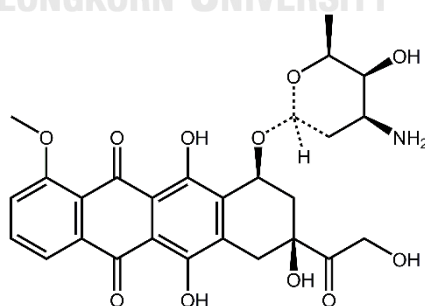
Figure 17 *The O-glycosidic bond connects between the doxorubicinone moiety and the daunosamine sugar of DOX. The dash bonds represent the acetal linkage.*

Table 2. *Pseudo-first order kinetic parameters for stability of DOX analogues in buffer pH 4, 5.5 and 7.4.*

	R^2			k_{obs}			$t_{1/2}$ (h)		
	pH 4	pH 5.5	pH 7.4	pH 4	pH 5.5	pH 7.4	pH 4	pH 5.5	pH 7.4
DOX	0.9681	0.9117	0.9988	0.0037	0.0084	0.0601	189	82	12
3a	0.9575	0.9540	0.9732	0.0022	0.0022	0.0307	313	315	23
3b-1	0.9649	0.9890	0.9975	0.0021	0.0029	0.0371	333	243	19
3b-2	0.9679	0.9289	0.9657	0.0029	0.0012	0.0220	239	558	32
3c-1	0.9595	0.9226	0.9689	0.2197	0.1959	0.2296	3	4	3
3c-2	0.9496	0.9034	0.9025	0.2691	0.2785	0.2472	3	2	3
3d-1	0.9472	0.9936	0.9964	0.0032	0.0035	0.0383	220	199	18
3d-2	0.9108	0.9806	0.9910	0.0020	0.0033	0.0325	343	213	21
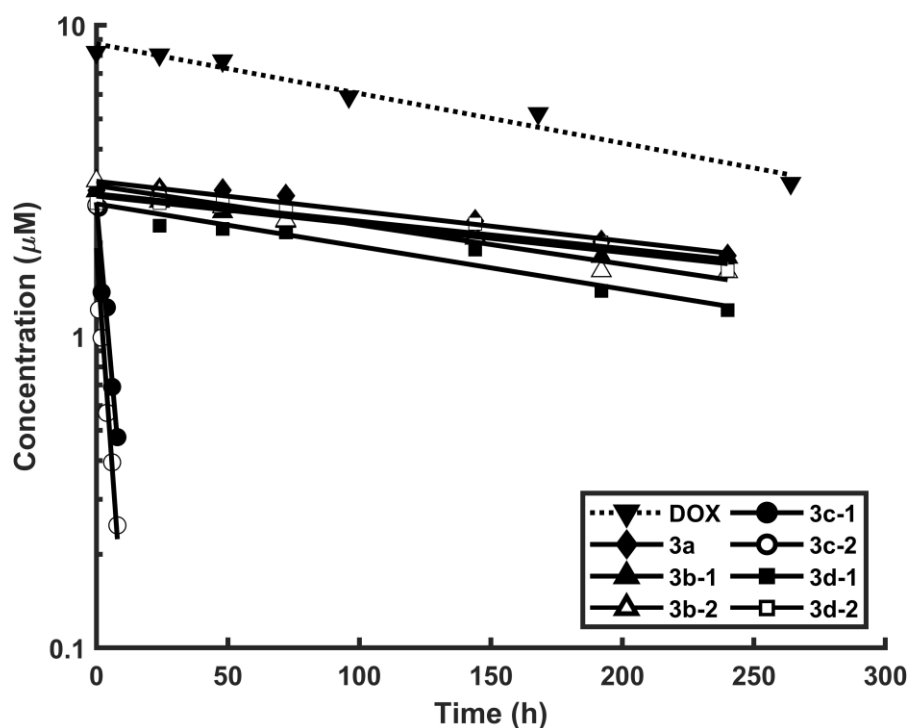
Figure 18 *Pseudo first order plots of stability profiles of DOX and seven DOX analogues at 37°C in acetate buffer pH 4.*
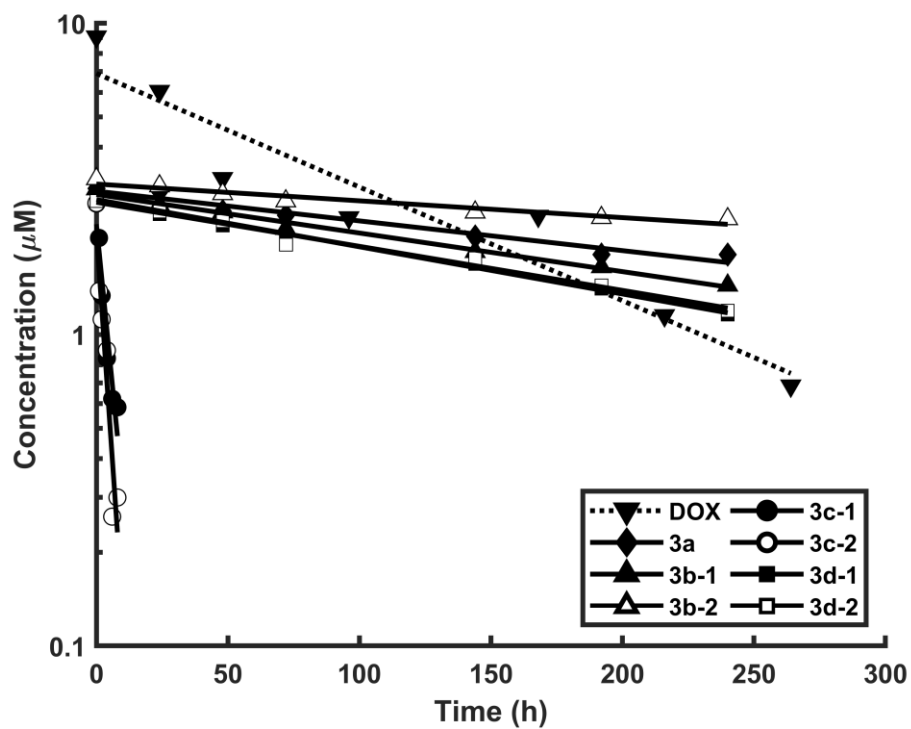
Figure 19 *Pseudo first order plots of stability profiles of DOX and seven DOX analogues at 37°C in phosphate buffer pH 5.5.*
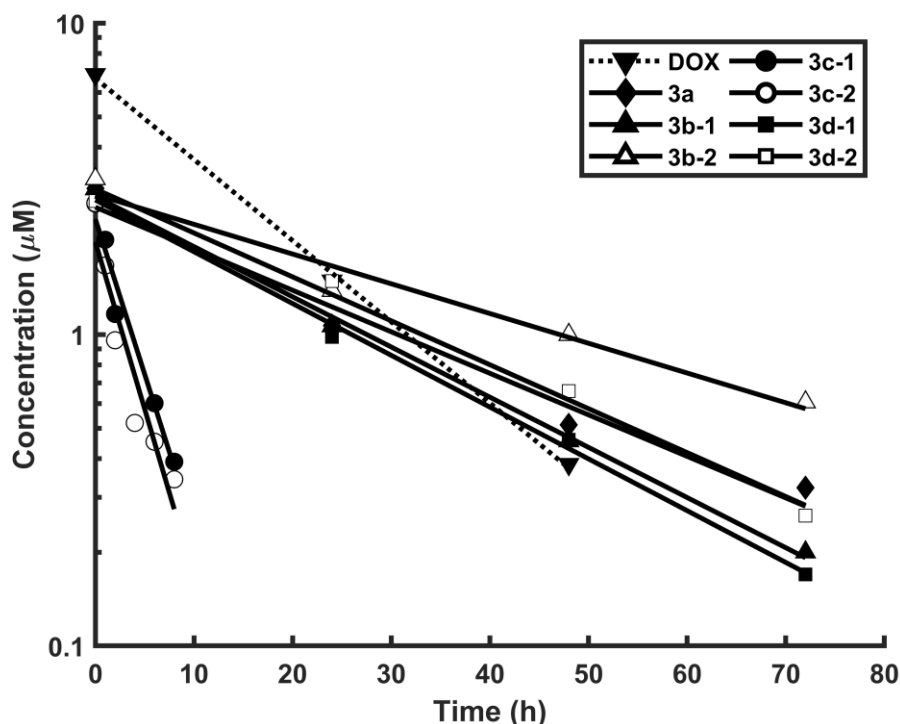
Figure 20 *Pseudo first order plots of stability profiles of DOX and seven DOX analogues at 37°C in phosphate buffer pH 7.4.*

4.1.4 Cell cytotoxicity and selectivity

The cytotoxic effects of DOX analogues and free DOX against MDA-MB-231 and MCF-7 breast cancer cells, as well as MCF-10A non-cancerous breast cell were evaluated. The DOX analogue 3a had similar cytotoxicity level to DOX against both breast cancer cell lines whereas other analogues were significantly less cytotoxic than DOX (Appendix D). In contrary, the DOX analogue 3a was significantly less cytotoxic than other DOX analogues and the DOX against MCF-10A non-cancerous breast cell (one-way ANOVA; $p < 0.01$, Appendix D).

Furthermore, we found out that the selectivity index of the DOX analogue 3a was higher than DOX with the DOX analogue 3a being the most selective against MDA-MB-231 and MCF7 (Table 3). The selectivity index should be greater than three as an indication of the potential suitability of compounds for use as a cancer therapeutic (Bézivin et al. 2003; Oliveira et al. 2015). On this

note, the DOX analogue 3a was deemed to be a potential anti-cancer model for further development.

The beta-thiopropanamide linker was responsible to introduce cancer selectivity to DOX. Compared to other linkers, it is the most accessible for the enzyme cleavage, which makes its enzyme-responsiveness in cancer cells. The amide bond in the DOX analogue 3a was readily cleaved by some overexpressed enzymes such as cathepsins B, an intracellular protease enzymes that are overexpressed in human breast cancer cells (Bengsch et al. 2014; Ruan et al. 2015; T. Sun et al. 2016). This enabled the DOX analogue 3a to exert a higher level of cytotoxicity in breast cancer cells. Apparently, the DOX analogue 3a had slower degradation kinetics at pH 4.0 compared to the DOX analogue 3b-2. The enzyme- instead of pH-responsiveness could aptly explained the cell selective behaviour of the DOX analogue 3a.
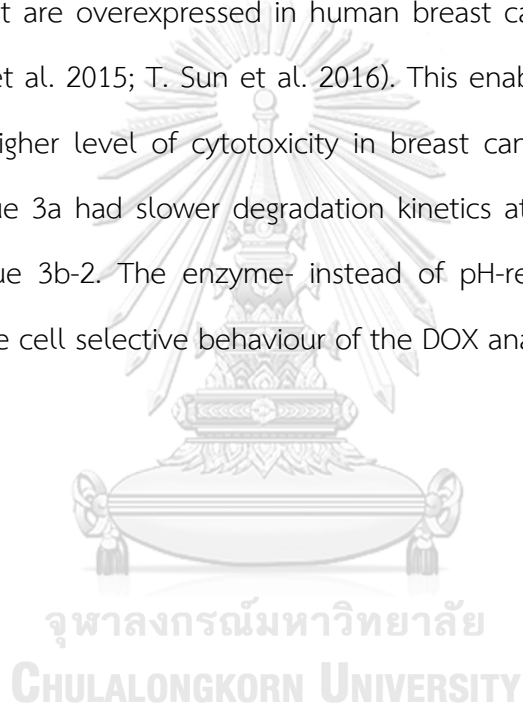
Table 3. Mean IC_{50} values for cytotoxicity of seven DOX analogues versus free DOX of different cancer cell lines. The selectivity indexes of conjugates were calculated as the IC_{50} ratio of MCF-10A/MDA-MB-231 and MCF-10A/MCF-7.

Treatment	$IC_{50} \pm SD$ (µM)			Selectivity Index	
	MDA-MB-231	MCF-7	MCF-10A	MCF-10A/ MDA-MB-231	MCF-10A/ MCF-7
DOX	0.066±0.015	0.254±0.036	0.409±0.017	6.24	1.61
3a	0.110±0.021	0.295±0.027	2.619±0.224	23.85	8.89
3b-1	>10	>10	>10	-	-
3b-2	4.904±0.730	>10	>10	-	-
3c-1	6.353±0.221	>10	>10	-	-
3c-2	3.010±0.184	8.042±0.332	>10	-	-
3d-1	8.298±0.627	>10	9.374±0.491	1.13	-
3d-2	3.404±0.268	>10	>10	-	-

จุฬาลงกรณ์มหาวิทยาลัย

CHULALONGKORN UNIVERSITY
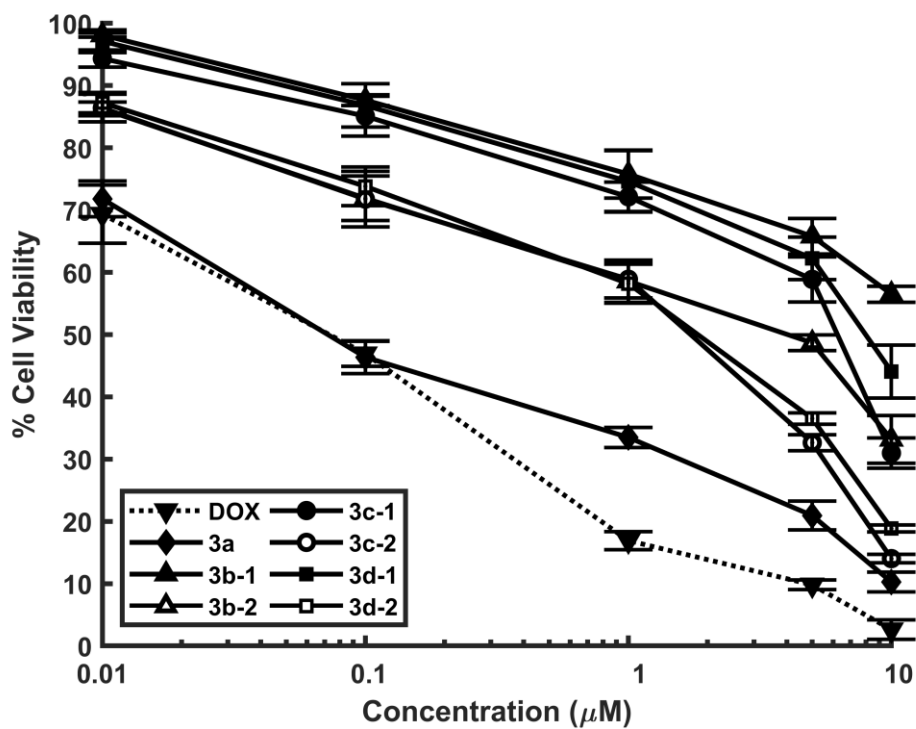
Figure 21 *Cytotoxicity of seven DOX analogues compared to free Dox for MDA-MB-231 breast cancer cells. All treatments were applied at various concentrations for 24 h, and cell viability was determined using MTT assay. The experiment was performed in four replicates, and data were plotted as the mean ± standard deviation.*
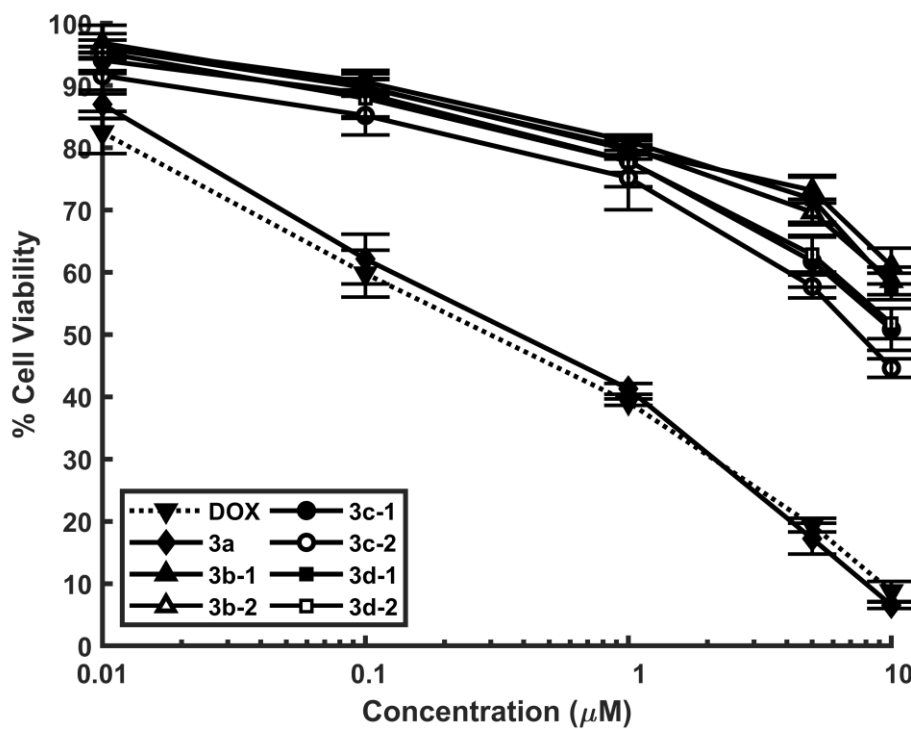
Figure 22 Cytotoxicity of seven DOX analogues compared to free Dox for MCF-7 breast cancer cells. All treatments were applied at various concentrations for 24 h, and cell viability was determined using MTT assay. The experiment was performed in four replicates, and data were plotted as the mean ± standard deviation.
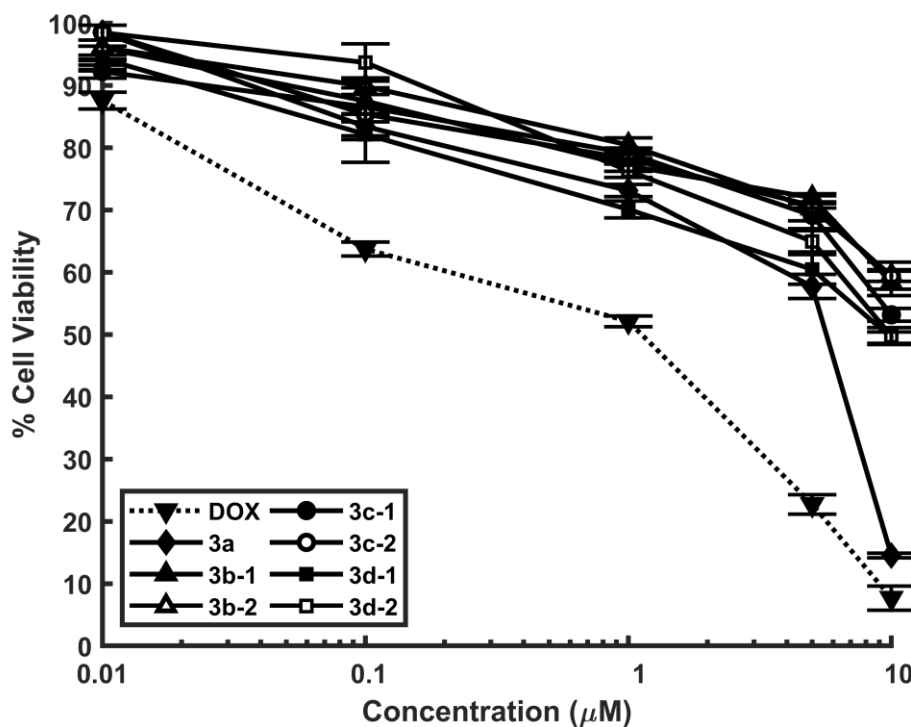
Figure 23 *Cytotoxicity of seven DOX analogues compared to free DOX for MCF-10A noncancerous breast cells. All treatments were applied at various concentrations for 24 h, and cell viability was determined using MTT assay. The experiment was performed in four replicates, and data were plotted as the mean ± standard deviation.*

4.1.5 Molecular docking

From the *in vitro* stability data, it suggested that the hydrolysis of all DOX analogues were not accelerated under an acidic condition of tumor microenvironment and lysosome of cancer cells. It is possible that the cleavage of these analogues is from the overexpressed enzyme of cancer cells since the DOX analogues 3a, which was the least steric analogue, was the most cytotoxic product compared to others. The molecular docking study between the DOX analogue 3a and the overexpressed enzymes in breast cancer cells, cathepsin B, D and L, was performed to propose this implication. Molecular docking study suggested that the DOX analogue 3a can bind to cathepsin L with the lowest

binding energy compared to cathepsins B and D (Table 4). The cathepsin L is most likely the responsible enzyme that cleaves the DOX analogue 3a in the MDA-MB-231 and MCF-7 cell lines. As shown in Figure 24-26, the distances between the carbonyl carbon of the DOX analogue 3a and the active residue of cathepsins were 4.0 Å (CYS25) for cathepsin L (Dana and Pathak 2020), 8.4 Å (CYS29) for cathepsin B (Ruan et al. 2015), 9.3 Å (ASP33) and 6.3 (ASP231) for cathepsin D (Minarowska et al. 2008). Moreover, the DOX analogue 3a can be docked to cathepsin L with the lowest binding energy. The DOX analogue 3a could be regarded to demonstrate a higher affinity for cathepsin which aptly explained their cytotoxicity and selectivity actions towards the breast cancer cells.

Table 4 *The molecular docking results of the 3a analogue and cathepsins.*

Cathepsins	PDB code	Binding energy (kcal/mol)
B	1HUC	-4.97
D	1LYB	-5.20
L	3HHA	-7.90
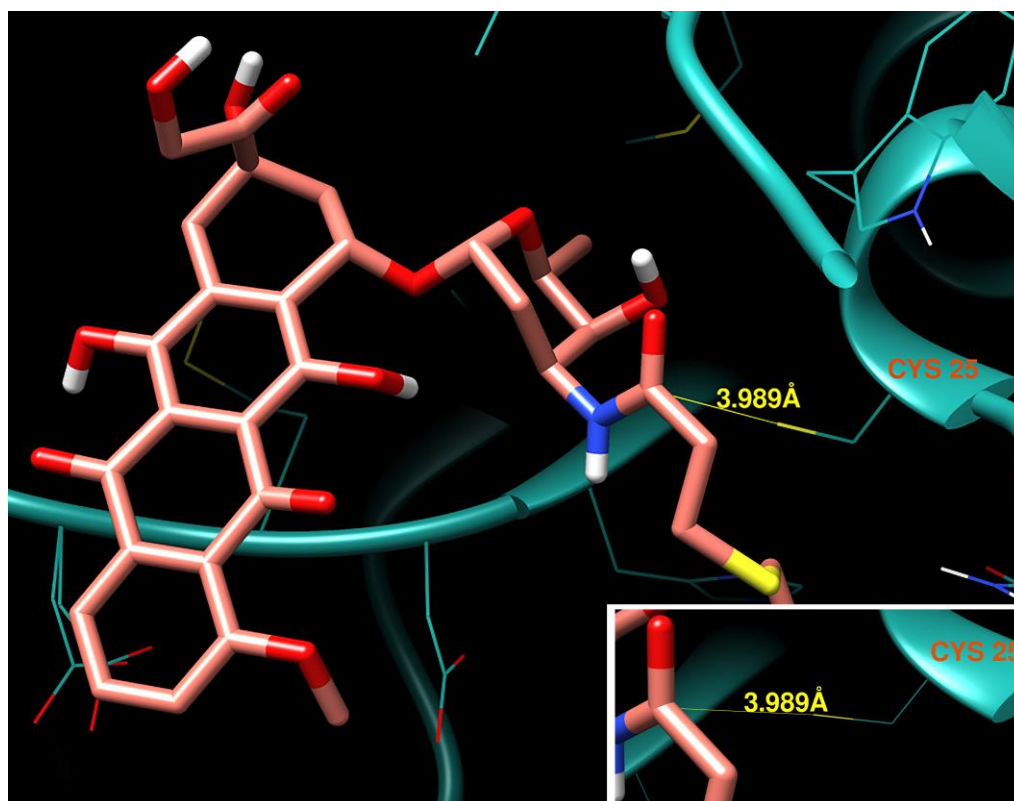
Figure 24 *Docked structures of 3a analogue and cathepsin L.*
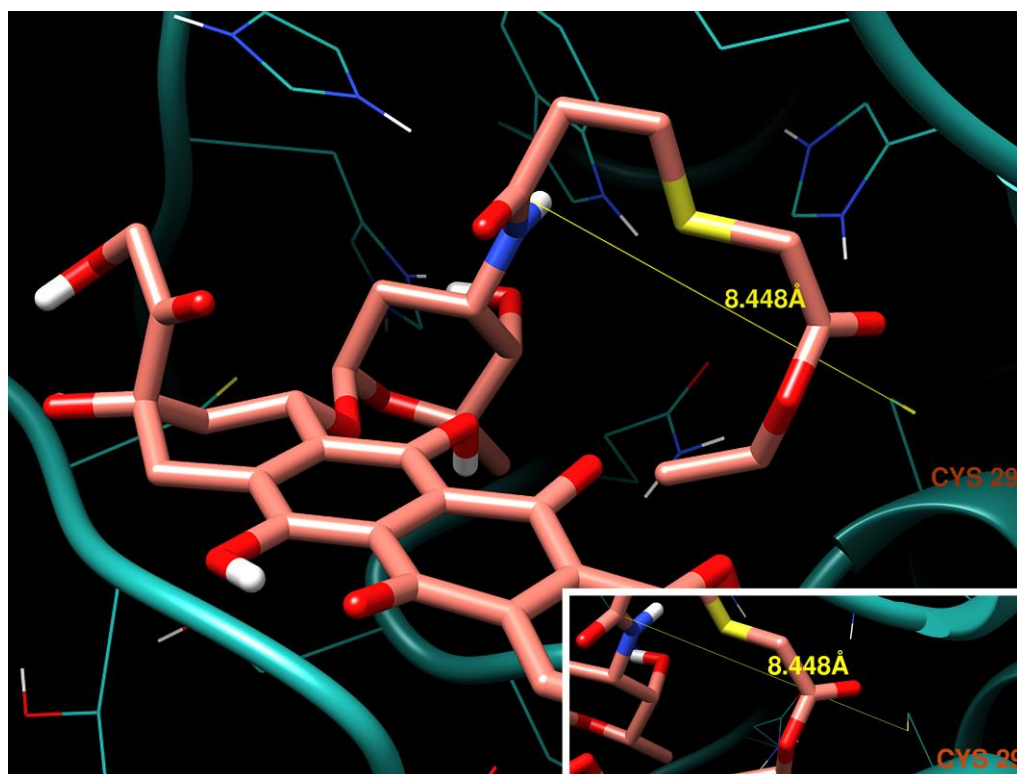
Figure 25 *Docked structures of 3a analogue and cathepsin B.*
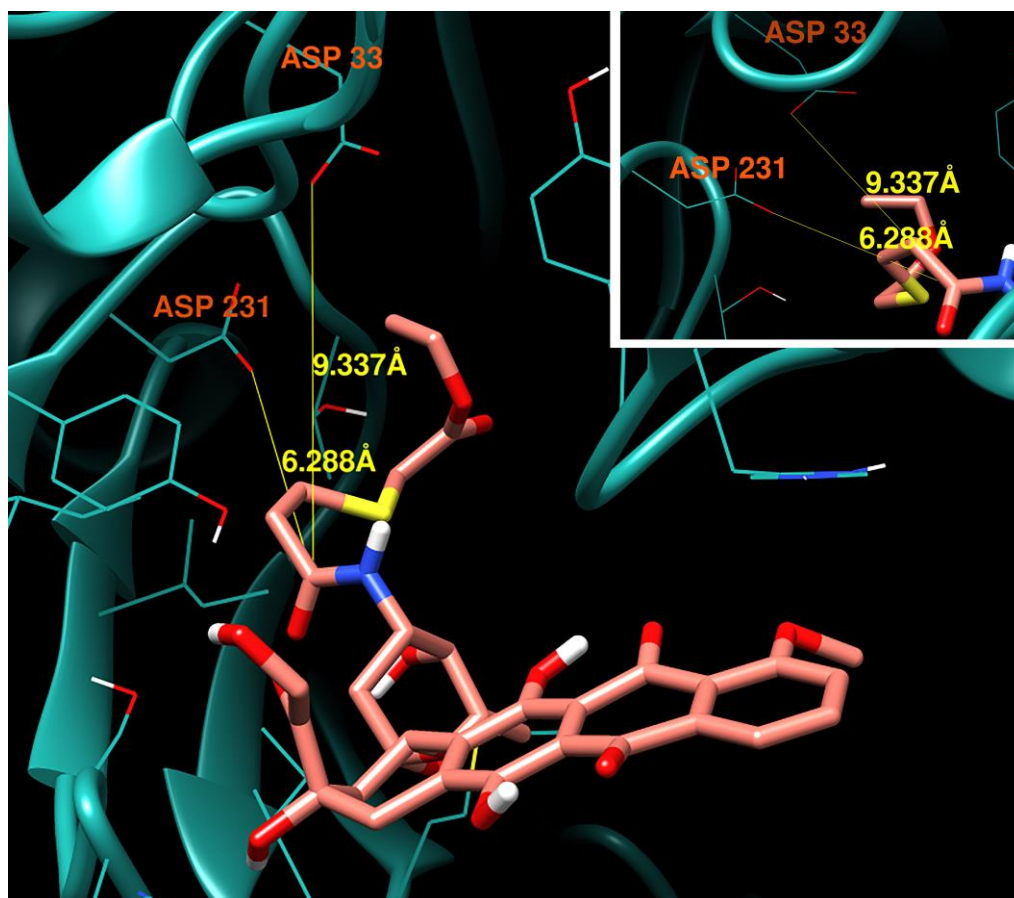
Figure 26 *Docked structures of 3a analogue and cathepsin D.*

4.2. Experimental results of polymer-DOX conjugates

4.2.1 Synthesis of P-A-DOX and P-DOX conjugates

The methyl protons of daunosamine sugar of DOX was represented by NMR peaks around 1.18 ppm, while the methoxy proton of DOX was detected at 4.00 ppm (Appendix C; Figure 73). The chemical shift of methylene protons at 5′ position of DOX was upfield shift to 1.44 ppm and methine protons at 4′ position was downfield shift to 4.73 ppm in P-A-DOX (Appendix C; Figure 73). These results indicated the amide bond formation in which the carbonyl moiety of the amide bond was responsible for the alteration of the above chemical shifts. Furthermore, the methylene protons of acrylic acid at 3″ and 4″ positions were profiled with chemical shifts at 2.90 and 2.26 ppm, respectively, following the covalent bond formation between mPEG-SH and acrylic acid in P-A-DOX. Similar observation was noted with reference to the P-DOX conjugate where the chemical shifts on 5′ and 4′ protons of DOX were detected at 1.43 and 4.72 ppm, respectively, and the protons of the mPEG chain at–2″ positions were identified at 3.69 ppm (Appendix C; Figure 74). The methylene protons were formed following the covalent conjugation between the mPEG-NHS and DOX.

4.2.1.1. mPEG-S-acrylic acid

The final product was obtained as white powder with 99.6% yield (602 mg). The conjugation status of P-A-DOX was assessed by 400 MHz ^{1}H-nuclear magnetic resonance (NMR) spectrometry technique (Varian 400 MR, Agilent Technologies, USA). The ^{1}H NMR spectrum of mPEG-S-acrylic acid conjugate (400 MHz, DMSO-d_6) (Appendix C; Figure 72) was assigned as follows: δ 3.69 (dd, *J* = 5.8, 3.8 Hz, 2H), 3.64 (t, *J* = 6.4 Hz,

2H), 3.52 (s, 170H), 3.34 (dd, J = 5.7, 4.0 Hz, 2H), 3.25 (s, 3H), 2.90 (t, J = 6.4 Hz, 2H), 2.18 (d, J = 14.5 Hz, 2H).

4.2.1.2. P-A-DOX conjugate

The final product was obtained as red powder with 64.1% yield (135 mg). The conjugation status of P-A-DOX was assessed by 500 MHz ^{1}H-nuclear magnetic resonance (NMR) spectrometry technique (Bruker AVANCE III HD/OXFORD 500 MHz, Bruker, USA). The synthesized P-A-DOX conjugate was structurally confirmed by ^{1}H NMR. The spectrum of ^{1}H NMR (500 MHz, DMSO-d_6) (Appendix C; Figure 73) was assigned as follows: δ 14.07 (s, 1H), 13.31 (s, 1H), 8.00 – 7.92 (m, 2H), 7.82 (s, 1H), 7.72 (dd, J = 7.6, 2.9 Hz, 1H), 5.48 (s, 1H), 5.24 (s, 1H), 4.97 (s, 1H), 4.73 (d, J = 5.4 Hz, 1H), 4.58 (s, 1H), 4.14 (d, J = 23.8 Hz, 1H), 4.00 (s, 3H), 3.52 (s, 3200H), 3.33 (s, 259H), 3.05 (t, J = 6.3 Hz, 1H), 2.90 (t, J = 6.4 Hz, 2H), 2.64 (s, 1H), 2.37 (s, 1H), 2.26 (d, J = 14.8 Hz, 2H), 1.89 (s, 1H), 1.44 (d, J = 15.1 Hz, 1H), 1.18 (t, J = 7.0 Hz, 3H).

4.2.1.3. P-DOX conjugate

The final product was obtained as red powder with 76.1% yield (158 mg). The synthesized P-DOX conjugate was structurally confirmed by ^{1}H NMR. The spectrum of ^{1}H NMR (500 MHz, DMSO-d_6) (Appendix C; Figure 74) was assigned as follows: δ 14.07 (s, 1H), 13.30 (s, 1H), 7.97 – 7.91 (m, 2H), 7.68 (dd, J = 6.3, 3.5 Hz, 1H), 7.55 (d, J = 8.2 Hz, 1H), 5.47 (s, 1H), 5.24 (s, 1H), 4.97 (s, 1H), 4.83 (t, J = 6.0 Hz, 1H), 4.72 (d, J = 6.0 Hz, 1H), 4.57 (d, J = 6.0 Hz, 1H), 4.16 (d, J = 6.9 Hz, 1H), 4.00 (s, 3H), 3.72 – 3.67 (m, 2H), 3.52 (s, 1352H), 3.32 (s, 186H), 3.00 (s, 1H), 2.68 (s, 1H), 2.38 – 2.25 (m, 2H), 2.16 (dd, J = 16.0, 10.2 Hz, 1H), 1.84 (s, 1H), 1.49 – 1.40 (m, 1H), 1.13 (d, J = 6.5 Hz, 3H).

4.2.2 DOX content

The maximum DOX content for P-A-DOX and P-DOX are 5.23 and 4.95 %(w/w), respectively. However, the DOX contents of P-A-DOX and P-DOX conjugates obtained from the HPLC analysis were 1.17 ± 0.06 %(w/w) and 4.55 ± 0.06 %(w/w), respectively. The low DOX content of P-A-DOX was ascribed to the presence of unreacted mPEG-SH and mPEG-S-acrylic acid in P-A-DOX conjugate. The unreacted mPEG-S-acrylic acid (data not shown) and mPEG-SH were not removed from the conjugate as they were found to be non-cytotoxic (Didychuk et al. 2008; Song et al. 2012).

4.2.3 *In vitro* drug release and stability

Both P-DOX and P-A-DOX conjugates released DOX at low levels in pH 4.0 and 7.4 medium, with the extent of DOX release being higher in the acidic medium (Figure 27-28). The difference of DOX release from the both conjugates compared to the DOX analogues may be due to the high concentration of the conjugates in buffer solution at the beginning of incubation time. The P-DOX conjugate released DOX at 5.43 ± 0.01 % at pH 4.0 within 48 h. Less than 1% of DOX was released from the P-DOX conjugate at pH 7.4 within 264 h. The P-A-DOX conjugate released DOX 4.09 ± 0.01 % at pH 4 within 96 h and less than 1% of DOX at pH 7.4 within 264 h. In comparison with the previously report of the 10-kDa polymer-DOX conjugate covalently linked by amide bond where the DOX was released by 10 % and 25 % within 48 h at pH 7.4 and 5.6, respectively (Qiao et al. 2018), the P-DOX and P-A-DOX conjugates showed a marginal preference in drug release at a lower pH medium.

At pH 4, the remaining P-DOX and P-A-DOX conjugates at 264 h were 65.5 ± 1.4 % and 67.3 ± 1.2 %, respectively, while DOX released from P-DOX and P-A-DOX were 5.03 ± 0.05 % and 2.91 ± 0.02 %, respectively. At pH 7.4, the remaining P-DOX and P-A-DOX conjugates at 264 h were 55.5 ± 3.3 % and 45.4

± 0.8 %, respectively, while there was minimal DOX detected from the P-DOX and P-A-DOX conjugates. A major fraction of the released DOX underwent degradation during the dissolution process particularly at a higher pH as indicated by the stability study of free DOX, showing that at pH 4, DOX were dramatically reduced to 37.9 ± 0.4 % within 264 h and completely degraded within 96 h at pH 7.4 (Figure 29). DOX conjugation to polymeric backbone in the presence or absence of the *beta*-thiopropanamide linker protected the drug from the systemic circulation to a greater extent than in the acidic microenvironment of cancer cells. The *beta*-thiopropanamide linker did not appear to provide any remarkable benefit in conferring pH-responsiveness to the conjugate when drug release or degradation was concerned at the vicinity of cancer.

The degradation of P-DOX, P-A-DOX and DOX to doxorubicinone followed pseudo first-order kinetics ($r^2 > 0.9$, Figure 30). The degradation kinetics of P-DOX and P-A-DOX were shown in Table 5 which was not significantly different (one-way ANOVA; $p > 0.01$, Appendix D) at both pHs. The P-DOX and P-A-DOX conjugates exhibited substantially low k_{obs} and high $t_{1/2}$ values at pH 4.0 and 7.4 compared to DOX (one-way ANOVA; $p < 0.01$, Appendix D). The chemical stability of both conjugates was possibly due to the steric effect of high molecular weight PEG which prevented the accessibility of proton ions and water molecules responsible for DOX hydrolysis.
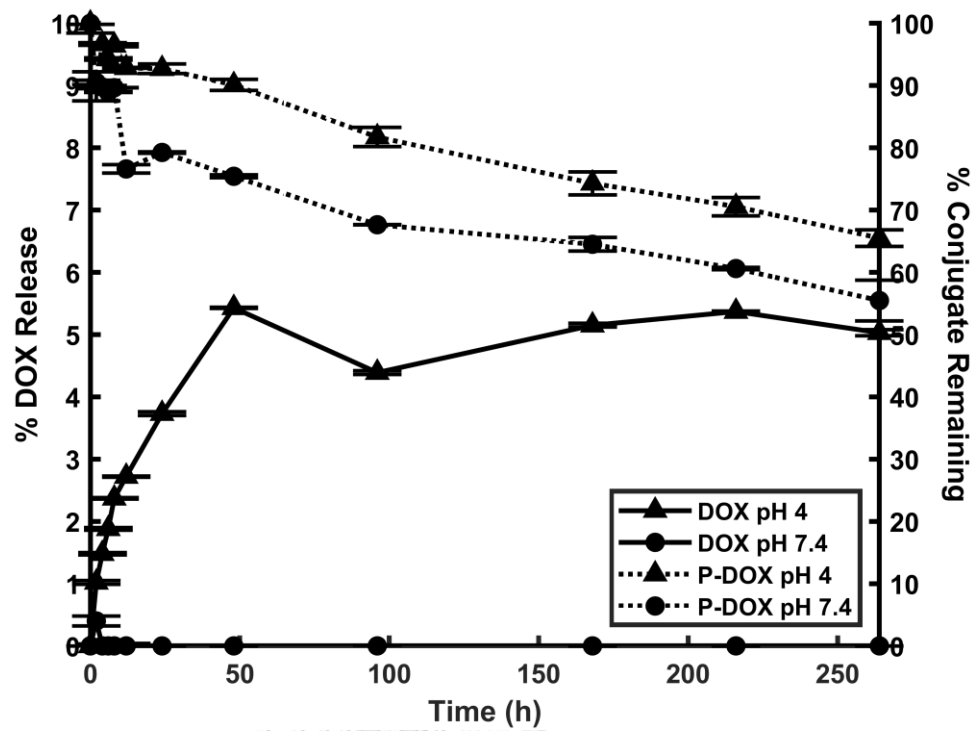
Figure 27 *Profiles of DOX release and remaining amount of P-DOX conjugate at pH 4.0 and 7.4, — DOX; ---- conjugate.*
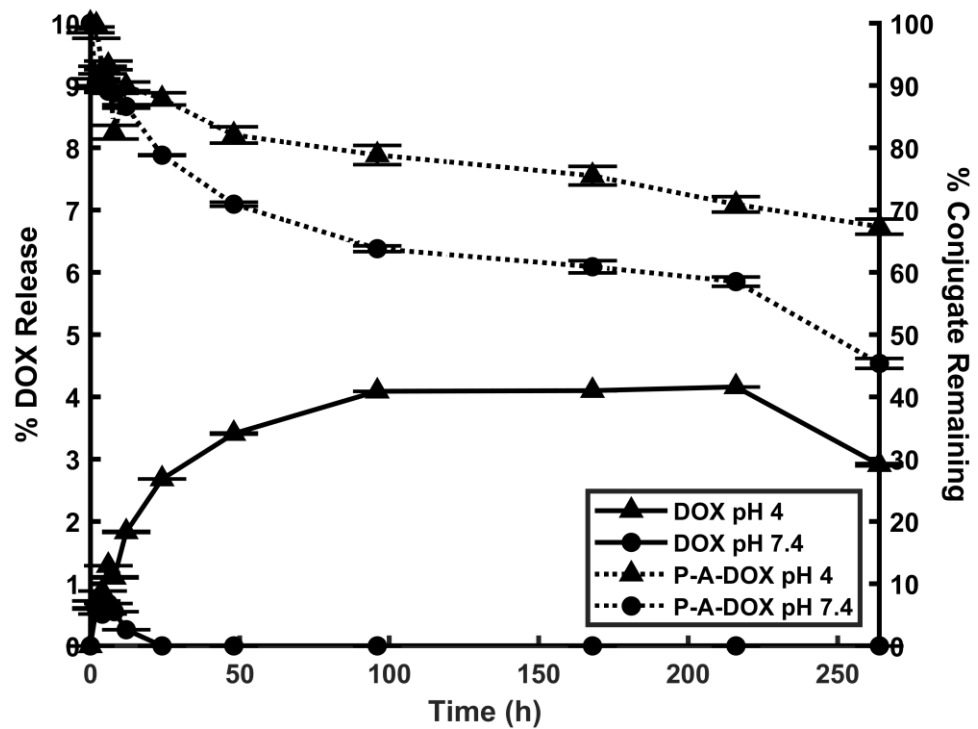
Figure 28 *Profiles of DOX release and remaining amount of P-A-DOX conjugate at pH 4.0 and 7.4, — DOX; ---- conjugate.*
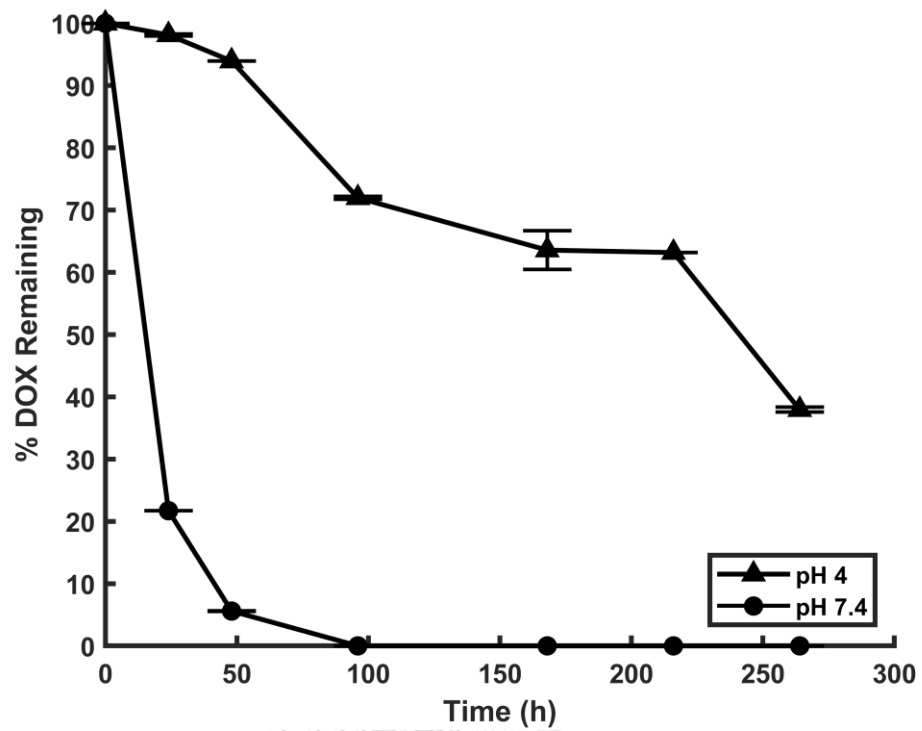
Figure 29 *Profiles of DOX degradation.*
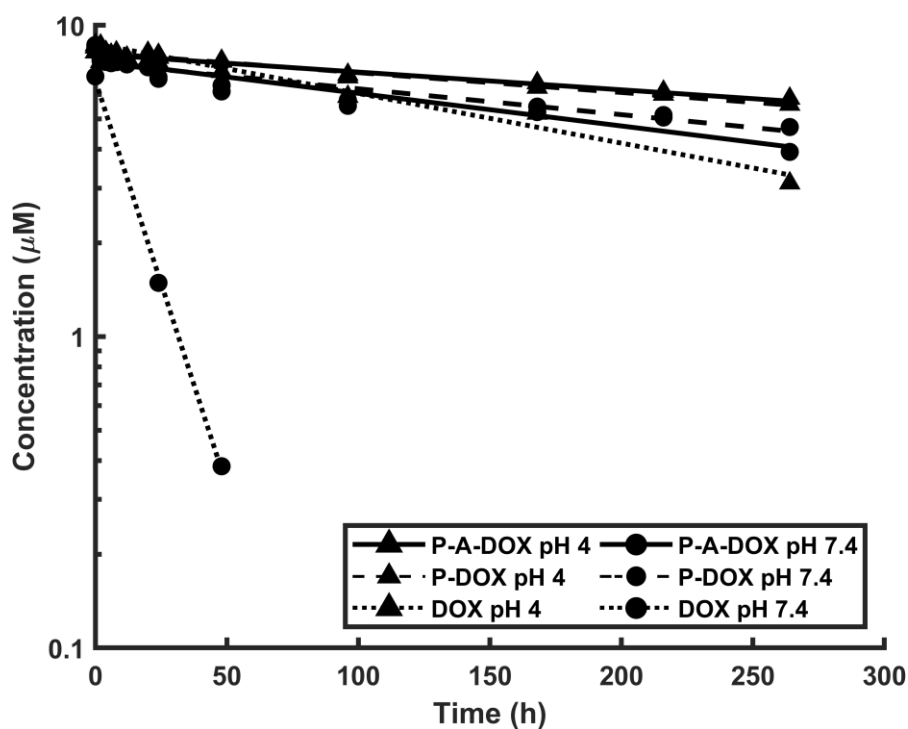
Figure 30 *Pseudo-first order degradation kinetic plots of P-A-DOX, P-DOX and DOX.*

Table 5 *Pseudo-first order kinetic parameters of P-A-DOX, P-DOX and DOX in pH 4 and 7.4.*

	R^2		k_{obs}		$t_{1/2}$ (h)	
	pH 4	pH 7.4	pH 4	pH 7.4	pH 4	pH 7.4
P-A-DOX	0.9022	0.9149	0.0013	0.0024	529	287
P-DOX	0.9637	0.9098	0.0015	0.0019	473	361
DOX	0.9681	0.9988	0.0037	0.0601	189	12

4.2.4 Cell cytotoxicity and selectivity

The cytotoxic effects of P-A-DOX, P-DOX, the intermediate mPEG-S-acrylic acid, and free DOX against MDA-MB-231 and MCF-7 breast cancer cells compared to MCF-10A non-cancerous breast cell were evaluated. P-A-DOX, P-DOX and DOX exhibited cytotoxic effect whereas mPEG-S-acrylic acid showed no cytotoxic effect against all cell lines (Figure 31-33). The P-A-DOX and P-DOX conjugates were characterized by a significantly higher cytotoxicity level than DOX against both breast cancer cell lines (one-way ANOVA; $p < 0.01$, Appendix D). On the contrary, the P-A-DOX conjugate was significantly less cytotoxic than P-DOX and DOX against MCF-10A non-cancerous breast cell (one-way ANOVA; $p < 0.01$, Appendix D). The difference of cytotoxicity of the P-A-DOX conjugate in breast cancer cells and normal breast cells may be influenced by the enzymatic cleavage of the *beta*-thiopropanamide linker that it may be extensively cleaved by an overexpressed enzyme in breast cancer cells but it may be slightly cleaved in normal breast cells. This resulted in the difference of DOX release.

The selectivity index of P-A-DOX and P-DOX conjugates were higher than DOX with P-A-DOX being the most selective compound against MDA-MB-231 and MCF-7 (Table 6). The selectivity index should be greater than three as an indication of the potential suitability of compounds as cancer chemotherapeutic agents (Bézivin et al. 2003; Oliveira et al. 2015). On this note, the P-A-DOX conjugate is deemed to be a potential anti-cancer model for further development.

The order of the cytotoxic selectivity progressed in the following order: P-A-DOX > P-DOX > DOX (Table 6). Both PEGylation and *beta*-thiopropanamide linker were responsible to introduce cancer selectivity to DOX. It has been suggested that PEGylation can enhance cellular uptake of cytotoxic compounds

into cancer cells via P-glycoprotein inhibition in cancer cells (Hodaei et al. 2015; Hugger et al. 2002). The enhanced cytotoxic selectivity of the P-A-DOX and P-DOX conjugates against DOX was probably due to an increase in intracellular uptake of conjugates by the breast cancer cells, which the conjugates may be internalize into cancer cells by a combination of passive diffusion and caveolae-mediated endocytosis as mentioned in a publication (Wang et al. 2020). The amide bond in the P-A-DOX conjugate was readily cleaved by some overexpressed enzymes such as cathepsins, an intracellular protease enzymes that are overexpressed in human breast cancer cells (Bengsch et al. 2014; Ruan et al. 2015; T. Sun et al. 2016). This enabled the P-A-DOX conjugate to exert a higher cytotoxicity and selectivity towards breast cancer cells by the promotion of the *beta*-thiopropanamide linker. Apparently, both P-A-DOX and P-DOX conjugates had similar DOX release and degradation kinetics as a function of pH. The enzyme- instead of pH-responsiveness could aptly explained the cell selective behavior of the P-A-DOX conjugate.
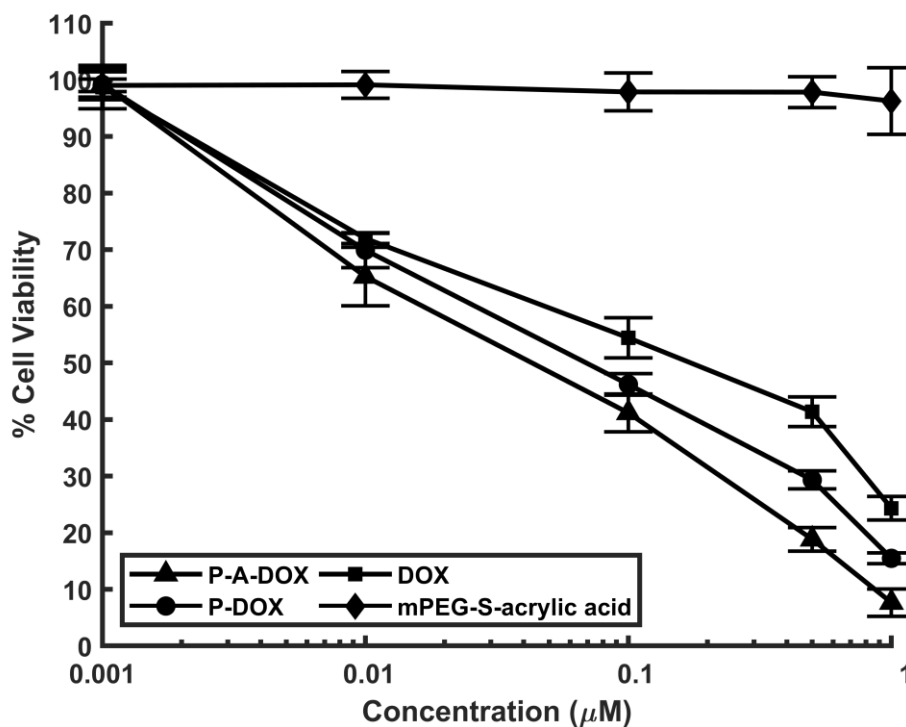
Figure 31 *Cytotoxicity of P-A-DOX, P-DOX conjugates, DOX and mPEG-S-acrylic acid. The cytotoxicity of conjugates was compared to that of the free Dox against MDA-MB-231 breast cancer cell. All treatments were applied at various concentrations for 72 h, and cell viability was determined using MTT assay. The experiment was performed in four replicates, and data were plotted as the mean ± standard deviation.*
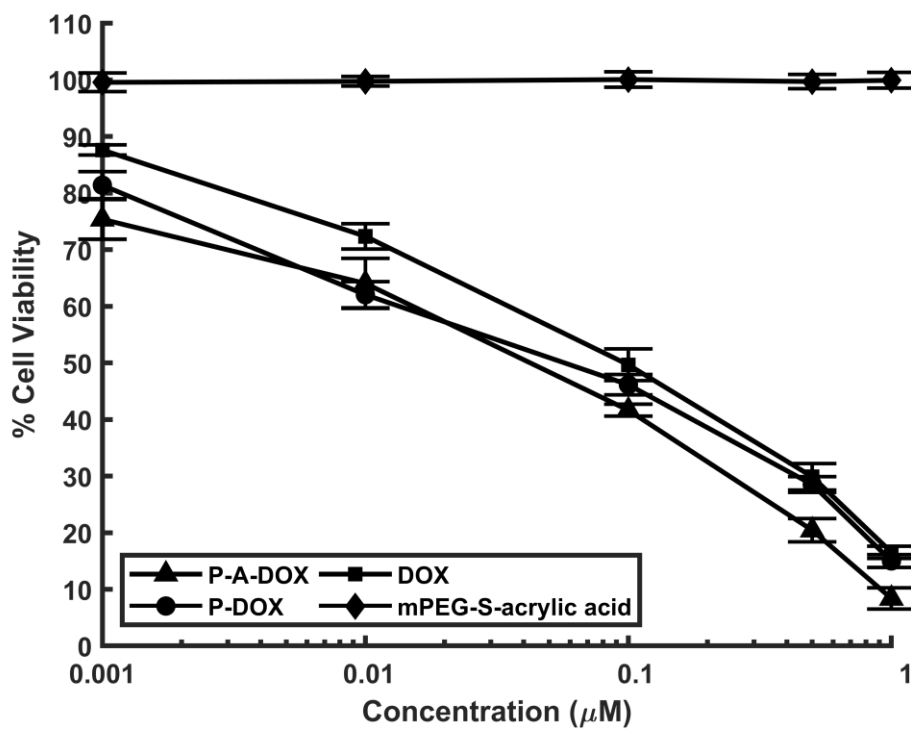
Figure 32 *Cytotoxicity of P-A-DOX, P-DOX conjugates, DOX and mPEG-S-acrylic acid. The cytotoxicity of conjugates was compared to that of the free Dox against MCF-7 breast cancer cell. All treatments were applied at various concentrations for 72 h, and cell viability was determined using MTT assay. The experiment was performed in four replicates, and data were plotted as the mean ± standard deviation.*
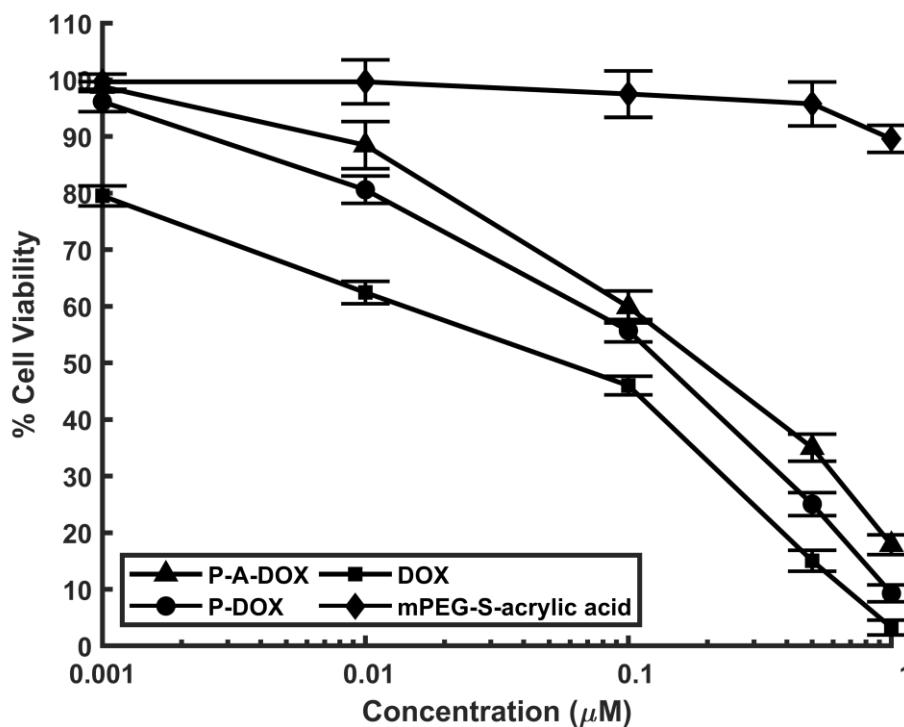
Figure 33 *Cytotoxicity of P-A-DOX, P-DOX conjugates, DOX and mPEG-S-acrylic acid. The cytotoxicity of conjugates was compared to that of the free Dox against MCF-10A noncancerous cell. All treatments were applied at various concentrations for 72 h, and cell viability was determined using MTT assay. The experiment was performed in four replicates, and data were plotted as the mean ± standard deviation.*

Table 6 *Mean IC_{50} values of P-A-DOX and P-DOX conjugates against DOX in MDA-MB-231, MCF-7 and MCF-10A cell lines.*

Treatment	IC_{50} (µM)			Selectivity Index	
	MDA-MB-231	MCF-7	MCF-10A	MCF-10A/ MDA-MB-231	MCF-10A/ MCF-7
P-A-DOX	0.042±0.004	0.024±0.003	0.131±0.018	3.13	5.43
P-DOX	0.065±0.005	0.038±0.005	0.072±0.002	1.10	1.89
DOX	0.125±0.011	0.062±0.008	0.025±0.001	0.20	0.39
mPEG-S-acrylic acid	>1	>1	>1	-	-

4.2.5 Molecular docking

Molecular docking study suggested that both P-DOX and P-A-DOX conjugates can bind to cathepsin L with the lowest binding energy compared to cathepsins B and D (Table 7). Even though the docked molecules (only 5 units of PEG) may not represent the actual activity of the whole molecules of P-DOX and P-A-DOX conjugates due to the software limitation, it is likely that cathepsin L is the responsible enzyme that catalyse the hydrolytic cleavage of P-DOX and P-A-DOX in the cancer cells. As shown in Figure 34-35, P-DOX and P-A-DOX can be docked in the active site of cathepsin L in proximity to Cys25, the amino acid residue which is responsible for the hydrolytic cleavage of an amide bond (Dana and Pathak 2020). The distance between the carbonyl carbon of the P-DOX and the sulfhydryl group of Cys25 is about 5.6 Å (Figure 34), while the carbonyl carbon of the P-A-DOX conjugate is about 3.6 Å away from Cys25 (Figure 35). It is noteworthy that the carbonyl carbon of the P-A-DOX conjugate is closer to Cys25 than that of the P-DOX. This allows the hydrolysis of the amide bond of P-A-DOX can occur more efficiently, resulting

in better cytotoxic selectivity against breast cancer cells of P-A-DOX compared to P-DOX and free DOX.

Table 7 *The molecular docking profiles of the P-DOX and P-A-DOX (with 5 units of PEG) with cathepsins.*

Cathepsins	PDB code	Binding energy (kcal/mol)	
		P-DOX	P-A-DOX
B	1HUC	-1.95	-1.89
D	1LYB	-3.36	-1.99
L	3HHA	-5.56	-4.45
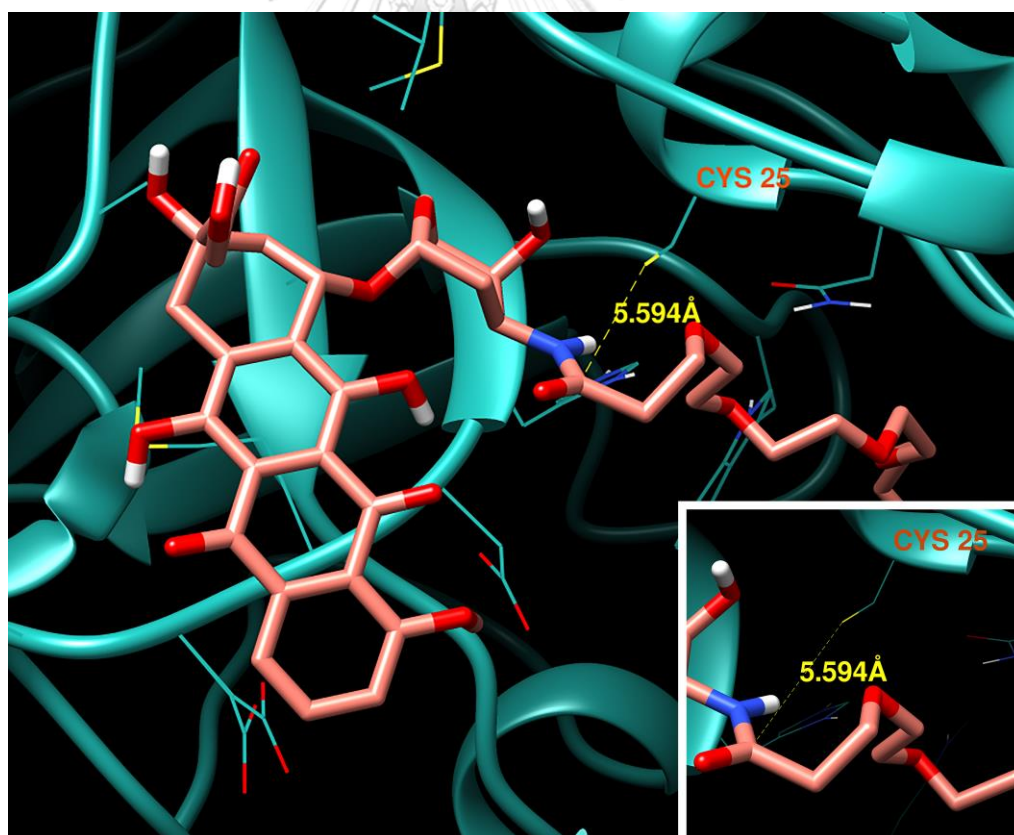
Figure 34 *Molecularly docked structures of cathepsin L with P-DOX (with 5 units of PEG).*
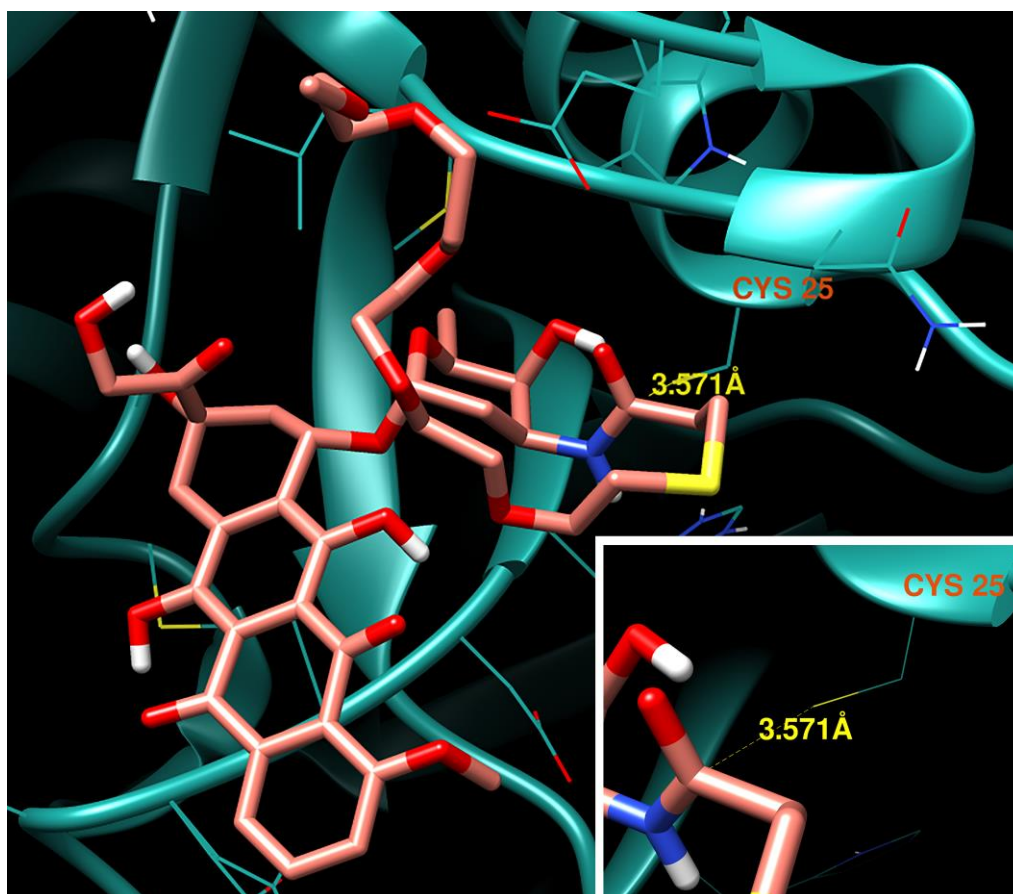
Figure 35 *Molecularly docked structures of cathepsin L with P-A-DOX (with 5 units of PEG).*

จุฬาลงกรณ์มหาวิทยาลัย

CHULALONGKORN UNIVERSITY

CHAPTER 5

DISCUSSION AND CONCLUSION

Doxorubicin (DOX) is a widely used anticancer drug to treat various types of cancers and usually co-administered with other chemotherapeutic drugs. In spite of it is an effective anticancer drug, the non-specific cell killing characteristic hinders its use in cancer treatment (Tacar et al. 2013). Further, the DOX exerts cardiotoxicity. The coupling of amide bond with a sulfur atom in the form of a linker between drug and polymer is envisaged to bring about conjugate stability in the blood, stimuli-responsiveness towards the cancer cells from the perspective dysregulated pH and overexpressed proteases of cancer cells such as cathepsins and matrix metalloproteinases. This study aims to design a *beta*-thiopropanamide linker (-S-CH2-CH2-CONH-) that incorporates a *beta* position sulfur atom to an amide functional group for using as a stimuli responsive linker for polymer-DOX conjugate. This novel linker was expected to raise the selectivity of DOX towards breast cancer cells.

The *beta*-thiopropanamide linker showed high cytotoxic selectivity towards MDA-MB-231 and MDF-7 breast cancer cells over MCF-10A non-cancerous breast cells. It can imply that such selectivity towards breast cancer cells may from the enzymatic process within the cells. The experimental data of DOX analogues showed that the DOX analogue 3a, which is the *beta*-thiopropanamide linker without substitution, gave high cytotoxic selectivity over other DOX analogues. This result indicated that the substitution of any moieties lower cytotoxicity of the DOX analogues that may be relevant to the reduction in accessibility of the responsible enzyme. The least steric structure of *beta*-thiopropanamide linker may provide the highest accessibility to the responsible enzyme compared to other linkers with substituents. It is possible that a protease enzyme in cathepsin family is the responsible enzymes for the enzymatic hydrolysis of the *beta*-thiopropanamide linker because cathepsins are overexpressed in breast cancer cells (Lah et al. 2000).

The molecular docking experiment showed that cathepsin L may be a responsible enzyme; however, it is needed a further experiment to prove the computational result for example, the enzymatic hydrolysis by the cathepsin L or the lysosomal fraction.

However, the *beta*-thiopropanamide linker had no pH-responsive effect since its kinetics showed low k_{obs} and high $t_{1/2}$ values at pH 4.0 and 5.5 compared to that at pH 7.4 (Table 2). The other linkers with the substitutions did not provide a pH-responsive effect because they showed an identical or a poorer kinetics profile. This rejects a hypothesis that an inductive effect from a *beta* position sulfur atom incorporated to an amide functional group may enhance a pH-responsive effect. In addition, the *beta*-thiopropanamide linker with or without substituent provide a slightly increase in the stability of DOX analogue in physiological pH compare to DOX (Table 2) except the phenyl substituent. This indicated that incorporation of a linker to DOX may reduce the chance of hydrolysis of DOX in the physiological condition due to the steric effect.

The outstanding experimental data of the *beta*-thiopropanamide linker form the DOX analogue 3a led us to synthesize the mPEG-DOX conjugate with the *beta*-thiopropanamide linker (P-A-DOX). The selective cytotoxicity of P-A-DOX was better than DOX, however, it was lower than that of DOX analogue in both breast cancer cells. This phenomenon may result from the enhancement of the cellular uptake of conjugates from PEG towards all cell lines especially the normal breast cells. The selectivity of the P-A-DOX conjugate only causes from the enzymatic process because the *in vitro* hydrolysis data indicated that the P-A-DOX conjugate did not possess pH-responsive effect. The P-A-DOX conjugate can enhance the cancer cell selectivity better than P-DOX that envisages the influence of the beta-sulfur atom in the enzymatic cleavage of amide bond. This idea is supported by the molecular docking result that showed the better docked structure compared to the P-DOX

conjugate. The responsible enzyme was cathepsin L, which was the same as that of the DOX analogue 3a. The conjugated PEG chain provided higher stability and a sustained release property in physiological pH compared to the DOX analogue and DOX, which resulted from the steric effect of high molecular weight polymer. The PEG also increased the cytotoxicity of DOX that may cause from the P-gp inhibition of PEG resulting an increase in cellular uptake. The high molecular weight PEG (more than 5000 kDa) can internalize cancer cells by a combination of passive diffusion and caveolae mediated endocytosis (Wang et al. 2020). This showed that the polymer conjugation can be used to increase the selectivity and stability of the drug delivery system and reduce the toxicity of an anticancer drug during the systemic circulation.

Besides, the high stability and sustained release property of P-A-DOX and P-DOX conjugates may be influenced by the nanoparticle system. There is a publication revealed that PEG-DOX conjugate was able to form nanoparticles in water (Rao et al. 2017). From this evidence, the nanoparticle aggregation of P-A-DOX and P-DOX conjugates should be evaluated and characterized in terms of morphology and stability of their nanoparticle system using some electron microscopy techniques for examples, transmission electron microscopy (TEM) and scanning electron microscopy (SEM), scanning probe microscopy (SPM) technique and dynamic light scattering (DLS) technique. Moreover, the enzymatic cleavage mechanisms of the beta-thiopropanamide linker are still unclear and needed more detail to clarify what is the cleaving enzyme and where is the linker cleaved. This needs an experiment to assess the DOX release of P-A-DOX inside and outside of a cell. One straightforward method is the HPLC analysis of intracellular and extracellular matrices.

In summary, the *beta*-thiopropanamide linker can produce significantly selective cytotoxicity towards MDA-MB-231 and MDF-7 breast cancer cells compared to MCF-10A non-cancerous breast cell. The *beta*-thiopropanamide linker could impart cancer enzyme-responsiveness to the conjugate, thereby was envisaged to promote

intracellular drug release and cytotoxic action. The linker can be used in the polymer-DOX conjugate with no compromised selective cytotoxicity. The developed linkage can be applied not only for doxorubicin but also for other cytotoxic drugs containing an amine group. The ultimate objective is to incorporate this potential biodegradable linkage to other polymer drug conjugates or nanoparticulate system to produce high selective drug delivery towards cancer cells. In a broader sense, to refine the chemical characteristics of the *beta*-thiopropanamide linkage, further studies are recommended to find out if this linker enhances the cellular uptake and to determine the cleavage mechanisms of the conjugate in cancer cells.

REFERENCES

Abuchowski, A., et al. (1977), 'Effect of covalent attachment of polyethylene glycol on immunogenicity and circulating life of bovine liver catalase', *Journal of Biological Chemistry,* 252 (11), 3582-6.

Beijnen, J. H., van der Houwen, O. A. G. J., and Underberg, W. J. M. (1986), 'Aspects of the degradation kinetics of doxorubicin in aqueous solution', *International Journal of Pharmaceutics,* 32 (2), 123-31.

Bengsch, F., et al. (2014), 'Cell type-dependent pathogenic functions of overexpressed human cathepsin B in murine breast cancer progression', *Oncogene,* 33 (36), 4474-84.

Bézivin, C., et al. (2003), 'Cytotoxic activity of some lichen extracts on murine and human cancer cell lines', *Phytomedicine,* 10 (6), 499-503.

Chan, J. W., et al. (2010), 'Nucleophile-Initiated Thiol-Michael Reactions: Effect of Organocatalyst, Thiol, and Ene', *Macromolecules,* 43 (15), 6381-88.

Chen, K., et al. (2016), 'Synthesis and characterization of a PAMAM-OH derivative containing an acid-labile beta-thiopropionate bond for gene delivery', *International Journal of Pharmaceutics* 509 (1-2), 314-27.

Chen, Y., et al. (2011), 'Anticancer efficacy enhancement and attenuation of side effects of doxorubicin with titanium dioxide nanoparticles', *International Journal of Nanomedicine,* 6, 2321-6.

Chhikara, B. S., et al. (2011), 'Fatty acyl amide derivatives of doxorubicin: synthesis and in vitro anticancer activities', *European Journal of Medicinal Chemistry,* 46 (6), 2037-42.

Dana, D. and Pathak, S. K. (2020), 'A Review of Small Molecule Inhibitors and Functional Probes of Human Cathepsin L', *Molecules,* 25 (3).

Didychuk, Candice, et al. (2008), *Synthesis and in vitro cytotoxicity of mPEG-SH modified gold nanorods* (SPIE BiOS, 6856: SPIE).

Dillman, R. O., et al. (1988), 'Superiority of an acid-labile daunorubicin-monoclonal antibody immunoconjugate compared to free drug', *Cancer Research,* 48 (21),

6097-102.

Gao, Q. H., et al. (2012), 'A polymer-drug conjugate for doxorubicin: Synthesis and biological evaluation of pluronic F127-doxorubicin amide conjugates', *Journal of Applied Polymer Science,* 124 (6), 4953-60.

Hershman, D. L., et al. (2008), 'Doxorubicin, cardiac risk factors, and cardiac toxicity in elderly patients with diffuse B-cell non-Hodgkin's lymphoma', *Journal of Clinical Oncology,* 26 (19), 3159-65.

Hodaei, Darya, et al. (2015), 'Effects of polyethylene glycols on intestinal efflux pump expression and activity in Caco-2 cells', *Brazilian Journal of Pharmaceutical Sciences,* 51, 745-53.

Hrdina, R., et al. (2000), 'Anthracycline-induced cardiotoxicity', *Acta Medica (Hradec Kralove),* 43 (3), 75-82.

Hugger, E. D., Audus, K. L., and Borchardt, R. T. (2002), 'Effects of poly(ethylene glycol) on efflux transporter activity in Caco-2 cell monolayers', *Journal of Pharmaceutical Sciences,* 91 (9), 1980-90.

Ishibashi, O., et al. (1999), 'Breast cancer cells express cathepsins B and L but not cathepsins K or H', *Cancer Biochemistry Biophysics,* 17 (1-2), 69-78.

Janssen, M. J. H., et al. (1985), 'Doxorubicin decomposition on storage. Effect of pH, type of buffer and liposome encapsulation', *International Journal of Pharmaceutics,* 23 (1), 1-11.

Kakinoki, A., et al. (2008), 'Synthesis of poly(vinyl alcohol)-doxorubicin conjugates containing cis-aconityl acid-cleavable bond and its isomer dependent doxorubicin release', *Biological and Pharmaceutical Bulletin,* 31 (1), 103-10.

Kaushik, D. and Bansal, G. (2015), 'Four new degradation products of doxorubicin: An application of forced degradation study and hyphenated chromatographic techniques', *Journal of Pharmaceutical Analysis,* 5 (5), 285-95.

Kluger, Ronald and Lam, C. H. (1978), 'Carboxylic acid participation in amide hydrolysis. External general base catalysis and general acid catalysis in reactions of norbornenylanilic acids', *Journal of the American Chemical Society,* 100 (7), 2191-97.

Lah, T. T., et al. (2000), 'Cells producing cathepsins D, B, and L in human breast

carcinoma and their association with prognosis', *Human Pathology,* 31 (2), 149-60.

Laurent-Matha, V., et al. (1998), 'Endocytosis of pro-cathepsin D into breast cancer cells is mostly independent of mannose-6-phosphate receptors', *Journal of Cell Science,* 111 (Pt 17), 2539-49.

Lee, S. J., et al. (2015), 'Enzyme-responsive doxorubicin release from dendrimer nanoparticles for anticancer drug delivery', *International Journal of Nanomedicine,* 10, 5489-503.

Li, Jingguo, et al. (2016), 'A pH-sensitive prodrug micelle self-assembled from multi-doxorubicin-tailed polyethylene glycol for cancer therapy', *RSC Advances,* 6 (11), 9160-63.

Li, N., et al. (2014), 'Amphiphilic peptide dendritic copolymer-doxorubicin nanoscale conjugate self-assembled to enzyme-responsive anti-cancer agent', *Biomaterials,* 35 (35), 9529-45.

Liu, B. and Thayumanavan, S. (2017), 'Substituent Effects on the pH Sensitivity of Acetals and Ketals and Their Correlation with Encapsulation Stability in Polymeric Nanogels', *Journal of the American Chemical Society,* 139 (6), 2306-17.

Lomovskaya, N., et al. (1999), 'Doxorubicin overproduction in Streptomyces peucetius: cloning and characterization of the dnrU ketoreductase and dnrV genes and the doxA cytochrome P-450 hydroxylase gene', *Journal of Bacteriology,* 181 (1), 305-18.

Lu, D., et al. (2009), 'A pH-sensitive nano drug delivery system derived from pullulan/doxorubicin conjugate', *Journal of Biomedical Materials Research Part B: Applied Biomaterials,* 89 (1), 177-83.

Lutz, J. F. and Hoth, A. (2006), 'Preparation of ideal PEG analogues with a tunable thermosensitivity by controlled radical copolymerization of 2-(2-methoxyethoxy)ethyl methacrylate and oligo(ethylene glycol) methacrylate', *Macromolecules,* 39 (2), 893-96.

Lv, S., et al. (2014), 'Well-defined polymer-drug conjugate engineered with redox and pH-sensitive release mechanism for efficient delivery of paclitaxel', *Journal of*

Controlled Release, 194, 220-7.

Mahesh, S., Tang, K. C., and Raj, M. (2018), 'Amide Bond Activation of Biological Molecules', *Molecules,* 23 (10), 1-43.

Matsumura, Y. and Maeda, H. (1986), 'A new concept for macromolecular therapeutics in cancer chemotherapy: mechanism of tumoritropic accumulation of proteins and the antitumor agent smancs', *Cancer Research,* 46 (12 Pt 1), 6387-92.

Minarowska, A., et al. (2008), 'Human cathepsin D', *Folia Histochemica et Cytobiologica,* 46 (1), 23-38.

Nie, Q., et al. (2017), 'Conjugation to 10 kDa Linear PEG Extends Serum Half-Life and Preserves the Receptor-Binding Ability of mmTRAIL with Minimal Stimulation of PEG-Specific Antibodies', *Molecular Pharmaceutics,* 14 (2), 502-12.

Oishi, M., et al. (2003), 'pH-responsive oligodeoxynucleotide (ODN)-poly(ethylene glycol) conjugate through acid-labile beta-thiopropionate linkage: preparation and polyion complex micelle formation', *Biomacromolecules,* 4 (5), 1426-32.

Oishi, M., et al. (2005), 'Lactosylated poly(ethylene glycol)-siRNA conjugate through acid-labile beta-thiopropionate linkage to construct pH-sensitive polyion complex micelles achieving enhanced gene silencing in hepatoma cells', *Journal of the American Chemical Society,* 127 (6), 1624-5.

Oliveira, Pollyanna Francielli de, et al. (2015), 'Cytotoxicity screening of essential oils in cancer cell lines', *Revista Brasileira de Farmacognosia,* 25 (2), 183-88.

Pommier, Yves, et al. (2010), 'DNA Topoisomerases and Their Poisoning by Anticancer and Antibacterial Drugs', *Chemistry & Biology,* 17 (5), 421-33.

Pramanik, P., et al. (2016), 'pH-Triggered Sustained Drug Delivery from a Polymer Micelle having the beta-Thiopropionate Linkage', *Macromolecular Rapid Communications,* 37 (18), 1499-506.

Qiao, Y., et al. (2018), 'Preparation and biological evaluation of a novel pH-sensitive poly (beta-malic acid) conjugate for antitumor drug delivery', *International Journal of Molecular Medicine,* 42 (6), 3495-502.

Qiu, L., et al. (2017), 'Silver Nanoparticles Covered with pH-Sensitive Camptothecin-Loaded Polymer Prodrugs: Switchable Fluorescence "Off" or "On" and Drug Delivery Dynamics in Living Cells', *ACS Applied Materials & Interfaces,* 9 (46),

40887-97.

Qiu, Liang, et al. (2016), 'Unimolecular micelles of camptothecin-bonded hyperbranched star copolymers via [small beta]-thiopropionate linkage: synthesis and drug delivery', *Journal of Materials Chemistry B,* 4 (1), 141-51.

Radenkovic, Sandra, et al. (2017), 'Role of Proteases in Breast Cancer', in Sajal Chakraborti and Naranjan S. Dhalla (eds.), *Pathophysiological Aspects of Proteases* (Singapore: Springer Singapore), 3-22.

Rao, Ksvk, et al. (2017), 'Nanoparticles of pH-Responsive, PEG-Doxorubicin Conjugates: Interaction with an in Vitro Model of Lung Adenocarcinoma and Their Direct Formulation in Propellant-Based Portable Inhalers', *Molecular Pharmaceutics,* 14 (11), 3866-78.

Ratnatilaka Na Bhuket, Pahweenvaj, et al. (2019), 'Interspecies differences in stability kinetics and plasma esterases involved in hydrolytic activation of curcumin diethyl disuccinate, a prodrug of curcumin', *RSC Advances,* 9 (8), 4626-34.

Ruan, H., et al. (2015), 'Targeting Cathepsin B for Cancer Therapies', *Horizons in Cancer Research,* 56, 23-40.

Rudakova, E. V., Boltneva, N. P., and Makhaeva, G. F. (2011), 'Comparative analysis of esterase activities of human, mouse, and rat blood', *Bulletin of Experimental Biology and Medicine,* 152 (1), 73-5.

Schiavon, O., et al. (2004), 'PEG-Ara-C conjugates for controlled release', *European Journal of Medicinal Chemistry,* 39 (2), 123-33.

Schoenmakers, R. G., et al. (2004), 'The effect of the linker on the hydrolysis rate of drug-linked ester bonds', *Journal of Controlled Release,* 95 (2), 291-300.

Schöttler, Susanne, et al. (2016), 'Protein adsorption is required for stealth effect of poly(ethylene glycol)- and poly(phosphoester)-coated nanocarriers', *Nature Nanotechnology,* 11 (4), 372-77.

Shaffer, C. B., Critchfield, F. H., and Nair, J. H., 3rd (1950), 'The absorption and excretion of a liquid polyethylene glycol', *Journal of the American Pharmacists Association,* 39 (6), 340-4.

Silverman, L. and Barenholz, Y. (2015), 'In vitro experiments showing enhanced release of doxorubicin from Doxil(R) in the presence of ammonia may explain drug

release at tumor site', *Nanomedicine,* 11 (7), 1841-50.

Song, X. L., et al. (2012), 'Cytotoxicity of water-soluble mPEG-SH-coated silver nanoparticles in HL-7702 cells', *Cell Biology and Toxicology,* 28 (4), 225-37.

Sreedhar, A. and Zhao, Y. F. (2018), 'Dysregulated metabolic enzymes and metabolic reprogramming in cancer cells', *Biomedical Reports,* 8 (1), 3-10.

Sun, C. Y., et al. (2014), 'Doxorubicin conjugate of poly(ethylene glycol)-block-polyphosphoester for cancer therapy', *Advanced Healthcare Materials,* 3 (2), 261-72.

Sun, T., et al. (2016), 'Expression profile of cathepsins indicates the potential of cathepsins B and D as prognostic factors in breast cancer patients', *Oncology Letters,* 11 (1), 575-83.

Tacar, O., Sriamornsak, P., and Dass, C. R. (2013), 'Doxorubicin: an update on anticancer molecular action, toxicity and novel drug delivery systems', *Journal of Pharmacy and Pharmacology,* 65 (2), 157-70.

Tomlinson, R., et al. (2003), 'Polyacetal-doxorubicin conjugates designed for pH-dependent degradation', *Bioconjugate Chemistry,* 14 (6), 1096-106.

van Vlerken, Lilian E., Vyas, Tushar K., and Amiji, Mansoor M. (2007), 'Poly(ethylene glycol)-modified Nanocarriers for Tumor-targeted and Intracellular Delivery', *Pharmaceutical Research,* 24 (8), 1405-14.

Volkova, M. and Russell, R., 3rd (2011), 'Anthracycline cardiotoxicity: prevalence, pathogenesis and treatment', *Current Cardiology Reviews,* 7 (4), 214-20.

Wang, Tingting, et al. (2020), 'Impact of molecular weight on the mechanism of cellular uptake of polyethylene glycols (PEGs) with particular reference to P-glycoprotein', *Acta Pharmaceutica Sinica B*.

Wei, X., et al. (2016), 'Enzyme- and pH-Sensitive Branched Polymer-Doxorubicin Conjugate-Based Nanoscale Drug Delivery System for Cancer Therapy', *ACS Applied Materials & Interfaces,* 8 (18), 11765-78.

White, K. A., Grillo-Hill, B. K., and Barber, D. L. (2017), 'Cancer cell behaviors mediated by dysregulated pH dynamics at a glance', *Journal of Cell Science,* 130 (4), 663-69.

Yamaoka, T., Tabata, Y., and Ikada, Y. (1994), 'Distribution and tissue uptake of

poly(ethylene glycol) with different molecular weights after intravenous administration to mice', *Journal of Pharmaceutical Sciences,* 83 (4), 601-6.

Yang, Y., et al. (2013), 'Biodegradable and amphiphilic block copolymer-doxorubicin conjugate as polymeric nanoscale drug delivery vehicle for breast cancer therapy', *Biomaterials,* 34 (33), 8430-43.

Yu, Q., et al. (2015), 'Polymer-Doxorubicin Conjugate Micelles Based on Poly(ethylene glycol) and Poly(N-(2-hydroxypropyl) methacrylamide): Effect of Negative Charge and Molecular Weight on Biodistribution and Blood Clearance', *Biomacromolecules,* 16 (9), 2645-55.

APPENDIX A

Characterization of DOX, *beta*-thiopropanamide substituents and DOX analogues

1. Nuclear magnetic resonance (NMR) spectroscopy

Fifteen milligrams of DOX, beta-thiopropanamide substituents and DOX analogues were dissolved with dimethylsulfoxide-d_6 (DMSO-d_6). The solution was analyzed by nuclear magnetic resonance spectroscopy at 400 MHz (Varian 400 MR, Agilent Technologies, USA) and 500 MHz (Bruker AVANCE III HD/OXFORD 500 MHz, Bruker, USA). Spectra of ^{1}H-NMR and ^{13}C-NMR were recorded.
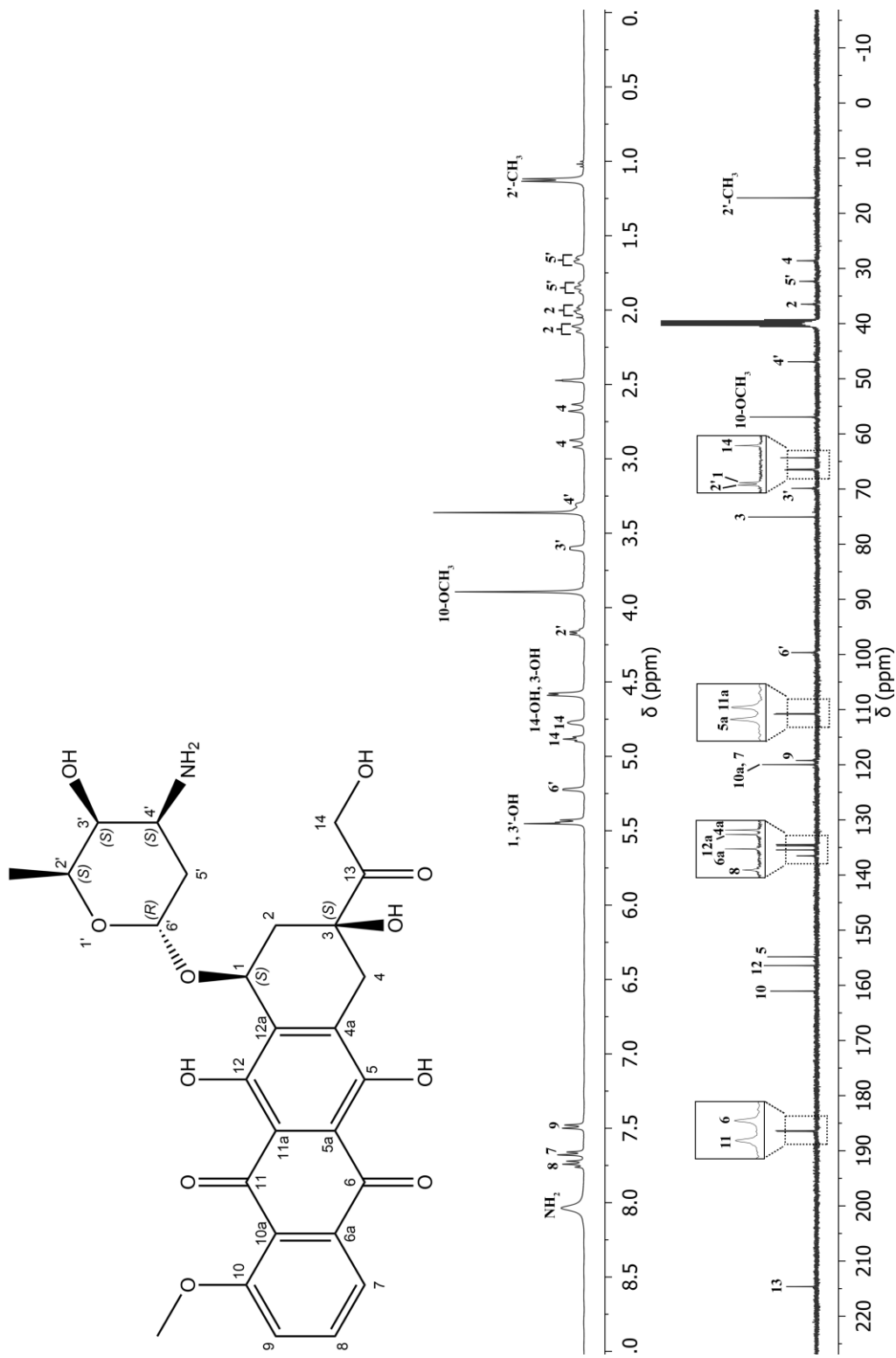
Figure 36 *Representative ^1H NMR spectrum of DOX in DMSO-d_6 (top) and ^{13}C NMR spectrum of DOX in DMSO-d_6 (bottom).*
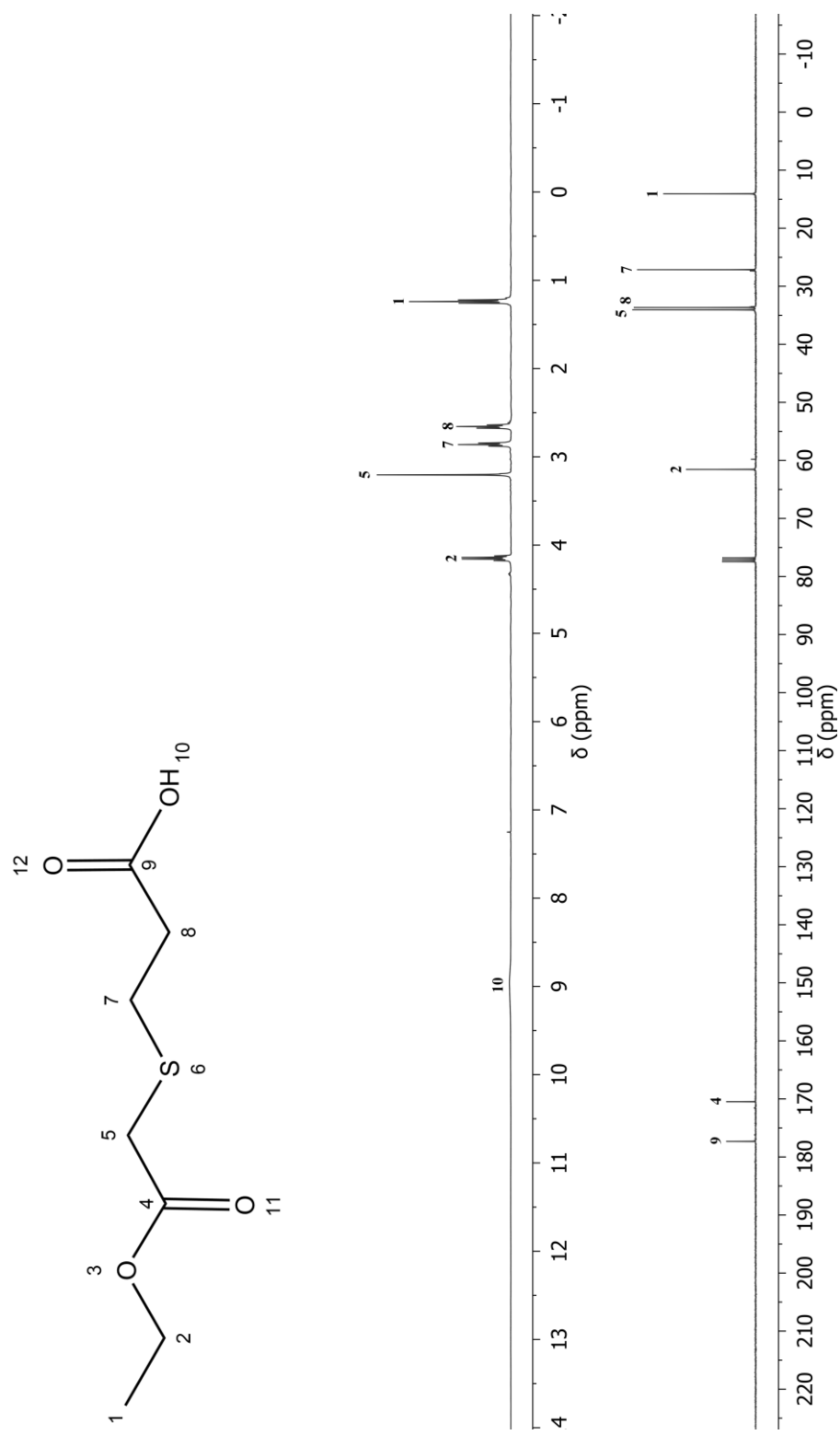
Figure 37 Representative ^1H NMR spectrum of compound 2a in $CDCl_3$ (top) and ^{13}C NMR spectrum of compound 2a in $CDCl_3$ (bottom).
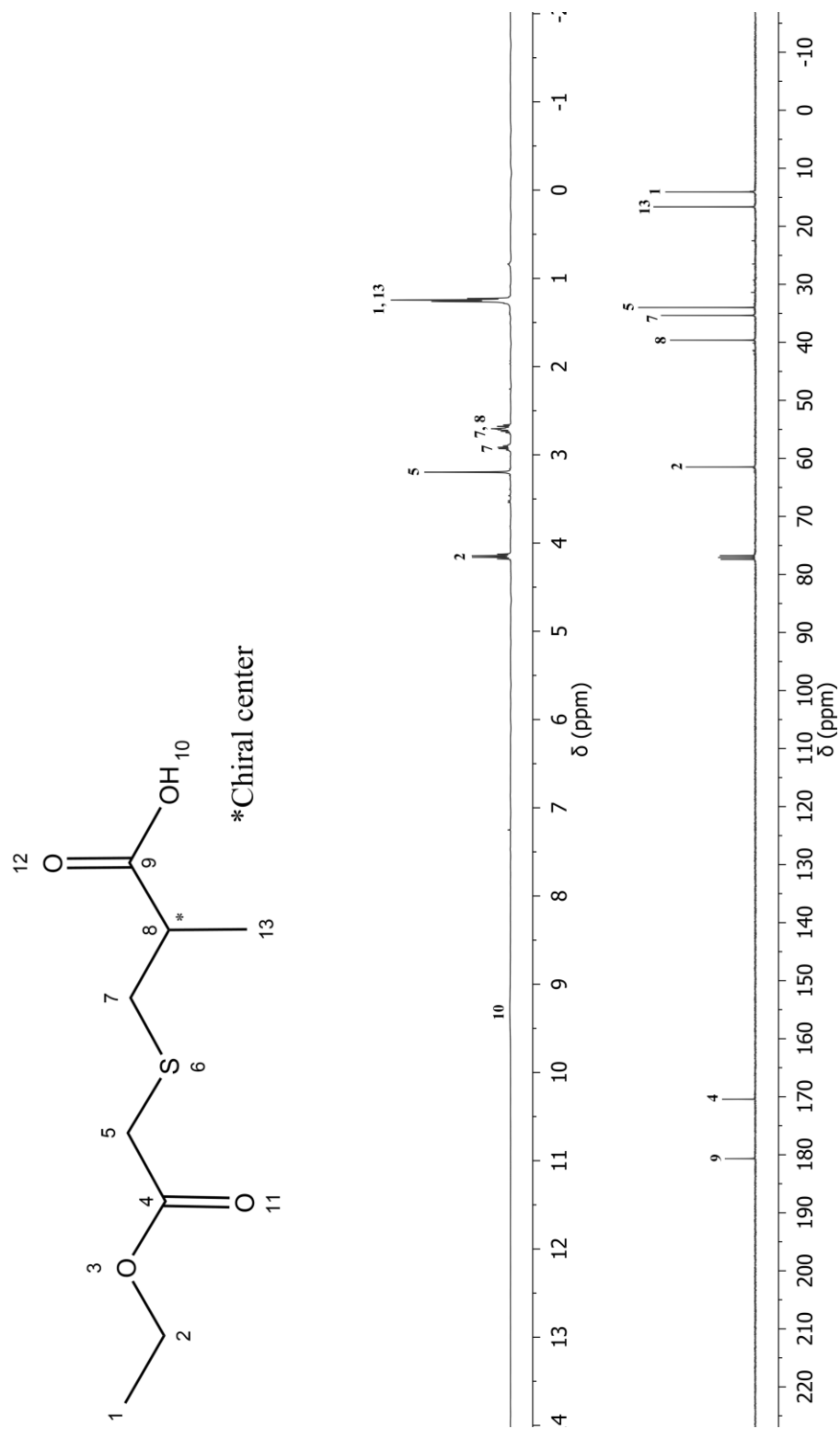
Figure 38 *Representative ^1H NMR spectrum of compound 2b in CDCl$_3$ (top) and ^{13}C NMR spectrum of compound 2b in CDCl$_3$ (bottom).*
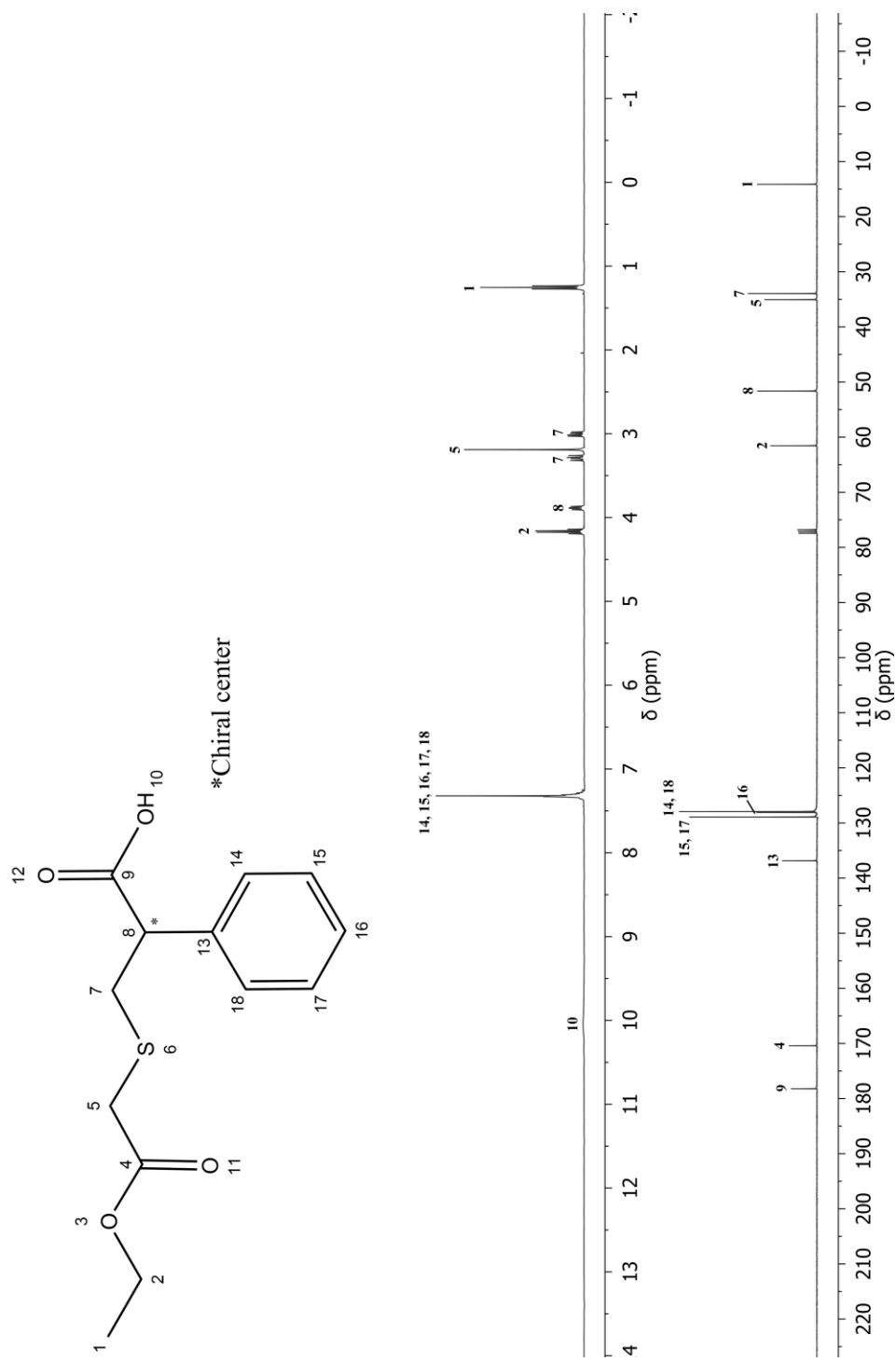
Figure 39 Representative ^1H NMR spectrum of compound 2c in CDCl$_3$ (top) and ^{13}C NMR spectrum of compound 2c in CDCl$_3$ (bottom).
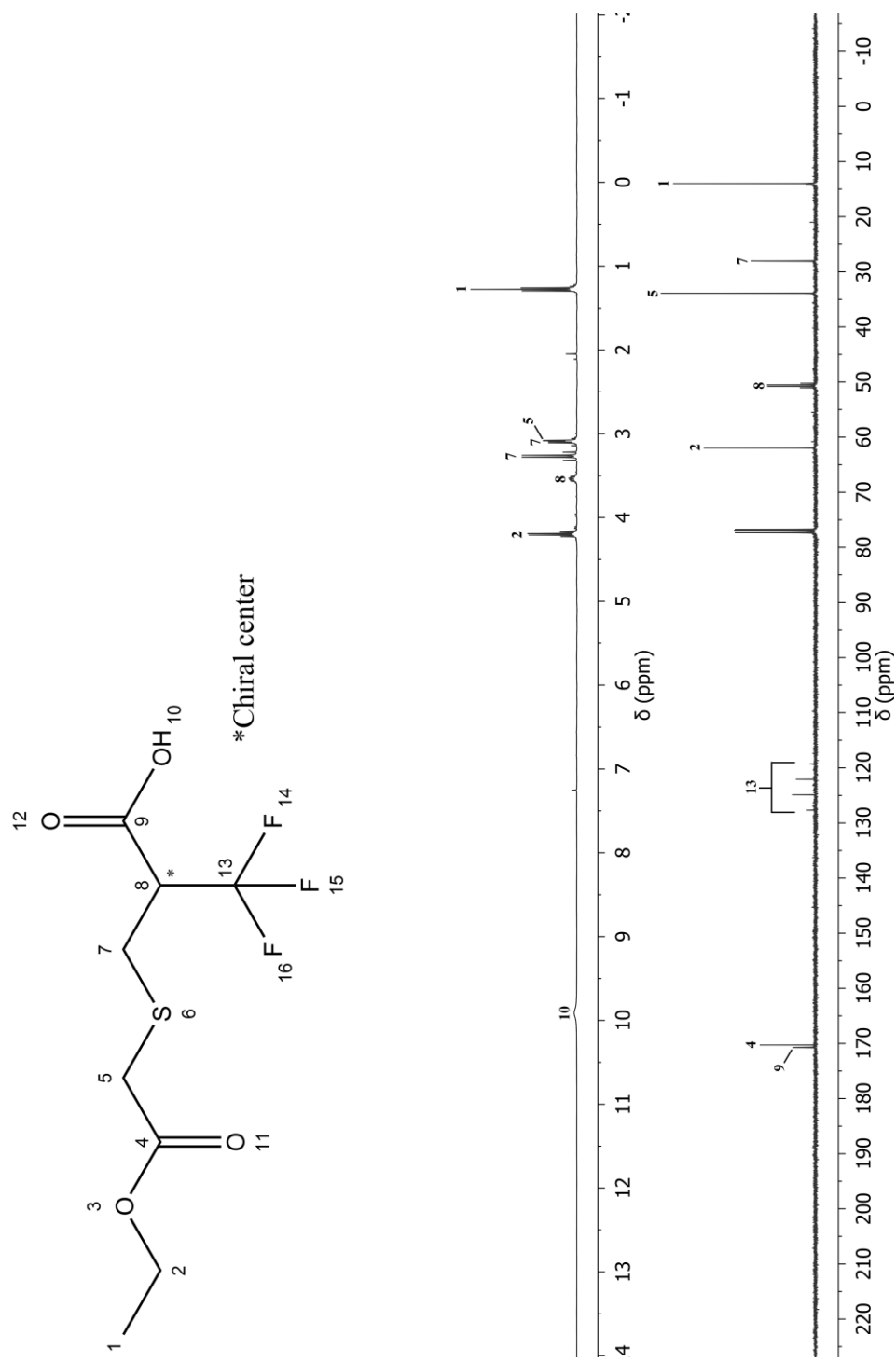
Figure 40 *Representative ^1H NMR spectrum of compound 2d in CDCl$_3$ (top) and ^{13}C NMR spectrum of compound 2d in CDCl$_3$ (bottom).*

94
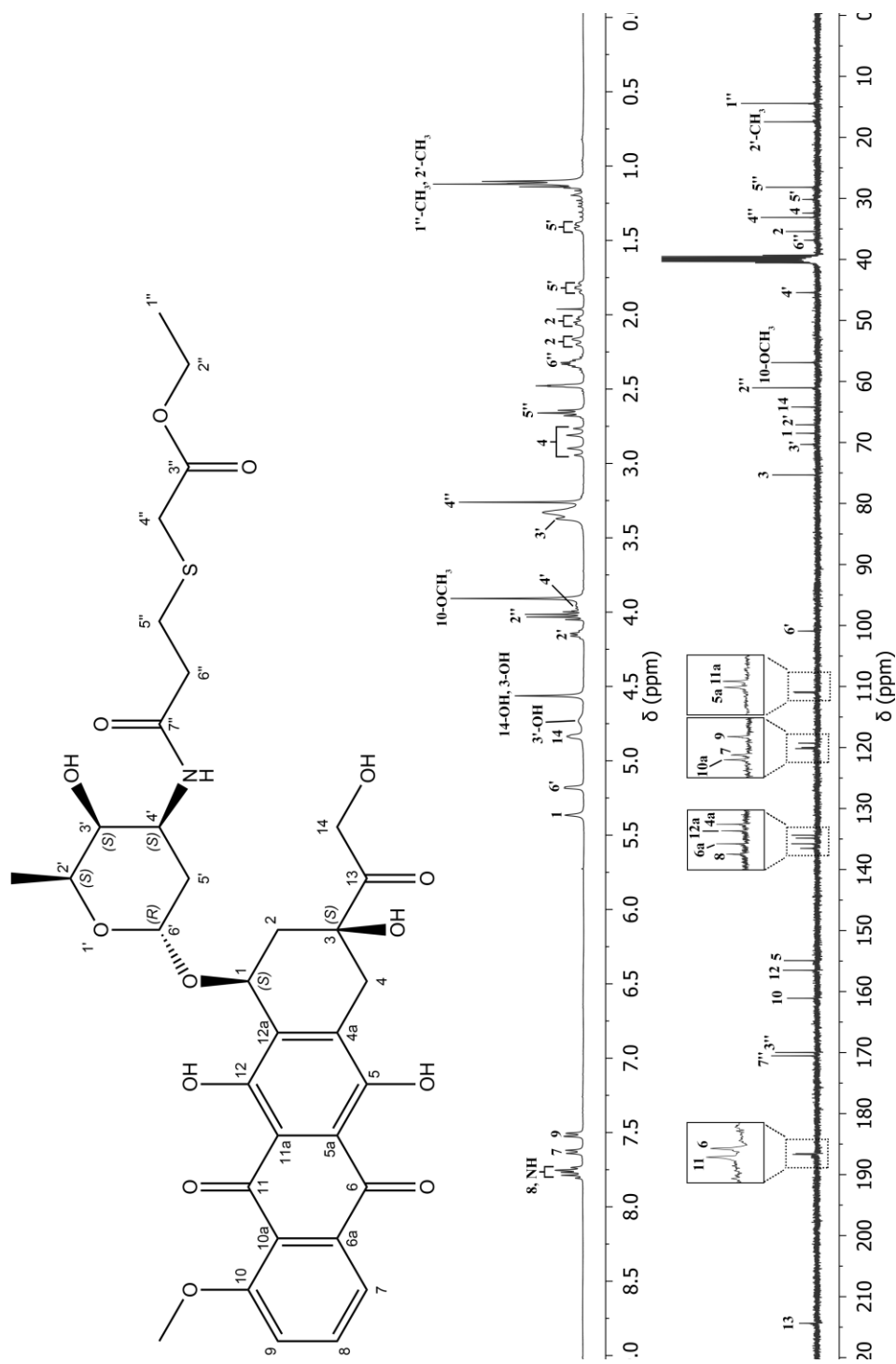
Figure 41 *Representative ^1H NMR spectrum of compound 3a in DMSO-d_6 (top) and ^{13}C NMR spectrum of compound 3a in DMSO-d_6 (bottom).*
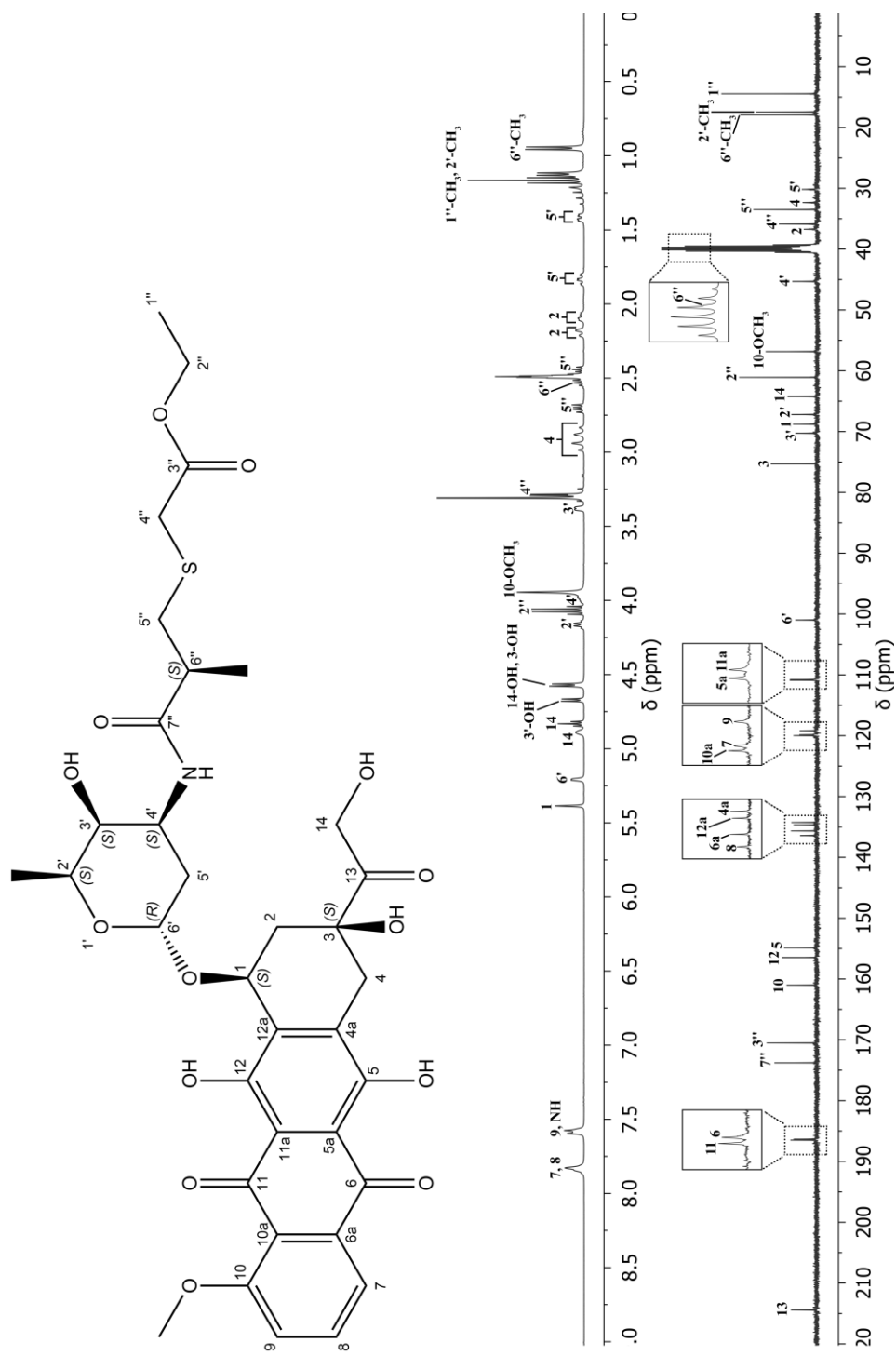
Figure 42 Representative ^1H NMR spectrum of compound 3b-1 in DMSO-d_6 (top) and ^{13}C NMR spectrum of compound 3b-1 in DMSO-d_6 (bottom).
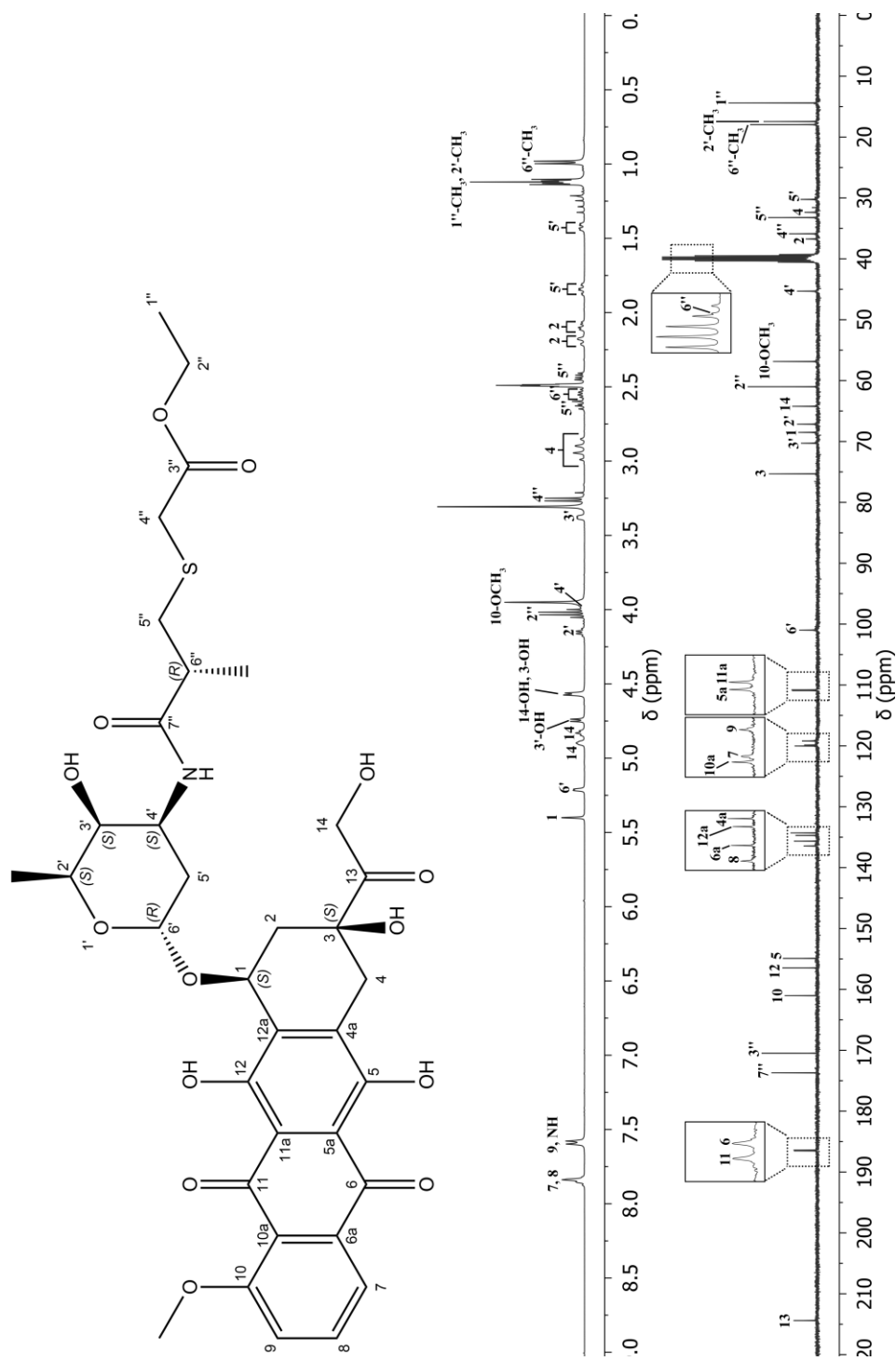
Figure 43 *Representative ^1H NMR spectrum of compound 3b-2 in DMSO-d$_6$ (top) and ^{13}C NMR spectrum of compound 3b-2 in DMSO-d$_6$ (bottom).*
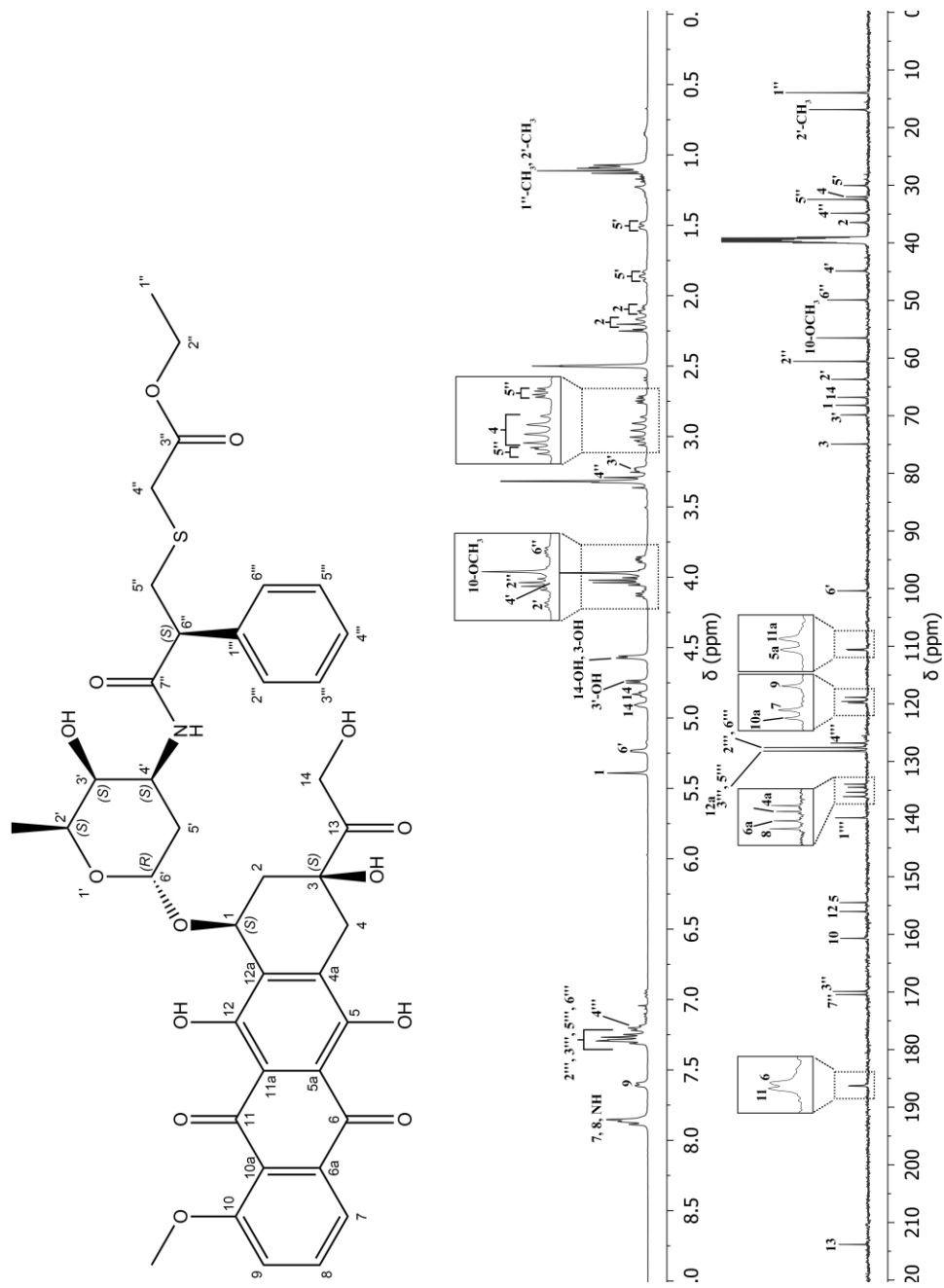
Figure 44 *Representative ^1H NMR spectrum of compound 3c-1 in DMSO-d_6 (top) and ^{13}C NMR spectrum of compound 3c-1 in DMSO-d_6 (bottom).*
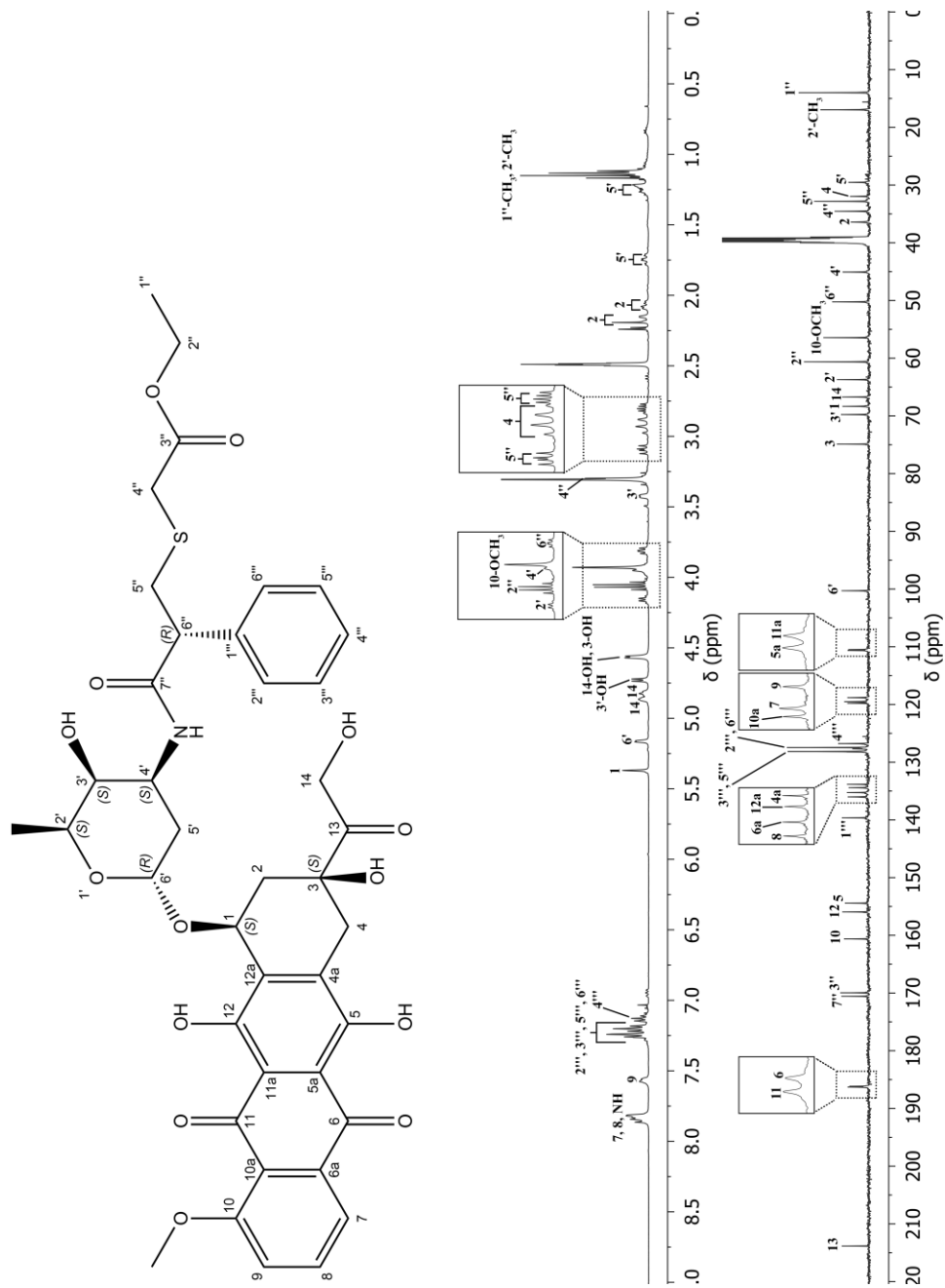
Figure 45 *Representative ^1H NMR spectrum of compound 3c-2 in DMSO-d_6 (top) and ^{13}C NMR spectrum of compound 3c-2 in DMSO-d_6 (bottom).*
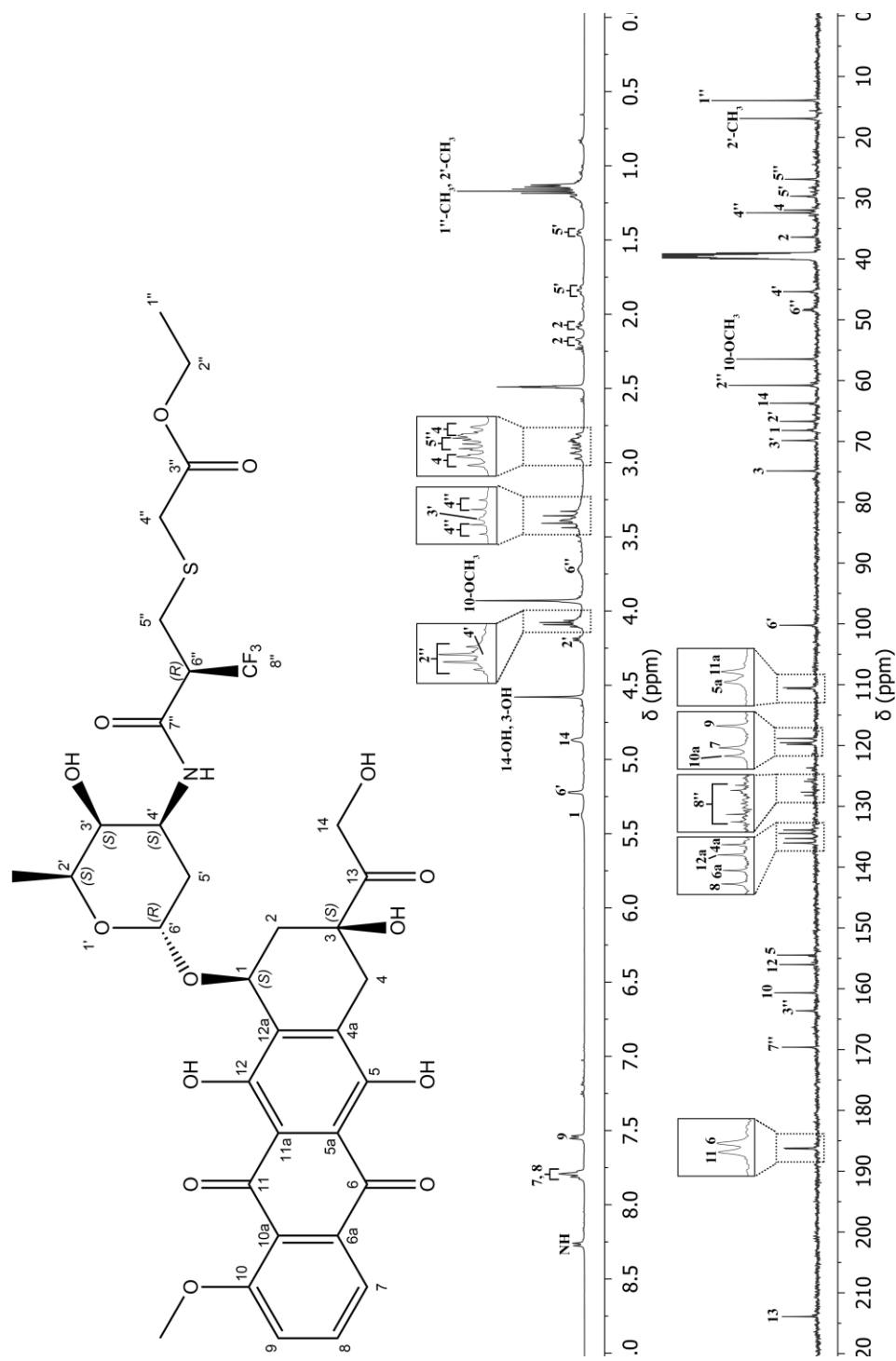
Figure 46 *Representative ^1H NMR spectrum of compound 3d-1 in DMSO-d_6 (top) and ^{13}C NMR spectrum of compound 3d-1 in DMSO-d_6 (bottom).*
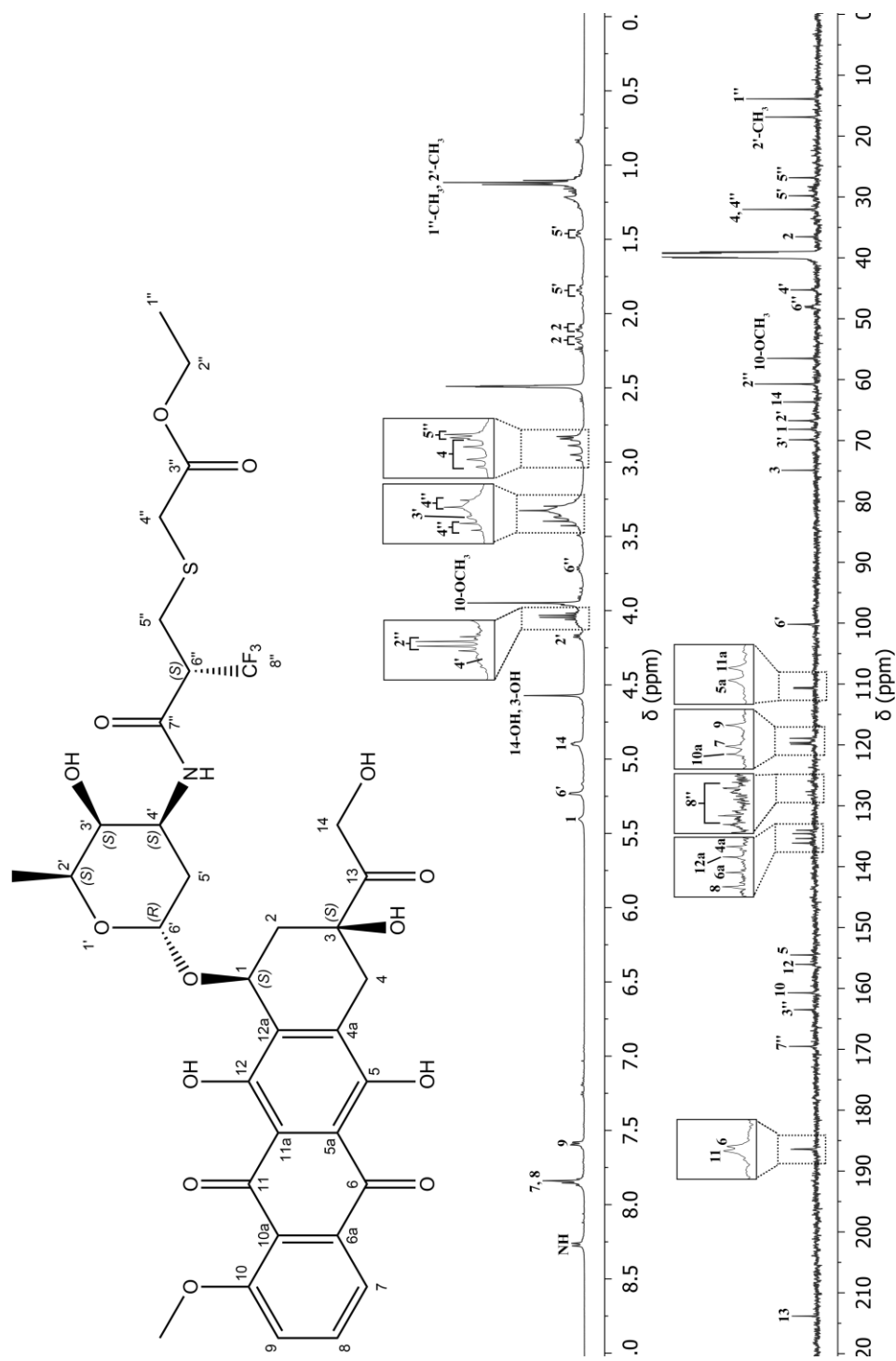
Figure 47 Representative ^1H NMR spectrum of compound 3d-2 in DMSO-d_6 (top) and ^{13}C NMR spectrum of compound 3d-2 in DMSO-d_6 (bottom).
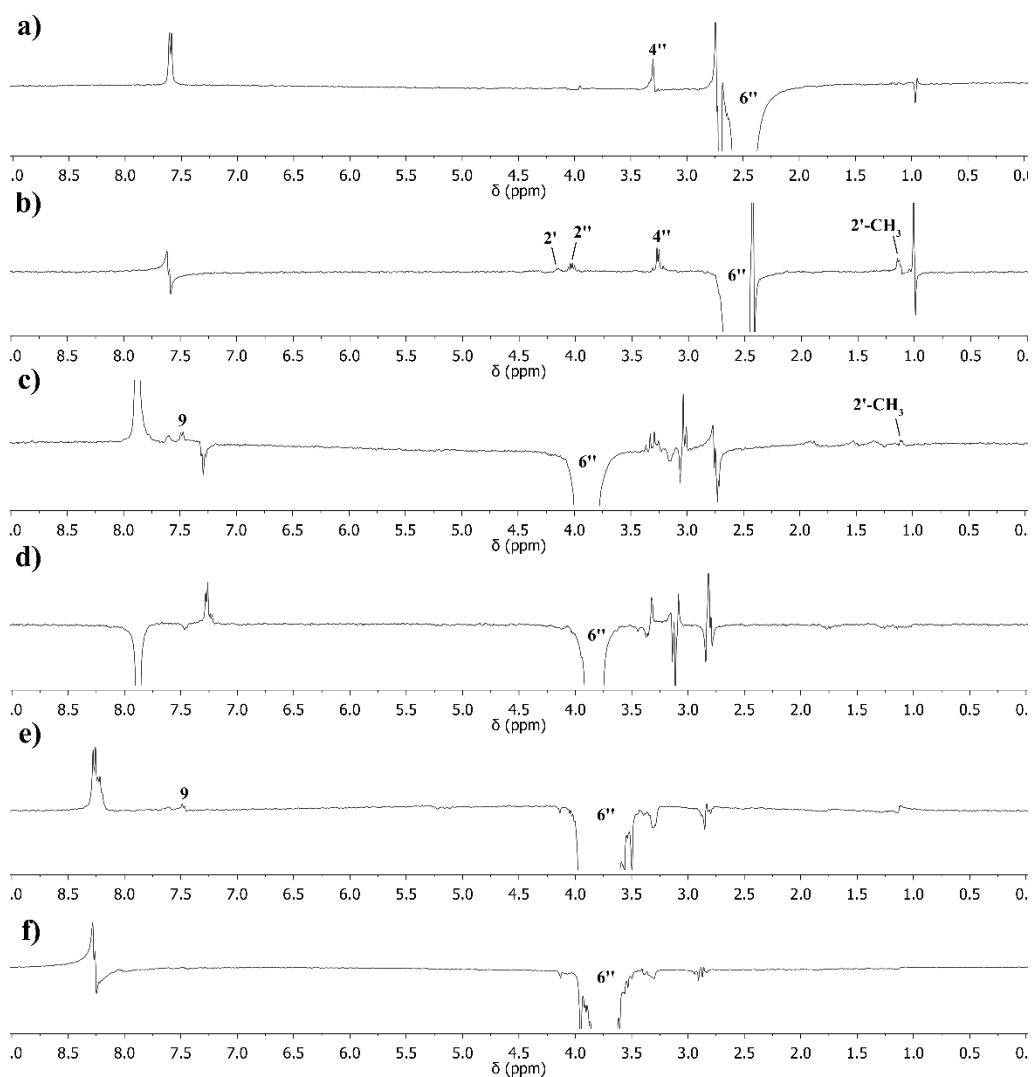
Figure 48 NOE difference spectra of diastereomeric compounds in DMSO-d_6. The NOE of a neighbor proton will present if it is close to 6"-proton. (a) 3b-1, (b) 3b-2, (c) 3c-1, (d) 3c-2, (e) 3d-1 and (f) 3d-2.

2. Mass spectrometry

DOX, beta-thiopropanamide substituents and DOX analogues was dissolved with methanol. The solution at 1 μg/ml was injected in mass spectrometer. Spectrum was recorded by electrospray ionization—time-of-flight mass spectrometry (ESI-TOF MS) technique (Bruker micrOTOF Q-II, Bruker, USA) and molecular weight was determined.
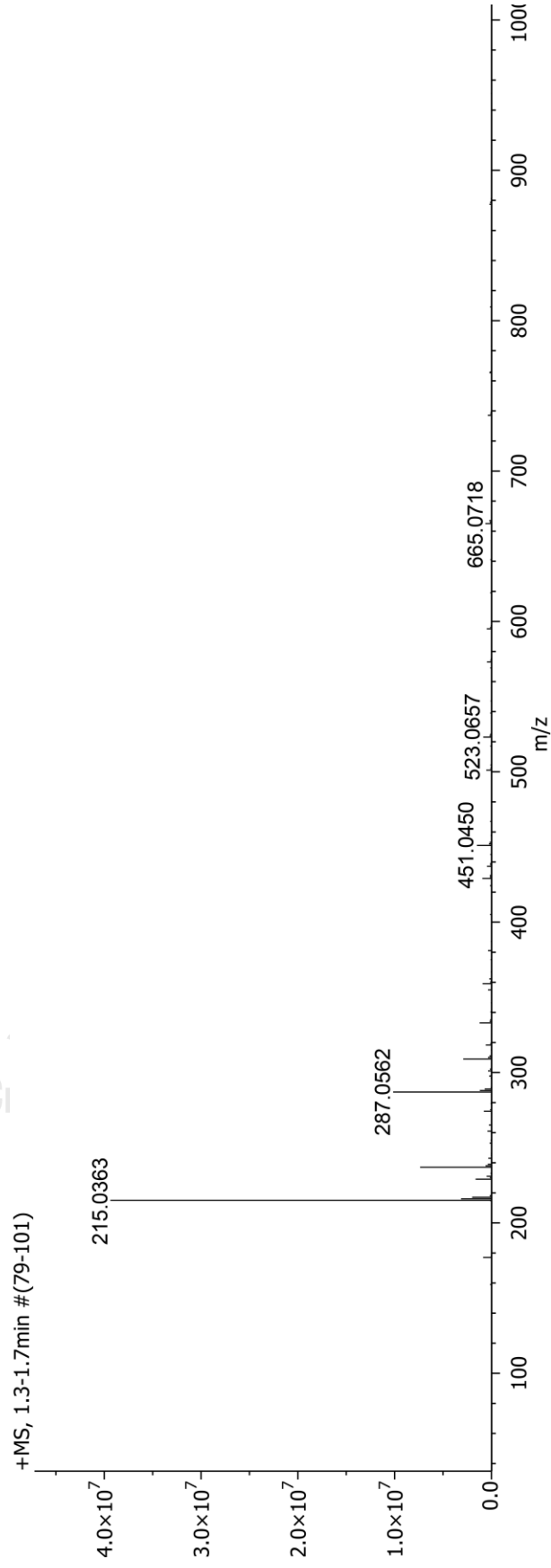
Figure 49 Representative mass spectrum of substituent 2a.

+MS, 1.6-2.0min #(94-122)

229.0524

316.1020

479.0761

707.1200

m/z
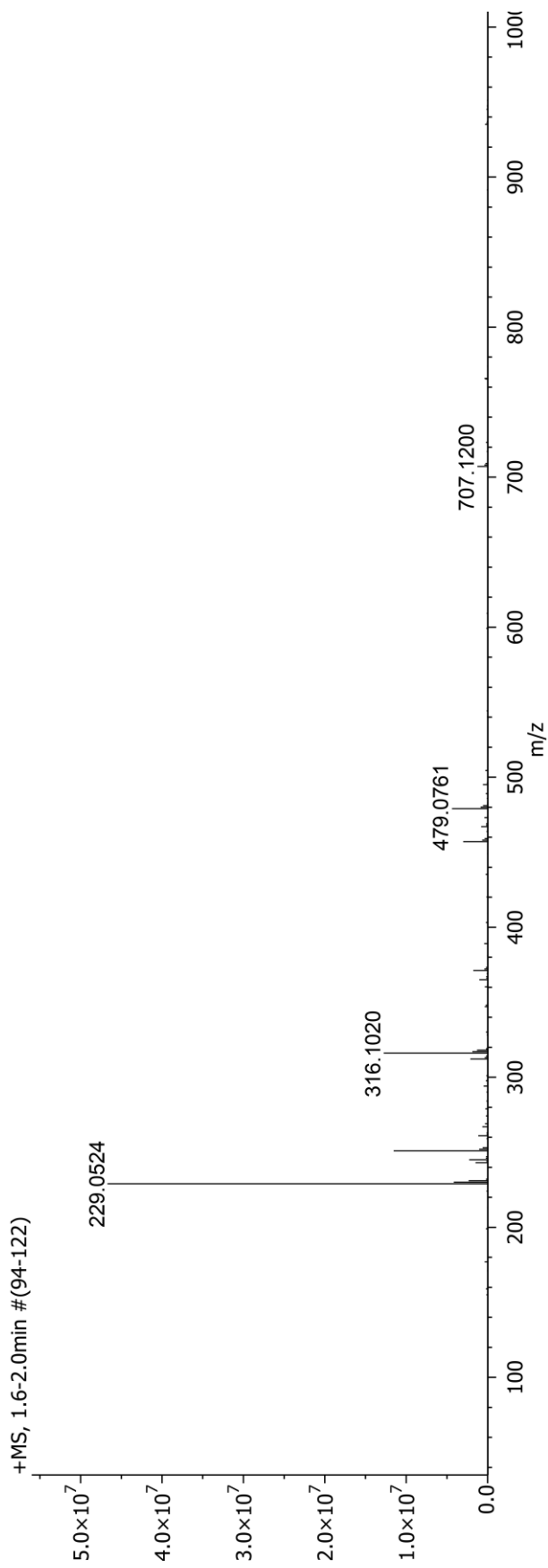
Figure 50 Representative mass spectrum of substituent 2b.

+MS, 1.9-2.4min #(113-145)
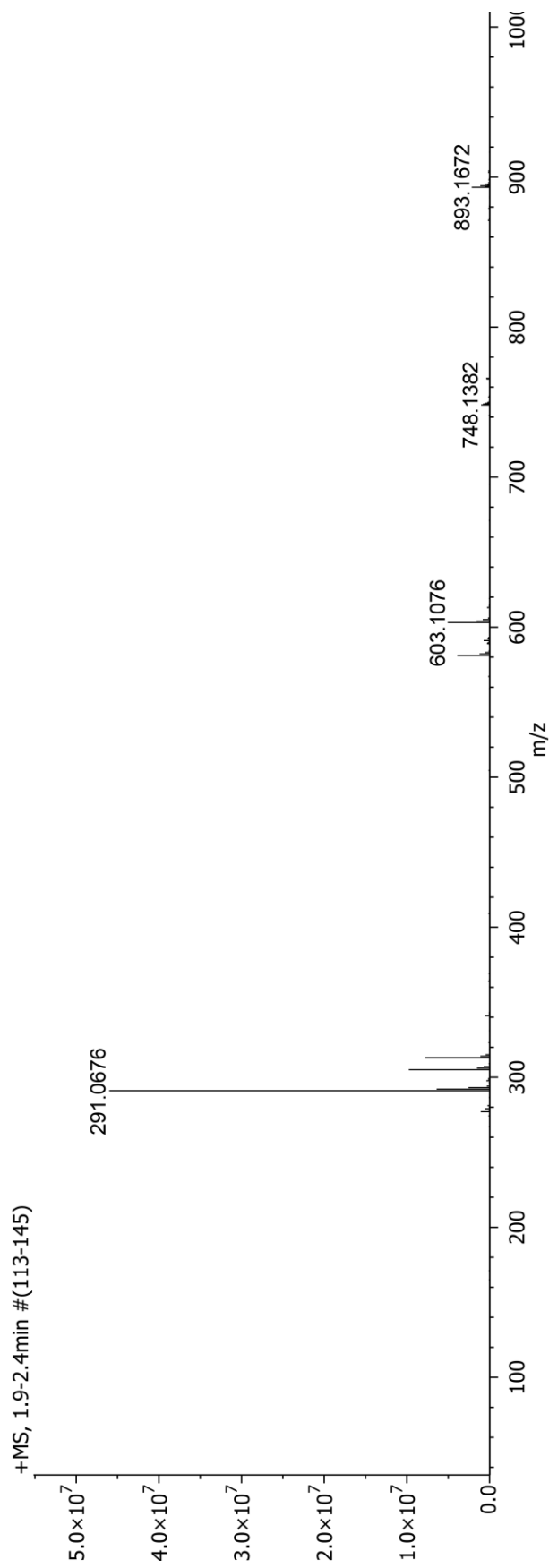
Figure 51 Representative mass spectrum of substituent 2c.

+MS, 1.2-1.7min #(72-100)

283.0239

224.1265

559.0212

819.0535

m/z
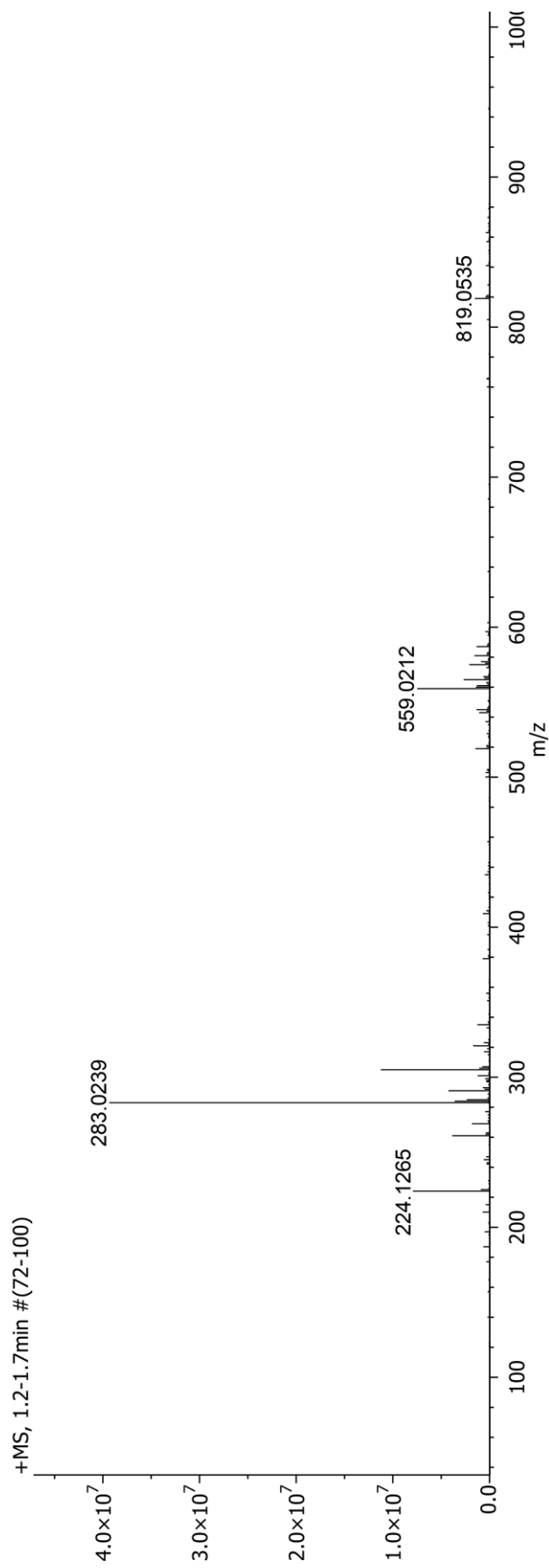
Figure 52 Representative mass spectrum of substituent 2d.

+MS, 1.2-1.6min #(72-98)

344.1135

740.1983

812.2170

m/z
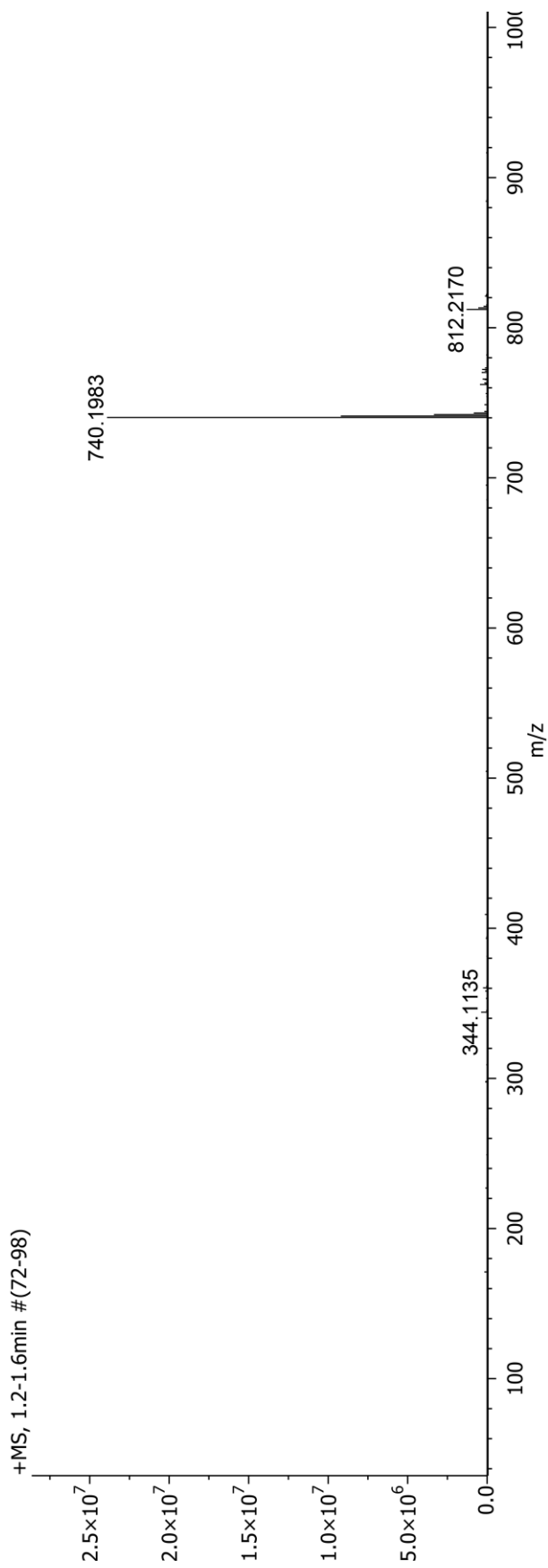
Figure 53 Representative mass spectrum of DOX analogue 3a.

+MS, 1.4-1.8min #(82-108)

171.0997   267.1570   360.3236   754.2157

m/z
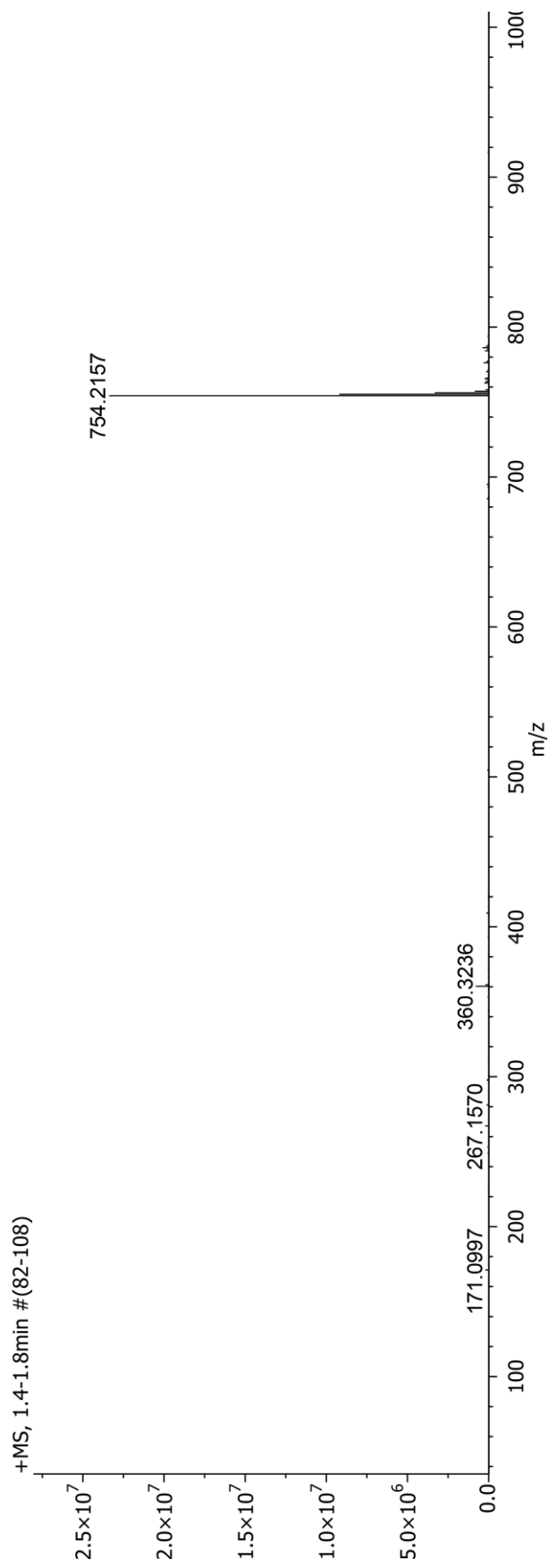
Figure 54 *Representative mass spectrum of DOX analogue 3b-1.*

+MS, 1.3-1.7min #(76-104)

754.2145

360.3231

m/z
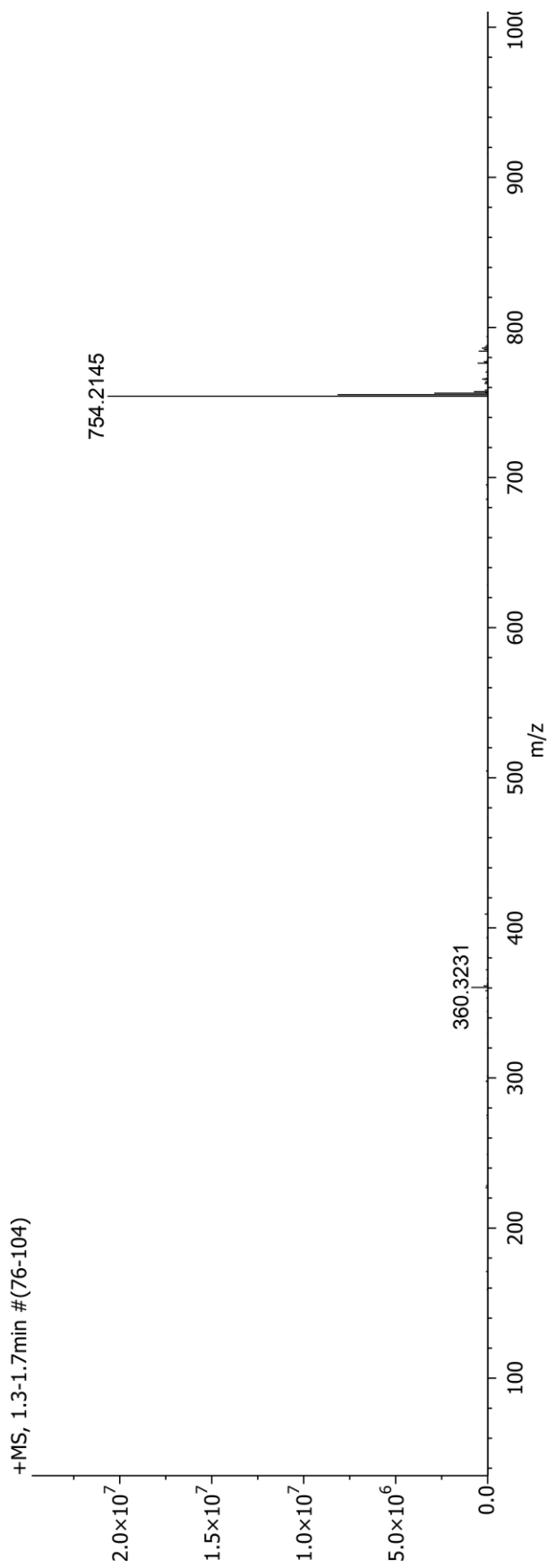
Figure 55 Representative mass spectrum of DOX analogue 3b-2.
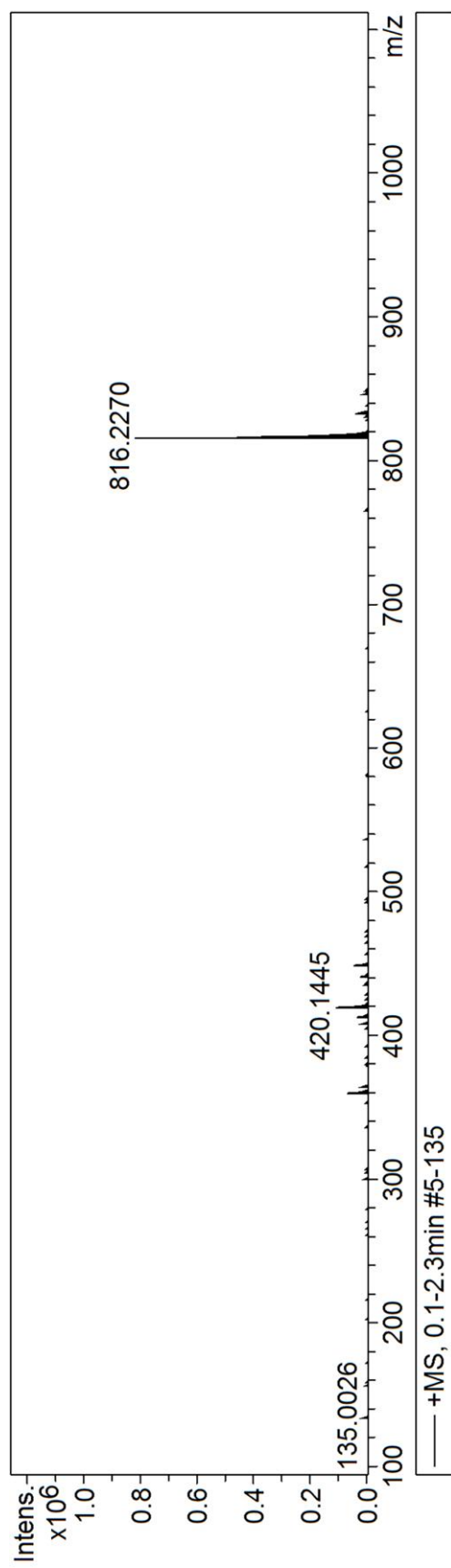
Figure 56 Representative mass spectrum of DOX analogue 3c-1.
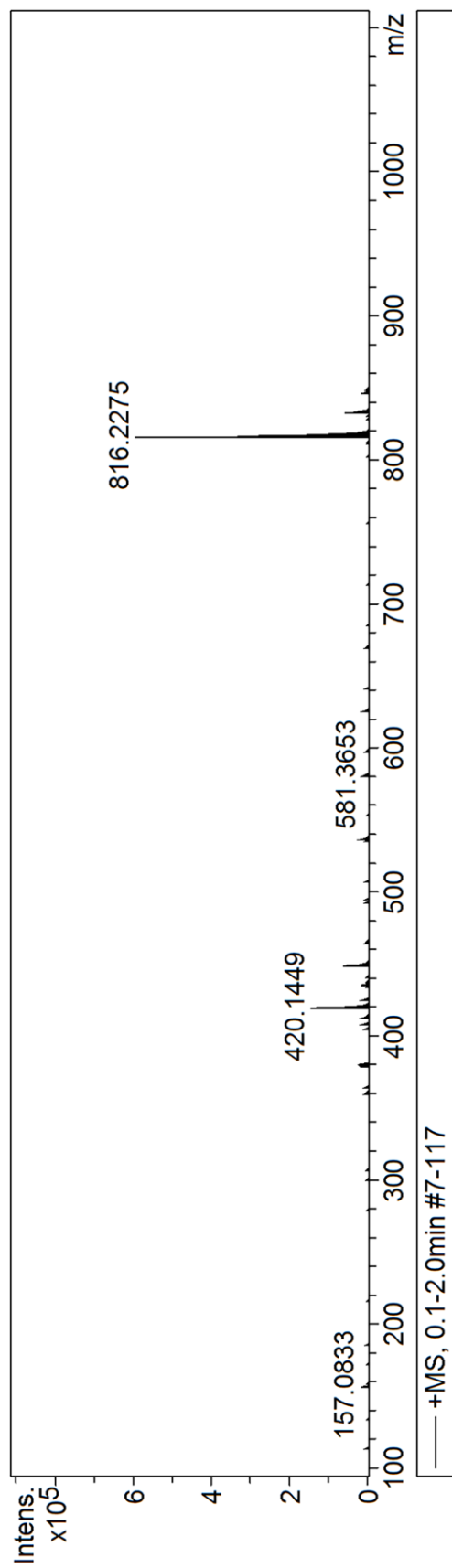
Figure 57 Representative mass spectrum of DOX analogue 3c-2.
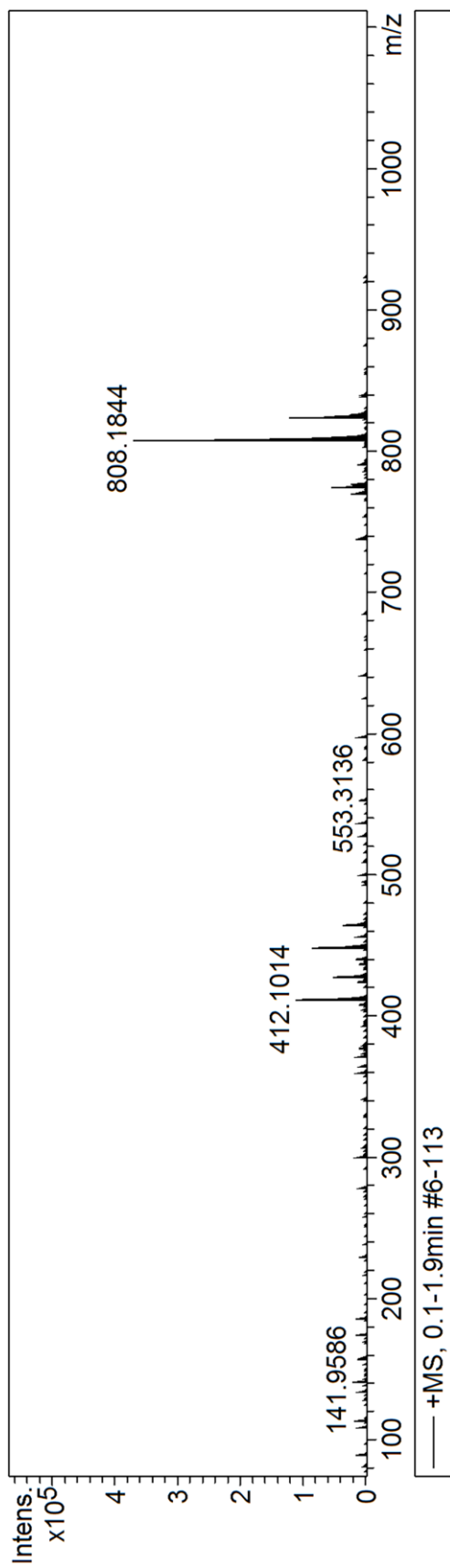
Figure 58 Representative mass spectrum of DOX analogue 3d-1.
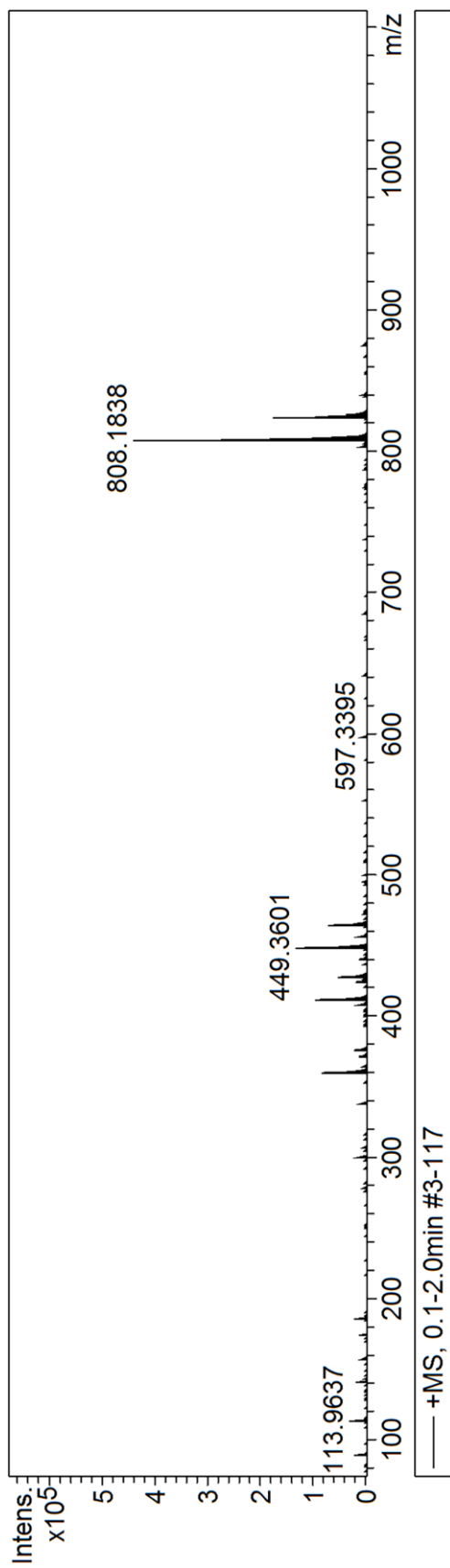
Figure 59 *Representative mass spectrum of DOX analogue 3d-2.*

APPENDIX B

HPLC chromatograms

1. Chromatogram of DOX, doxorubicinone and DOX analogues
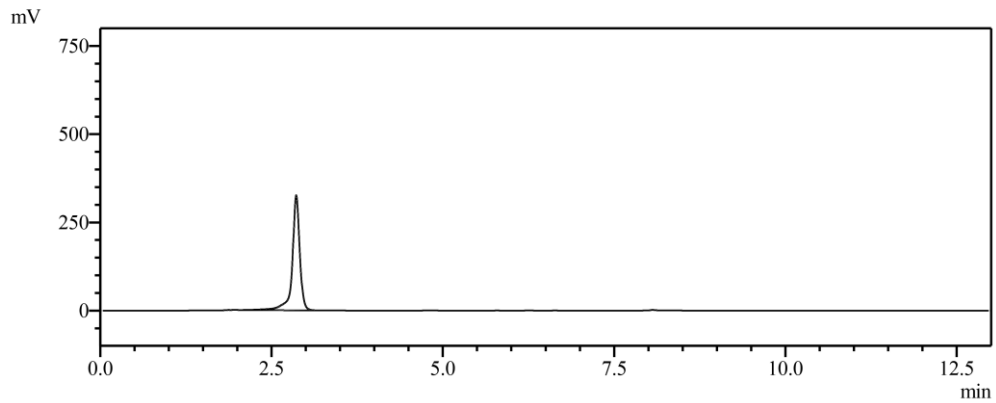
Figure 60 *HPLC chromatograms of doxorubicin standard with retention time at 2.8 minute*
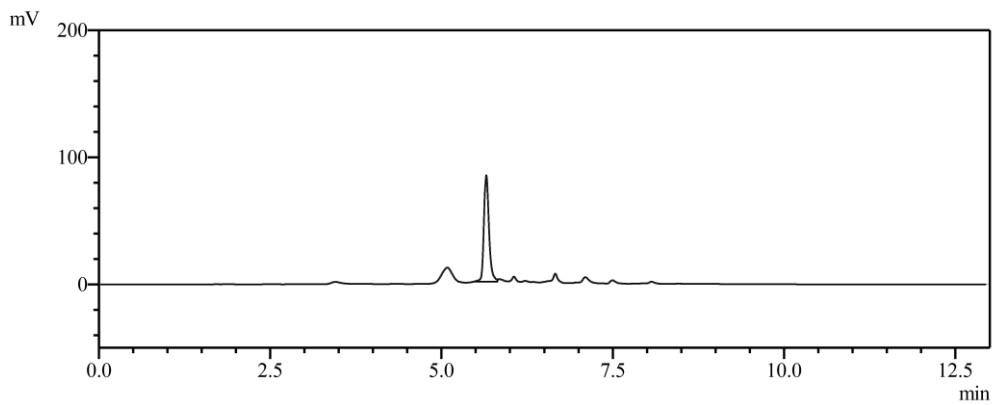
Figure 61 *HPLC chromatograms of doxorubicinone with retention time at 5.6 minute*
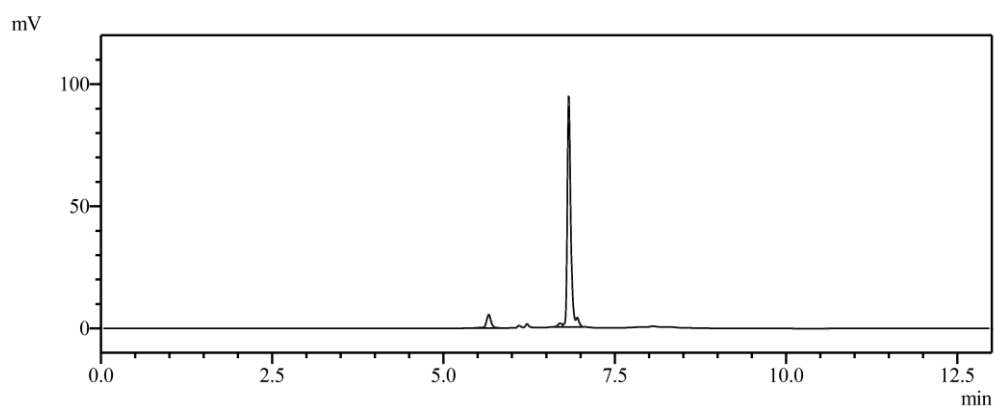
Figure 62 HPLC chromatograms of the DOX analogue 3a with retention time at 6.8 minute. The sample was taken after 24 h incubation at 37°C in acetate buffer pH 4.0
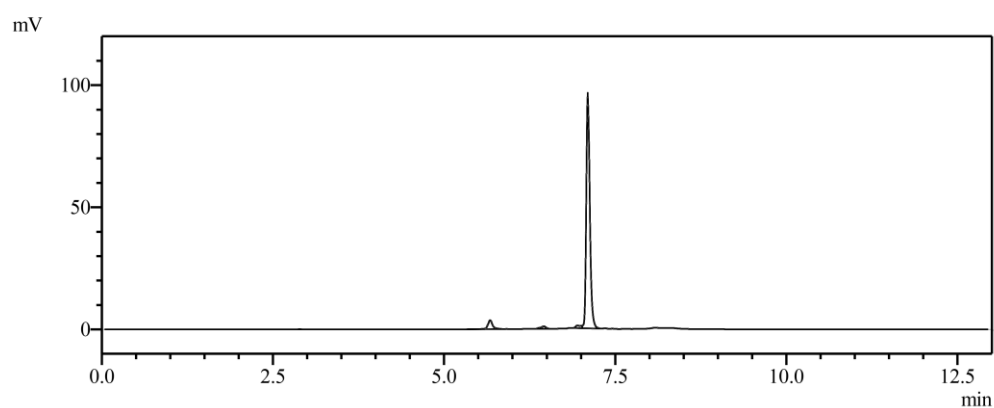
Figure 63 HPLC chromatograms of the DOX analogue 3b-1 with retention time at 6.9 minute. The sample was taken after 24 h incubation at 37°C in acetate buffer pH 4.0
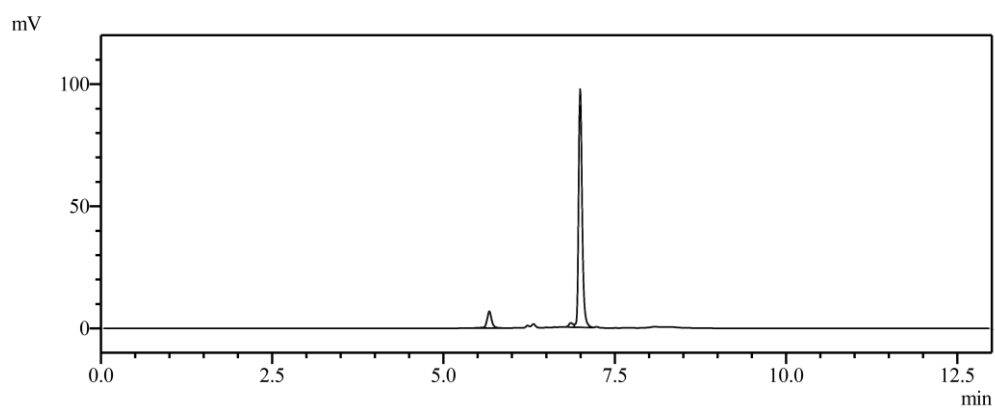
Figure 64 *HPLC chromatograms of the DOX analogue 3b-2 with retention time at 7.0 minute. The sample was taken after 24 h incubation at 37℃ in acetate buffer pH 4.0*
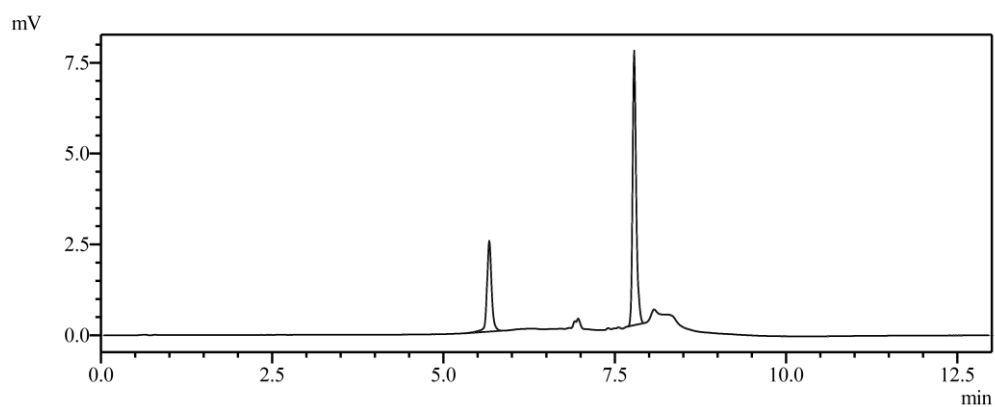
Figure 65 *HPLC chromatograms of the DOX analogue 3c-1 with retention time at 7.8 minute. The sample was taken after 8 h incubation at 37℃ in acetate buffer pH 4.0*
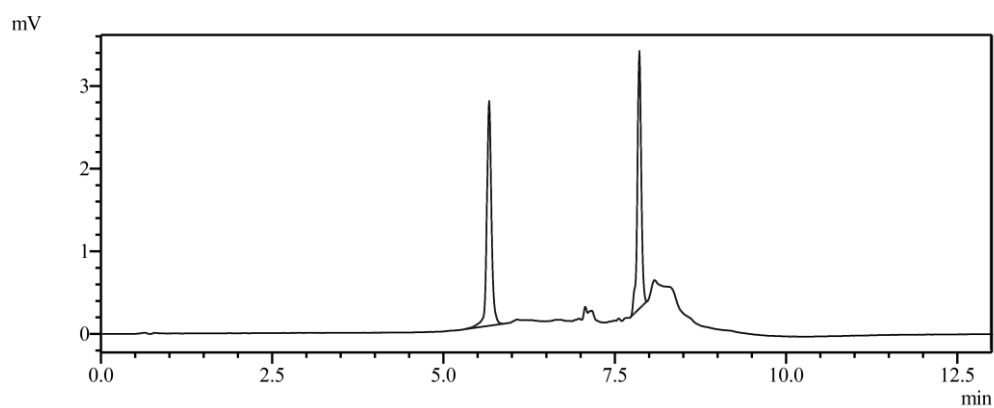
Figure 66 HPLC chromatograms of the DOX analogue 3c-2 with retention time at 7.9 minute. The sample was taken after 8 h incubation at 37℃ in acetate buffer pH 4.0
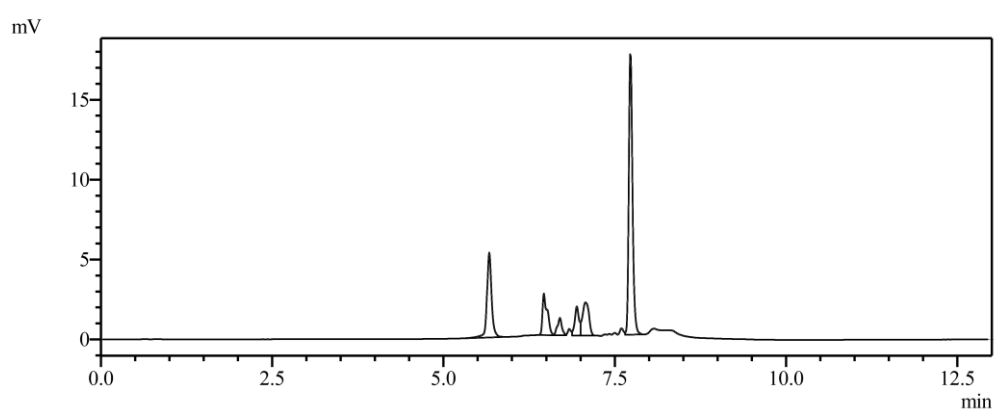
Figure 67 HPLC chromatograms of the DOX analogue 3d-1 with retention time at 7.7 minute. The sample was taken after 24 h incubation at 37℃ in acetate buffer pH 4.0
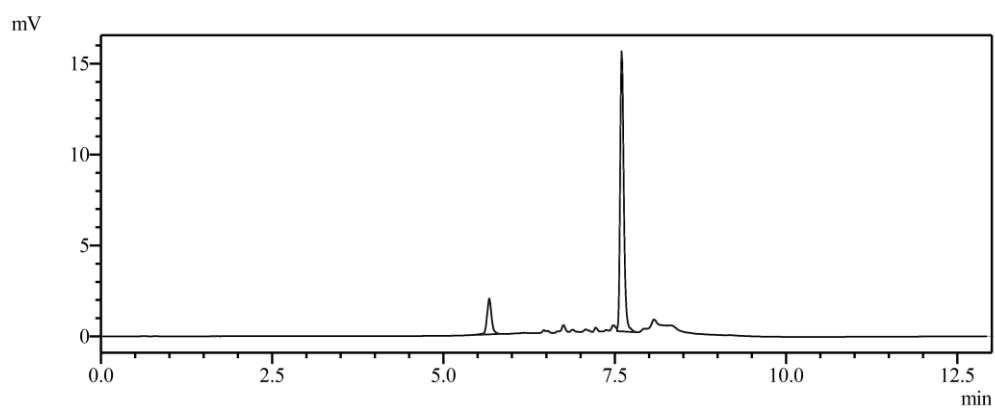
Figure 68 *HPLC chromatograms of the DOX analogue 3d-2 with retention time at 7.6 minute. The sample was taken after 24 h incubation at 37°C in acetate buffer pH 4.0*

2. Chromatogram of P-DOX and P-A-DOX conjugates
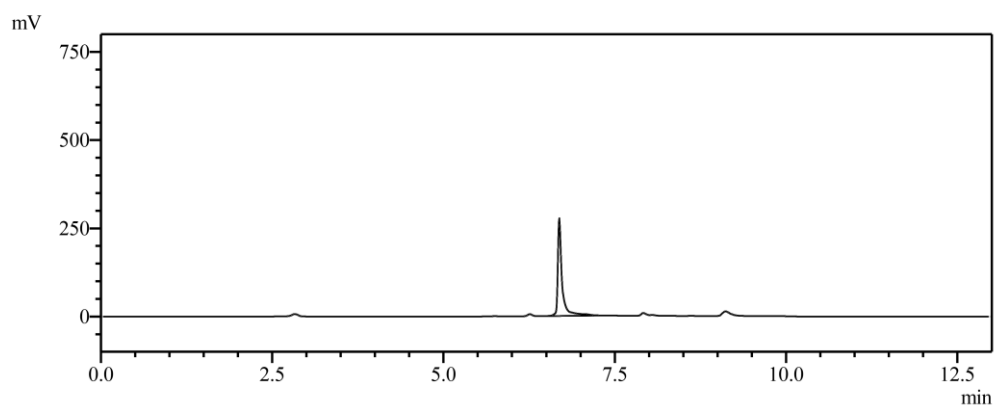
Figure 69 *HPLC chromatograms of the P-DOX conjugate with retention time at 6.7 minute. The sample was taken after 24 h incubation at 37°C in acetate buffer pH 4.0*
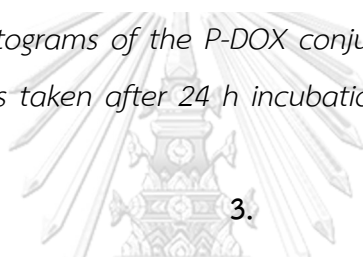
3.
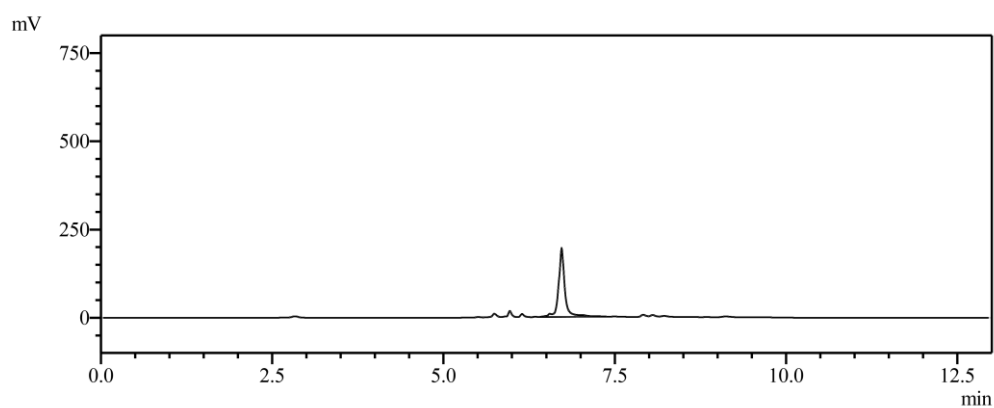
Figure 70 *HPLC chromatograms of the P-A-DOX conjugate with retention time at 6.6 minute. The sample was taken after 24 h incubation at 37°C in acetate buffer pH 4.0*

APPENDIX C

Characterization of mPEG-SH, mPEG-S-acrylic acid, P-DOX and P-A-DOX conjugates

1. Nuclear magnetic resonance (NMR) **spectroscopy**
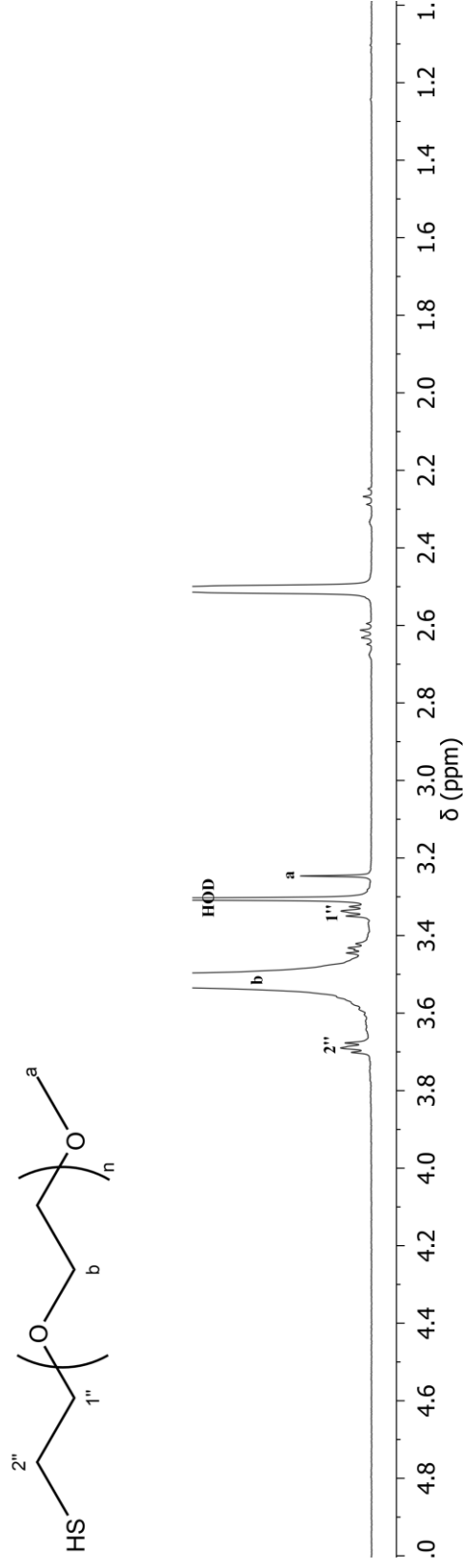
Figure 71 Representative ^{1}H NMR spectrum of mPEG-SH in DMSO-d_6
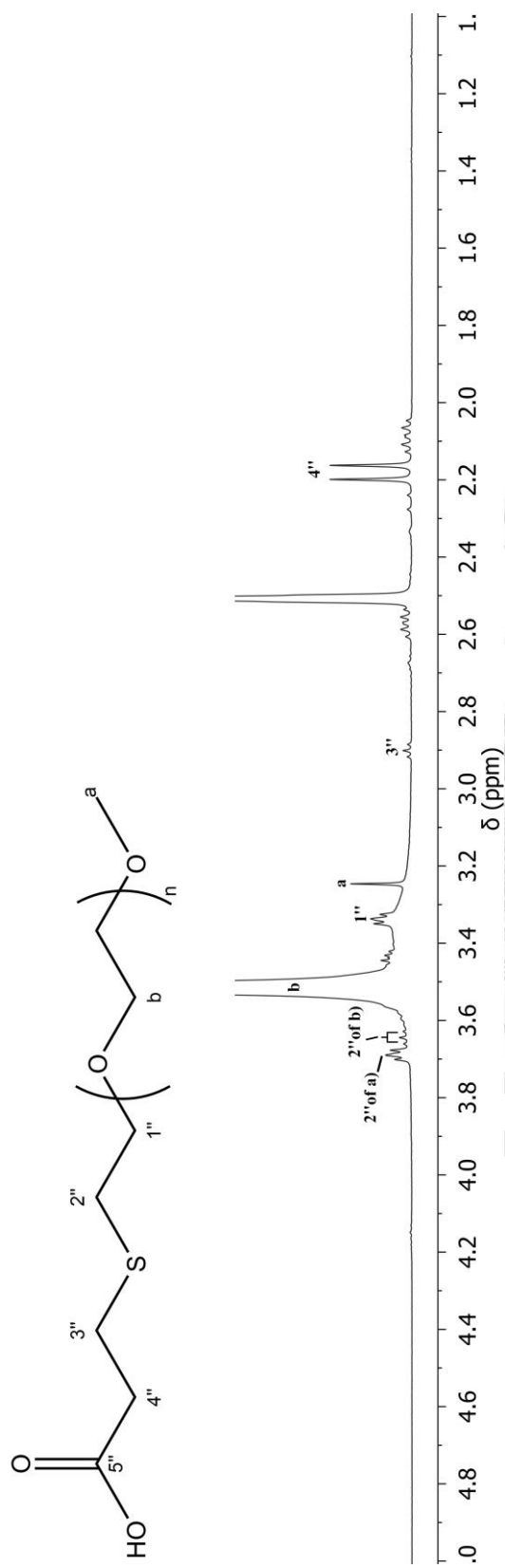
Figure 72 *Representative ^1H NMR spectrum of mPEG-S-acrylic acid in DMSO-d_6*

121
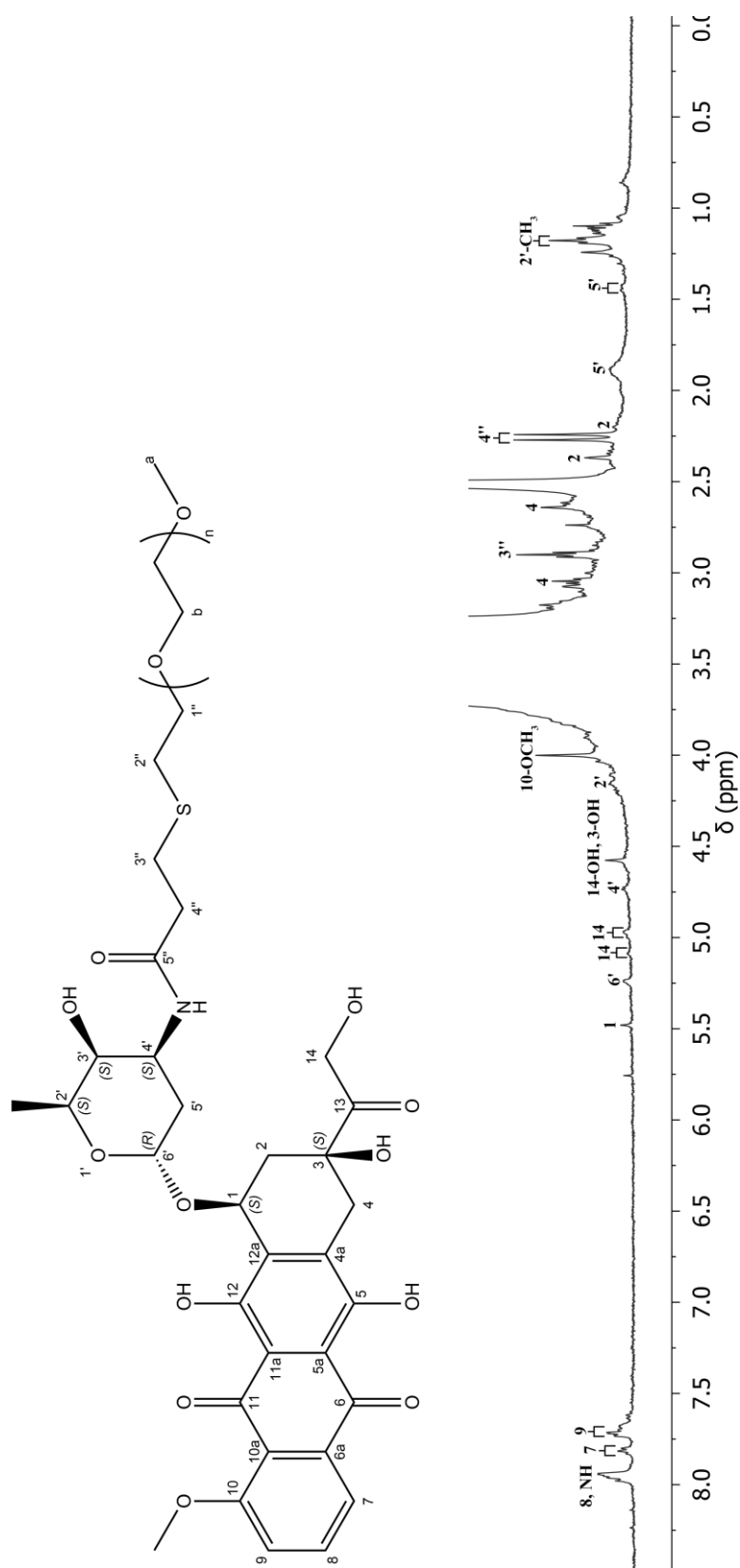
Figure 73 *Representative ^1H NMR spectrum of the P-A-DOX conjugate in DMSO-d_6*
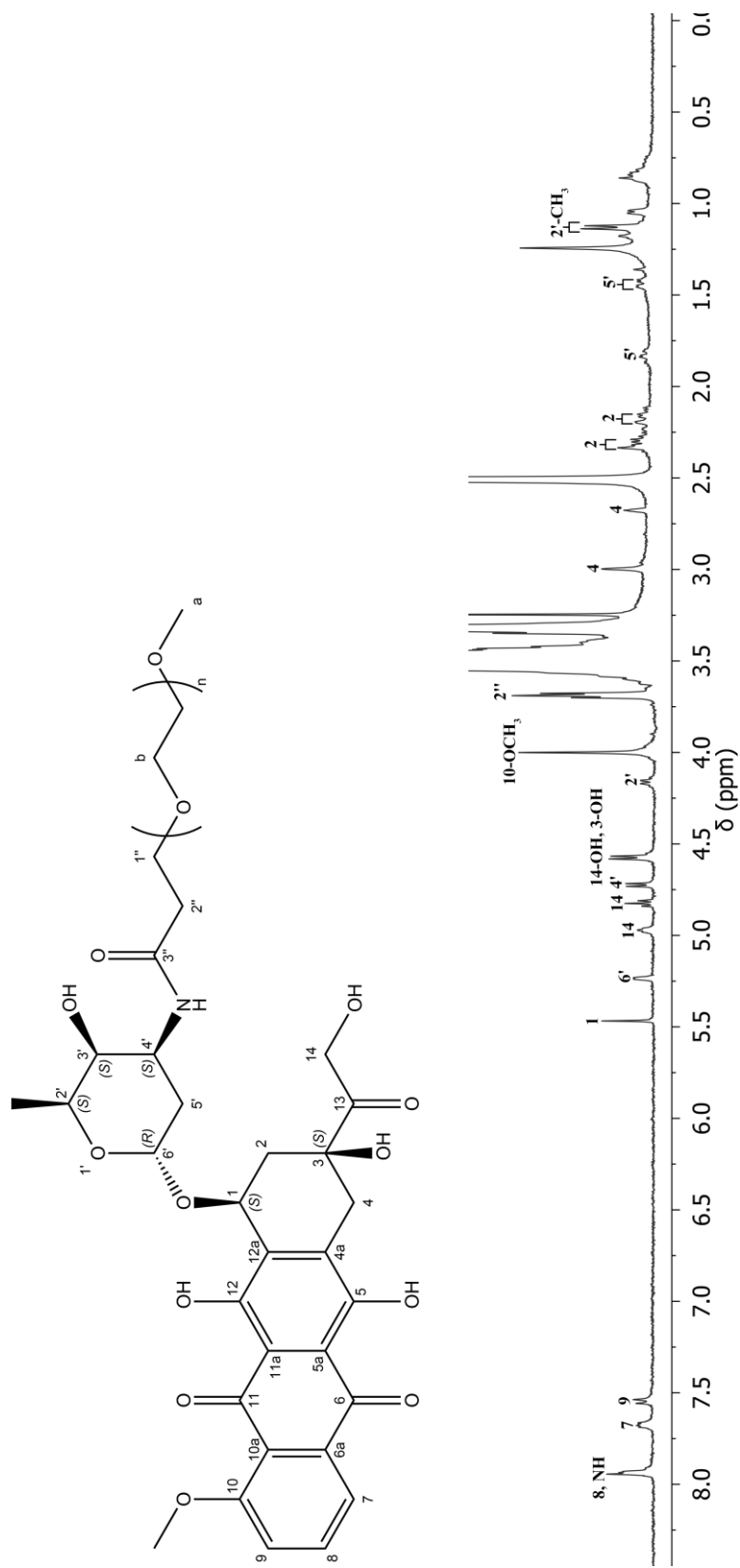
Figure 74 *Representative ^1H NMR spectrum of the P-DOX conjugate in DMSO-d_6*

APPENDIX D

Statistical analysis

1. Statistical analysis of *in vitro* stability of DOX and DOX analogues

   1.1. The Kinetic stability at pH 4.0 (significant level = 0.01)

One-Way ANOVA

		Sum of Squares	df	Mean Square	F	Sig.
$t_{1/2}$	Between Groups	391084.147	7	55869.164	3123.013	.000
	Within Groups	286.232	16	17.890		
	Total	391370.379	23			
k_{obs}	Between Groups	.267	7	.038	20164.527	.000
	Within Groups	.000	16	.000		
	Total	.267	23			

Multiple Comparisons (Post Hoc Test: Scheffe)

Dependent Variable		(I) Compound	(J) Compound	Mean Difference (I-J)	Std. Error	Sig.	99% Confidence Interval	
							Lower Bound	Upper Bound
$t_{1/2}$	Scheffe	3a	3b-1	-19.689667*	3.453453	.005	-38.02279	-1.35654
			3b-2	74.092667*	3.453453	.000	55.75954	92.42579
			3c-1	310.016333*	3.453453	.000	291.68321	328.34946
			3c-2	310.595667*	3.453453	.000	292.26254	328.92879
			3d-1	93.465000*	3.453453	.000	75.13187	111.79813
			3d-2	-29.490667*	3.453453	.000	-47.82379	-11.15754
			DOX	124.507667*	3.453453	.000	106.17454	142.84079
		3b-1	3a	19.689667*	3.453453	.005	1.35654	38.02279
			3b-2	93.782333*	3.453453	.000	75.44921	112.11546
			3c-1	329.706000*	3.453453	.000	311.37287	348.03913
			3c-2	330.285333*	3.453453	.000	311.95221	348.61846
			3d-1	113.154667*	3.453453	.000	94.82154	131.48779
			3d-2	-9.801000	3.453453	.382	-28.13413	8.53213
			DOX	144.197333*	3.453453	.000	125.86421	162.53046
		3b-2	3a	-74.092667*	3.453453	.000	-92.42579	-55.75954
			3b-1	-93.782333*	3.453453	.000	-112.11546	-75.44921
			3c-1	235.923667*	3.453453	.000	217.59054	254.25679

			3c-2	236.503000*	3.453453	.000	218.16987	254.83613
			3d-1	19.372333*	3.453453	.006	1.03921	37.70546
			3d-2	-103.583333*	3.453453	.000	-121.91646	-85.25021
			DOX	50.415000*	3.453453	.000	32.08187	68.74813
		3c-1	3a	-310.016333*	3.453453	.000	-328.34946	-291.68321
			3b-1	-329.706000*	3.453453	.000	-348.03913	-311.37287
			3b-2	-235.923667*	3.453453	.000	-254.25679	-217.59054
			3c-2	.579333	3.453453	1.000	-17.75379	18.91246
			3d-1	-216.551333*	3.453453	.000	-234.88446	-198.21821
			3d-2	-339.507000*	3.453453	.000	-357.84013	-321.17387
			DOX	-185.508667*	3.453453	.000	-203.84179	-167.17554
		3c-2	3a	-310.595667*	3.453453	.000	-328.92879	-292.26254
			3b-1	-330.285333*	3.453453	.000	-348.61846	-311.95221
			3b-2	-236.503000*	3.453453	.000	-254.83613	-218.16987
			3c-1	-.579333	3.453453	1.000	-18.91246	17.75379
			3d-1	-217.130667*	3.453453	.000	-235.46379	-198.79754
			3d-2	-340.086333*	3.453453	.000	-358.41946	-321.75321
			DOX	-186.088000*	3.453453	.000	-204.42113	-167.75487
		3d-1	3a	-93.465000*	3.453453	.000	-111.79813	-75.13187
			3b-1	-113.154667*	3.453453	.000	-131.48779	-94.82154
			3b-2	-19.372333*	3.453453	.006	-37.70546	-1.03921
			3c-1	216.551333*	3.453453	.000	198.21821	234.88446
			3c-2	217.130667*	3.453453	.000	198.79754	235.46379
			3d-2	-122.955667*	3.453453	.000	-141.28879	-104.62254
			DOX	31.042667*	3.453453	.000	12.70954	49.37579
		3d-2	3a	29.490667*	3.453453	.000	11.15754	47.82379
			3b-1	9.801000	3.453453	.382	-8.53213	28.13413
			3b-2	103.583333*	3.453453	.000	85.25021	121.91646
			3c-1	339.507000*	3.453453	.000	321.17387	357.84013
			3c-2	340.086333*	3.453453	.000	321.75321	358.41946
			3d-1	122.955667*	3.453453	.000	104.62254	141.28879
			DOX	153.998333*	3.453453	.000	135.66521	172.33146
		DOX	3a	-124.507667*	3.453453	.000	-142.84079	-106.17454
			3b-1	-144.197333*	3.453453	.000	-162.53046	-125.86421
			3b-2	-50.415000*	3.453453	.000	-68.74813	-32.08187
			3c-1	185.508667*	3.453453	.000	167.17554	203.84179

k_{obs}	Scheffe							
			3c-2	186.088000*	3.453453	.000	167.75487	204.42113
			3d-1	-31.042667*	3.453453	.000	-49.37579	-12.70954
			3d-2	-153.998333*	3.453453	.000	-172.33146	-135.66521
k_{obs}	Scheffe	3a	3b-1	.000131000	.001122025	1.000	-.00582542	.00608742
			3b-2	-.000685000	.001122025	1.000	-.00664142	.00527142
			3c-1	-.217459333*	.001122025	.000	-.22341576	-.21150291
			3c-2	-.266861667*	.001122025	.000	-.27281809	-.26090524
			3d-1	-.000940667	.001122025	.998	-.00689709	.00501576
			3d-2	.000191333	.001122025	1.000	-.00576509	.00614776
			DOX	-.001460667	.001122025	.968	-.00741709	.00449576
		3b-1	3a	-.000131000	.001122025	1.000	-.00608742	.00582542
			3b-2	-.000816000	.001122025	.999	-.00677242	.00514042
			3c-1	-.217590333*	.001122025	.000	-.22354676	-.21163391
			3c-2	-.266992667*	.001122025	.000	-.27294909	-.26103624
			3d-1	-.001071667	.001122025	.995	-.00702809	.00488476
			3d-2	.000060333	.001122025	1.000	-.00589609	.00601676
			DOX	-.001591667	.001122025	.949	-.00754809	.00436476
		3b-2	3a	.000685000	.001122025	1.000	-.00527142	.00664142
			3b-1	.000816000	.001122025	.999	-.00514042	.00677242
			3c-1	-.216774333*	.001122025	.000	-.22273076	-.21081791
			3c-2	-.266176667*	.001122025	.000	-.27213309	-.26022024
			3d-1	-.000255667	.001122025	1.000	-.00621209	.00570076
			3d-2	.000876333	.001122025	.998	-.00508009	.00683276
			DOX	-.000775667	.001122025	.999	-.00673209	.00518076
		3c-1	3a	.217459333*	.001122025	.000	.21150291	.22341576
			3b-1	.217590333*	.001122025	.000	.21163391	.22354676
			3b-2	.216774333*	.001122025	.000	.21081791	.22273076
			3c-2	-.049402333*	.001122025	.000	-.05535876	-.04344591
			3d-1	.216518667*	.001122025	.000	.21056224	.22247509
			3d-2	.217650667*	.001122025	.000	.21169424	.22360709
			DOX	.215998667*	.001122025	.000	.21004224	.22195509
		3c-2	3a	.266861667*	.001122025	.000	.26090524	.27281809
			3b-1	.266992667*	.001122025	.000	.26103624	.27294909
			3b-2	.266176667*	.001122025	.000	.26022024	.27213309
			3c-1	.049402333*	.001122025	.000	.04344591	.05535876
			3d-1	.265921000*	.001122025	.000	.25996458	.27187742

			3d-2	.267053000*	.001122025	.000	.26109658	.27300942
			DOX	.265401000*	.001122025	.000	.25944458	.27135742
		3d-1	3a	.000940667	.001122025	.998	-.00501576	.00689709
			3b-1	.001071667	.001122025	.995	-.00488476	.00702809
			3b-2	.000255667	.001122025	1.000	-.00570076	.00621209
			3c-1	-.216518667*	.001122025	.000	-.22247509	-.21056224
			3c-2	-.265921000*	.001122025	.000	-.27187742	-.25996458
			3d-2	.001132000	.001122025	.992	-.00482442	.00708842
			DOX	-.000520000	.001122025	1.000	-.00647642	.00543642
		3d-2	3a	-.000191333	.001122025	1.000	-.00614776	.00576509
			3b-1	-.000060333	.001122025	1.000	-.00601676	.00589609
			3b-2	-.000876333	.001122025	.998	-.00683276	.00508009
			3c-1	-.217650667*	.001122025	.000	-.22360709	-.21169424
			3c-2	-.267053000*	.001122025	.000	-.27300942	-.26109658
			3d-1	-.001132000	.001122025	.992	-.00708842	.00482442
			DOX	-.001652000	.001122025	.939	-.00760842	.00430442
		DOX	3a	.001460667	.001122025	.968	-.00449576	.00741709
			3b-1	.001591667	.001122025	.949	-.00436476	.00754809
			3b-2	.000775667	.001122025	.999	-.00518076	.00673209
			3c-1	-.215998667*	.001122025	.000	-.22195509	-.21004224
			3c-2	-.265401000*	.001122025	.000	-.27135742	-.25944458
			3d-1	.000520000	.001122025	1.000	-.00543642	.00647642
			3d-2	.001652000	.001122025	.939	-.00430442	.00760842

*. The mean difference is significant at the 0.01 level.

1.2. The Kinetic stability at pH 5.5 (significant level = 0.01)

One-Way ANOVA

		Sum of Squares	df	Mean Square	F	Sig.
$t_{1/2}$	Between Groups	705155.004	7	100736.429	10182.989	.000
	Within Groups	158.282	16	9.893		
	Total	705313.286	23			
k_{obs}	Between Groups	.256	7	.037	13655.645	.000
	Within Groups	.000	16	.000		
	Total	.256	23			

Multiple Comparisons (Post Hoc Test: Scheffe)

Dependent Variable		(I) Compound	(J) Compound	Mean Difference (I-J)	Std. Error	Sig.	99% Confidence Interval Lower Bound	99% Confidence Interval Upper Bound
$t_{1/2}$	Scheffe	3a	3b-1	72.634667*	2.568089	.000	59.00162	86.26772
			3b-2	-242.821333*	2.568089	.000	-256.45438	-229.18828
			3c-1	311.895667*	2.568089	.000	298.26262	325.52872
			3c-2	312.943667*	2.568089	.000	299.31062	326.57672
			3d-1	116.845000*	2.568089	.000	103.21195	130.47805
			3d-2	102.757333*	2.568089	.000	89.12428	116.39038
			DOX	232.954667*	2.568089	.000	219.32162	246.58772
		3b-1	3a	-72.634667*	2.568089	.000	-86.26772	-59.00162
			3b-2	-315.456000*	2.568089	.000	-329.08905	-301.82295
			3c-1	239.261000*	2.568089	.000	225.62795	252.89405
			3c-2	240.309000*	2.568089	.000	226.67595	253.94205
			3d-1	44.210333*	2.568089	.000	30.57728	57.84338
			3d-2	30.122667*	2.568089	.000	16.48962	43.75572
			DOX	160.320000*	2.568089	.000	146.68695	173.95305
		3b-2	3a	242.821333*	2.568089	.000	229.18828	256.45438
			3b-1	315.456000*	2.568089	.000	301.82295	329.08905
			3c-1	554.717000*	2.568089	.000	541.08395	568.35005
			3c-2	555.765000*	2.568089	.000	542.13195	569.39805
			3d-1	359.666333*	2.568089	.000	346.03328	373.29938
			3d-2	345.578667*	2.568089	.000	331.94562	359.21172
			DOX	475.776000*	2.568089	.000	462.14295	489.40905

		(I)	(J)	Mean Difference	Std. Error	Sig.	Lower Bound	Upper Bound
		3c-1	3a	-311.895667*	2.568089	.000	-325.52872	-298.26262
			3b-1	-239.261000*	2.568089	.000	-252.89405	-225.62795
			3b-2	-554.717000*	2.568089	.000	-568.35005	-541.08395
			3c-2	1.048000	2.568089	1.000	-12.58505	14.68105
			3d-1	-195.050667*	2.568089	.000	-208.68372	-181.41762
			3d-2	-209.138333*	2.568089	.000	-222.77138	-195.50528
			DOX	-78.941000*	2.568089	.000	-92.57405	-65.30795
		3c-2	3a	-312.943667*	2.568089	.000	-326.57672	-299.31062
			3b-1	-240.309000*	2.568089	.000	-253.94205	-226.67595
			3b-2	-555.765000*	2.568089	.000	-569.39805	-542.13195
			3c-1	-1.048000	2.568089	1.000	-14.68105	12.58505
			3d-1	-196.098667*	2.568089	.000	-209.73172	-182.46562
			3d-2	-210.186333*	2.568089	.000	-223.81938	-196.55328
			DOX	-79.989000*	2.568089	.000	-93.62205	-66.35595
		3d-1	3a	-116.845000*	2.568089	.000	-130.47805	-103.21195
			3b-1	-44.210333*	2.568089	.000	-57.84338	-30.57728
			3b-2	-359.666333*	2.568089	.000	-373.29938	-346.03328
			3c-1	195.050667*	2.568089	.000	181.41762	208.68372
			3c-2	196.098667*	2.568089	.000	182.46562	209.73172
			3d-2	-14.087667*	2.568089	.007	-27.72072	-.45462
			DOX	116.109667*	2.568089	.000	102.47662	129.74272
		3d-2	3a	-102.757333*	2.568089	.000	-116.39038	-89.12428
			3b-1	-30.122667*	2.568089	.000	-43.75572	-16.48962
			3b-2	-345.578667*	2.568089	.000	-359.21172	-331.94562
			3c-1	209.138333*	2.568089	.000	195.50528	222.77138
			3c-2	210.186333*	2.568089	.000	196.55328	223.81938
			3d-1	14.087667*	2.568089	.007	.45462	27.72072
			DOX	130.197333*	2.568089	.000	116.56428	143.83038
		DOX	3a	-232.954667*	2.568089	.000	-246.58772	-219.32162
			3b-1	-160.320000*	2.568089	.000	-173.95305	-146.68695
			3b-2	-475.776000*	2.568089	.000	-489.40905	-462.14295
			3c-1	78.941000*	2.568089	.000	65.30795	92.57405
			3c-2	79.989000*	2.568089	.000	66.35595	93.62205
			3d-1	-116.109667*	2.568089	.000	-129.74272	-102.47662
			3d-2	-130.197333*	2.568089	.000	-143.83038	-116.56428
k_{obs}	Scheffe	3a	3b-1	-.000657000	.001335780	1.000	-.00774817	.00643417

			3b-2	.000956000	.001335780	.999	-.00613517	.00804717
			3c-1	-.193740667*	.001335780	.000	-.20083184	-.18664949
			3c-2	-.276201667*	.001335780	.000	-.28329284	-.26911049
			3d-1	-.001292667	.001335780	.994	-.00838384	.00579851
			3d-2	-.001061667	.001335780	.998	-.00815284	.00602951
			DOX	-.006206000	.001335780	.029	-.01329717	.00088517
		3b-1	3a	.000657000	.001335780	1.000	-.00643417	.00774817
			3b-2	.001613000	.001335780	.979	-.00547817	.00870417
			3c-1	-.193083667*	.001335780	.000	-.20017484	-.18599249
			3c-2	-.275544667*	.001335780	.000	-.28263584	-.26845349
			3d-1	-.000635667	.001335780	1.000	-.00772684	.00645551
			3d-2	-.000404667	.001335780	1.000	-.00749584	.00668651
			DOX	-.005549000	.001335780	.064	-.01264017	.00154217
		3b-2	3a	-.000956000	.001335780	.999	-.00804717	.00613517
			3b-1	-.001613000	.001335780	.979	-.00870417	.00547817
			3c-1	-.194696667*	.001335780	.000	-.20178784	-.18760549
			3c-2	-.277157667*	.001335780	.000	-.28424884	-.27006649
			3d-1	-.002248667	.001335780	.886	-.00933984	.00484251
			3d-2	-.002017667	.001335780	.931	-.00910884	.00507351
			DOX	-.007162000*	.001335780	.009	-.01425317	-.00007083
		3c-1	3a	.193740667*	.001335780	.000	.18664949	.20083184
			3b-1	.193083667*	.001335780	.000	.18599249	.20017484
			3b-2	.194696667*	.001335780	.000	.18760549	.20178784
			3c-2	-.082461000*	.001335780	.000	-.08955217	-.07536983
			3d-1	.192448000*	.001335780	.000	.18535683	.19953917
			3d-2	.192679000*	.001335780	.000	.18558783	.19977017
			DOX	.187534667*	.001335780	.000	.18044349	.19462584
		3c-2	3a	.276201667*	.001335780	.000	.26911049	.28329284
			3b-1	.275544667*	.001335780	.000	.26845349	.28263584
			3b-2	.277157667*	.001335780	.000	.27006649	.28424884
			3c-1	.082461000*	.001335780	.000	.07536983	.08955217
			3d-1	.274909000*	.001335780	.000	.26781783	.28200017
			3d-2	.275140000*	.001335780	.000	.26804883	.28223117
			DOX	.269995667*	.001335780	.000	.26290449	.27708684
		3d-1	3a	.001292667	.001335780	.994	-.00579851	.00838384
			3b-1	.000635667	.001335780	1.000	-.00645551	.00772684

				Mean Difference	Std. Error	Sig.	Lower Bound	Upper Bound
			3b-2	.002248667	.001335780	.886	-.00484251	.00933984
			3c-1	-.192448000*	.001335780	.000	-.19953917	-.18535683
			3c-2	-.274909000*	.001335780	.000	-.28200017	-.26781783
			3d-2	.000231000	.001335780	1.000	-.00686017	.00732217
			DOX	-.004913333	.001335780	.130	-.01200451	.00217784
		3d-2	3a	.001061667	.001335780	.998	-.00602951	.00815284
			3b-1	.000404667	.001335780	1.000	-.00668651	.00749584
			3b-2	.002017667	.001335780	.931	-.00507351	.00910884
			3c-1	-.192679000*	.001335780	.000	-.19977017	-.18558783
			3c-2	-.275140000*	.001335780	.000	-.28223117	-.26804883
			3d-1	-.000231000	.001335780	1.000	-.00732217	.00686017
			DOX	-.005144333	.001335780	.101	-.01223551	.00194684
		DOX	3a	.006206000	.001335780	.029	-.00088517	.01329717
			3b-1	.005549000	.001335780	.064	-.00154217	.01264017
			3b-2	.007162000*	.001335780	.009	.00007083	.01425317
			3c-1	-.187534667*	.001335780	.000	-.19462584	-.18044349
			3c-2	-.269995667*	.001335780	.000	-.27708684	-.26290449
			3d-1	.004913333	.001335780	.130	-.00217784	.01200451
			3d-2	.005144333	.001335780	.101	-.00194684	.01223551

*. The mean difference is significant at the 0.01 level.

จุฬาลงกรณ์มหาวิทยาลัย

CHULALONGKORN UNIVERSITY

1.3. The Kinetic stability at pH 7.4 (significant level = 0.01)

One-Way ANOVA

		Sum of Squares	df	Mean Square	F	Sig.
$t_{1/2}$	Between Groups	2056.667	7	293.810	27217.822	.000
	Within Groups	.173	16	.011		
	Total	2056.840	23			
k_{obs}	Between Groups	.186	7	.027	20674.162	.000
	Within Groups	.000	16	.000		
	Total	.186	23			

Multiple Comparisons (Post Hoc Test: Scheffe)

Dependent Variable		(I) Compound	(J) Compound	Mean Difference (I-J)	Std. Error	Sig.	99% Confidence Interval Lower Bound	Upper Bound
$t_{1/2}$	Scheffe	3a	3b-1	3.888667*	.084832	.000	3.43832	4.33901
			3b-2	-8.941000*	.084832	.000	-9.39134	-8.49066
			3c-1	19.541667*	.084832	.000	19.09132	19.99201
			3c-2	19.756333*	.084832	.000	19.30599	20.20668
			3d-1	4.465000*	.084832	.000	4.01466	4.91534
			3d-2	1.230000*	.084832	.000	.77966	1.68034
			DOX	11.024000*	.084832	.000	10.57366	11.47434
		3b-1	3a	-3.888667*	.084832	.000	-4.33901	-3.43832
			3b-2	-12.829667*	.084832	.000	-13.28001	-12.37932
			3c-1	15.653000*	.084832	.000	15.20266	16.10334
			3c-2	15.867667*	.084832	.000	15.41732	16.31801
			3d-1	.576333*	.084832	.001	.12599	1.02668
			3d-2	-2.658667*	.084832	.000	-3.10901	-2.20832
			DOX	7.135333*	.084832	.000	6.68499	7.58568
		3b-2	3a	8.941000*	.084832	.000	8.49066	9.39134
			3b-1	12.829667*	.084832	.000	12.37932	13.28001
			3c-1	28.482667*	.084832	.000	28.03232	28.93301
			3c-2	28.697333*	.084832	.000	28.24699	29.14768
			3d-1	13.406000*	.084832	.000	12.95566	13.85634
			3d-2	10.171000*	.084832	.000	9.72066	10.62134
			DOX	19.965000*	.084832	.000	19.51466	20.41534

		3c-1	3a	-19.541667*	.084832	.000	-19.99201	-19.09132
			3b-1	-15.653000*	.084832	.000	-16.10334	-15.20266
			3b-2	-28.482667*	.084832	.000	-28.93301	-28.03232
			3c-2	.214667	.084832	.520	-.23568	.66501
			3d-1	-15.076667*	.084832	.000	-15.52701	-14.62632
			3d-2	-18.311667*	.084832	.000	-18.76201	-17.86132
			DOX	-8.517667*	.084832	.000	-8.96801	-8.06732
		3c-2	3a	-19.756333*	.084832	.000	-20.20668	-19.30599
			3b-1	-15.867667*	.084832	.000	-16.31801	-15.41732
			3b-2	-28.697333*	.084832	.000	-29.14768	-28.24699
			3c-1	-.214667	.084832	.520	-.66501	.23568
			3d-1	-15.291333*	.084832	.000	-15.74168	-14.84099
			3d-2	-18.526333*	.084832	.000	-18.97668	-18.07599
			DOX	-8.732333*	.084832	.000	-9.18268	-8.28199
		3d-1	3a	-4.465000*	.084832	.000	-4.91534	-4.01466
			3b-1	-.576333*	.084832	.001	-1.02668	-.12599
			3b-2	-13.406000*	.084832	.000	-13.85634	-12.95566
			3c-1	15.076667*	.084832	.000	14.62632	15.52701
			3c-2	15.291333*	.084832	.000	14.84099	15.74168
			3d-2	-3.235000*	.084832	.000	-3.68534	-2.78466
			DOX	6.559000*	.084832	.000	6.10866	7.00934
		3d-2	3a	-1.230000*	.084832	.000	-1.68034	-.77966
			3b-1	2.658667*	.084832	.000	2.20832	3.10901
			3b-2	-10.171000*	.084832	.000	-10.62134	-9.72066
			3c-1	18.311667*	.084832	.000	17.86132	18.76201
			3c-2	18.526333*	.084832	.000	18.07599	18.97668
			3d-1	3.235000*	.084832	.000	2.78466	3.68534
			DOX	9.794000*	.084832	.000	9.34366	10.24434
		DOX	3a	-11.024000*	.084832	.000	-11.47434	-10.57366
			3b-1	-7.135333*	.084832	.000	-7.58568	-6.68499
			3b-2	-19.965000*	.084832	.000	-20.41534	-19.51466
			3c-1	8.517667*	.084832	.000	8.06732	8.96801
			3c-2	8.732333*	.084832	.000	8.28199	9.18268
			3d-1	-6.559000*	.084832	.000	-7.00934	-6.10866
			3d-2	-9.794000*	.084832	.000	-10.24434	-9.34366
k_{obs}	Scheffe	3a	3b-1	-.006397667*	.000925080	.001	-.01130858	-.00148675

		3b-2	.008721667*	.000925080	.000	.00381075	.01363258
		3c-1	-.198887333*	.000925080	.000	-.20379825	-.19397642
		3c-2	-.216398333*	.000925080	.000	-.22130925	-.21148742
		3d-1	-.007579333*	.000925080	.000	-.01249025	-.00266842
		3d-2	-.001770000	.000925080	.805	-.00668092	.00314092
		DOX	-.029355667*	.000925080	.000	-.03426658	-.02444475
	3b-1	3a	.006397667*	.000925080	.001	.00148675	.01130858
		3b-2	.015119333*	.000925080	.000	.01020842	.02003025
		3c-1	-.192489667*	.000925080	.000	-.19740058	-.18757875
		3c-2	-.210000667*	.000925080	.000	-.21491158	-.20508975
		3d-1	-.001181667	.000925080	.971	-.00609258	.00372925
		3d-2	.004627667	.000925080	.017	-.00028325	.00953858
		DOX	-.022958000*	.000925080	.000	-.02786892	-.01804708
	3b-2	3a	-.008721667*	.000925080	.000	-.01363258	-.00381075
		3b-1	-.015119333*	.000925080	.000	-.02003025	-.01020842
		3c-1	-.207609000*	.000925080	.000	-.21251992	-.20269808
		3c-2	-.225120000*	.000925080	.000	-.23003092	-.22020908
		3d-1	-.016301000*	.000925080	.000	-.02121192	-.01139008
		3d-2	-.010491667*	.000925080	.000	-.01540258	-.00558075
		DOX	-.038077333*	.000925080	.000	-.04298825	-.03316642
	3c-1	3a	.198887333*	.000925080	.000	.19397642	.20379825
		3b-1	.192489667*	.000925080	.000	.18757875	.19740058
		3b-2	.207609000*	.000925080	.000	.20269808	.21251992
		3c-2	-.017511000*	.000925080	.000	-.02242192	-.01260008
		3d-1	.191308000*	.000925080	.000	.18639708	.19621892
		3d-2	.197117333*	.000925080	.000	.19220642	.20202825
		DOX	.169531667*	.000925080	.000	.16462075	.17444258
	3c-2	3a	.216398333*	.000925080	.000	.21148742	.22130925
		3b-1	.210000667*	.000925080	.000	.20508975	.21491158
		3b-2	.225120000*	.000925080	.000	.22020908	.23003092
		3c-1	.017511000*	.000925080	.000	.01260008	.02242192
		3d-1	.208819000*	.000925080	.000	.20390808	.21372992
		3d-2	.214628333*	.000925080	.000	.20971742	.21953925
		DOX	.187042667*	.000925080	.000	.18213175	.19195358
	3d-1	3a	.007579333*	.000925080	.000	.00266842	.01249025
		3b-1	.001181667	.000925080	.971	-.00372925	.00609258

			3b-2	.016301000*	.000925080	.000	.01139008	.02121192
			3c-1	-.191308000*	.000925080	.000	-.19621892	-.18639708
			3c-2	-.208819000*	.000925080	.000	-.21372992	-.20390808
			3d-2	.005809333*	.000925080	.002	.00089842	.01072025
			DOX	-.021776333*	.000925080	.000	-.02668725	-.01686542
		3d-2	3a	.001770000	.000925080	.805	-.00314092	.00668092
			3b-1	-.004627667	.000925080	.017	-.00953858	.00028325
			3b-2	.010491667*	.000925080	.000	.00558075	.01540258
			3c-1	-.197117333*	.000925080	.000	-.20202825	-.19220642
			3c-2	-.214628333*	.000925080	.000	-.21953925	-.20971742
			3d-1	-.005809333*	.000925080	.002	-.01072025	-.00089842
			DOX	-.027585667*	.000925080	.000	-.03249658	-.02267475
		DOX	3a	.029355667*	.000925080	.000	.02444475	.03426658
			3b-1	.022958000*	.000925080	.000	.01804708	.02786892
			3b-2	.038077333*	.000925080	.000	.03316642	.04298825
			3c-1	-.169531667*	.000925080	.000	-.17444258	-.16462075
			3c-2	-.187042667*	.000925080	.000	-.19195358	-.18213175
			3d-1	.021776333*	.000925080	.000	.01686542	.02668725
			3d-2	.027585667*	.000925080	.000	.02267475	.03249658

*. The mean difference is significant at the 0.01 level.

จุฬาลงกรณ์มหาวิทยาลัย

CHULALONGKORN UNIVERSITY

2. Statistical analysis of *cytotoxicity results* of DOX and DOX analogues

2.1. MDA-MB-231 cell line (significant level = 0.01)

One-Way ANOVA

IC_{50}

	Sum of Squares	df	Mean Square	F	Sig.
Between Groups	225.148	6	37.525	182.356	.000
Within Groups	4.321	21	.206		
Total	229.470	27			

Multiple Comparisons (Post Hoc Test: Scheffe)

Dependent Variable: IC_{50}

	(I) Treatment	(J) Treatment	Mean Difference (I-J)	Std. Error	Sig.	99% Confidence Interval	
						Lower Bound	Upper Bound
Scheffe	3a	3b-2	-4.794313750*	.320762918	.000	-6.32829690	-3.26033060
		3c-1	-6.243643750*	.320762918	.000	-7.77762690	-4.70966060
		3c-2	-2.900196250*	.320762918	.000	-4.43417940	-1.36621310
		3d-1	-8.188264750*	.320762918	.000	-9.72224790	-6.65428160
		3d-2	-3.293912000*	.320762918	.000	-4.82789515	-1.75992885
		DOX	.044272750	.320762918	1.000	-1.48971040	1.57825590
	3b-2	3a	4.794313750*	.320762918	.000	3.26033060	6.32829690
		3c-1	-1.449330000	.320762918	.017	-2.98331315	.08465315
		3c-2	1.894117500*	.320762918	.001	.36013435	3.42810065
		3d-1	-3.393951000*	.320762918	.000	-4.92793415	-1.85996785
		3d-2	1.500401750	.320762918	.012	-.03358140	3.03438490
		DOX	4.838586500*	.320762918	.000	3.30460335	6.37256965
	3c-1	3a	6.243643750*	.320762918	.000	4.70966060	7.77762690
		3b-2	1.449330000	.320762918	.017	-.08465315	2.98331315
		3c-2	3.343447500*	.320762918	.000	1.80946435	4.87743065
		3d-1	-1.944621000*	.320762918	.001	-3.47860415	-.41063785
		3d-2	2.949731750*	.320762918	.000	1.41574860	4.48371490
		DOX	6.287916500*	.320762918	.000	4.75393335	7.82189965
	3c-2	3a	2.900196250*	.320762918	.000	1.36621310	4.43417940
		3b-2	-1.894117500*	.320762918	.001	-3.42810065	-.36013435
		3c-1	-3.343447500*	.320762918	.000	-4.87743065	-1.80946435
		3d-1	-5.288068500*	.320762918	.000	-6.82205165	-3.75408535

		3d-2	-.393715750	.320762918	.953	-1.92769890	1.14026740
		DOX	2.944469000*	.320762918	.000	1.41048585	4.47845215
	3d-1	3a	8.188264750*	.320762918	.000	6.65428160	9.72224790
		3b-2	3.393951000*	.320762918	.000	1.85996785	4.92793415
		3c-1	1.944621000*	.320762918	.001	.41063785	3.47860415
		3c-2	5.288068500*	.320762918	.000	3.75408535	6.82205165
		3d-2	4.894352750*	.320762918	.000	3.36036960	6.42833590
		DOX	8.232537500*	.320762918	.000	6.69855435	9.76652065
	3d-2	3a	3.293912000*	.320762918	.000	1.75992885	4.82789515
		3b-2	-1.500401750	.320762918	.012	-3.03438490	.03358140
		3c-1	-2.949731750*	.320762918	.000	-4.48371490	-1.41574860
		3c-2	.393715750	.320762918	.953	-1.14026740	1.92769890
		3d-1	-4.894352750*	.320762918	.000	-6.42833590	-3.36036960
		DOX	3.338184750*	.320762918	.000	1.80420160	4.87216790
	DOX	3a	-.044272750	.320762918	1.000	-1.57825590	1.48971040
		3b-2	-4.838586500*	.320762918	.000	-6.37256965	-3.30460335
		3c-1	-6.287916500*	.320762918	.000	-7.82189965	-4.75393335
		3c-2	-2.944469000*	.320762918	.000	-4.47845215	-1.41048585
		3d-1	-8.232537500*	.320762918	.000	-9.76652065	-6.69855435
		3d-2	-3.338184750*	.320762918	.000	-4.87216790	-1.80420160

*. The mean difference is significant at the 0.01 level.

จุฬาลงกรณ์มหาวิทยาลัย

CHULALONGKORN UNIVERSITY

2.2. MCF-7 cell line (significant level = 0.01)

One-Way ANOVA

IC_{50}

	Sum of Squares	df	Mean Square	F	Sig.
Between Groups	160.879	2	80.440	1607.473	.000
Within Groups	.450	9	.050		
Total	161.330	11			

Multiple Comparisons (Post Hoc Test: Scheffe)

Dependent Variable: IC_{50}

	(I) Treatment	(J) Treatment	Mean Difference (I-J)	Std. Error	Sig.	99% Confidence Interval	
						Lower Bound	Upper Bound
Scheffe	3a	3c-2	-7.747101843[*]	.158178747	.000	-8.38066715	-7.11353653
		DOX	.040078907	.158178747	.969	-.59348640	.67364422
	3c-2	3a	7.747101843[*]	.158178747	.000	7.11353653	8.38066715
		DOX	7.787180750[*]	.158178747	.000	7.15361544	8.42074606
	DOX	3a	-.040078907	.158178747	.969	-.67364422	.59348640
		3c-2	-7.787180750[*]	.158178747	.000	-8.42074606	-7.15361544

[*]. The mean difference is significant at the 0.01 level.

จุฬาลงกรณ์มหาวิทยาลัย

CHULALONGKORN UNIVERSITY

2.3. MCF-10A cell line (significant level = 0.01)

One-Way ANOVA

IC_{50}

	Sum of Squares	df	Mean Square	F	Sig.
Between Groups	174.529	2	87.265	672.717	.000
Within Groups	1.167	9	.130		
Total	175.697	11			

Multiple Comparisons (Post Hoc Test: Scheffe)

Dependent Variable: IC_{50}

	(I) Treatment	(J) Treatment	Mean Difference (I-J)	Std. Error	Sig.	99% Confidence Interval	
						Lower Bound	Upper Bound
Scheffe	3a	3d-1	-6.755710266[*]	.254675922	.000	-7.77578302	-5.73563751
		DOX	2.209514734[*]	.254675922	.000	1.18944198	3.22958749
	3d-1	3a	6.755710266[*]	.254675922	.000	5.73563751	7.77578302
		DOX	8.965225000[*]	.254675922	.000	7.94515225	9.98529775
	DOX	3a	-2.209514734[*]	.254675922	.000	-3.22958749	-1.18944198
		3d-1	-8.965225000[*]	.254675922	.000	-9.98529775	-7.94515225

*. The mean difference is significant at the 0.01 level.

จุฬาลงกรณ์มหาวิทยาลัย

CHULALONGKORN UNIVERSITY

3. Statistical analysis of *in vitro* drug release and stability of P-A-DOX conjugate, P-DOX conjugate and DOX

   3.1. The Kinetic stability at pH 4.0 (significant level = 0.01)

One-Way ANOVA

		Sum of Squares	df	Mean Square	F	Sig.
$t_{1/2}$	Between Groups	183881.818	2	91940.909	36.789	.000
	Within Groups	14995.044	6	2499.174		
	Total	198876.862	8			
k_{obs}	Between Groups	.000	2	.000	101.430	.000
	Within Groups	.000	6	.000		
	Total	.000	8			

Multiple Comparisons (Post Hoc Test: Scheffe)

Dependent Variable		(I) Compound	(J) Compound	Mean Difference (I-J)	Std. Error	Sig.	99% Confidence Interval Lower Bound	99% Confidence Interval Upper Bound
$t_{1/2}$	Scheffe	DOX	P-A-DOX	-341.905000*	40.818085	.000	-532.70295	-151.10705
			P-DOX	-236.272000*	40.818085	.004	-427.06995	-45.47405
		P-A-DOX	DOX	341.905000*	40.818085	.000	151.10705	532.70295
			P-DOX	105.633000	40.818085	.106	-85.16495	296.43095
		P-DOX	DOX	236.272000*	40.818085	.004	45.47405	427.06995
			P-A-DOX	-105.633000	40.818085	.106	-296.43095	85.16495
k_{obs}	Scheffe	DOX	P-A-DOX	.002367667*	.000178760	.000	.00153208	.00320325
			P-DOX	.001994667*	.000178760	.000	.00115908	.00283025
		P-A-DOX	DOX	-.002367667*	.000178760	.000	-.00320325	-.00153208
			P-DOX	-.000373000	.000178760	.195	-.00120859	.00046259
		P-DOX	DOX	-.001994667*	.000178760	.000	-.00283025	-.00115908
			P-A-DOX	.000373000	.000178760	.195	-.00046259	.00120859

*. The mean difference is significant at the 0.01 level.

3.2. The Kinetic stability at pH 7.4 (significant level = 0.01)

One-Way ANOVA

		Sum of Squares	df	Mean Square	F	Sig.
$t_{1/2}$	Between Groups	209859.920	2	104929.960	80.807	.000
	Within Groups	7791.138	6	1298.523		
	Total	217651.059	8			
k_{obs}	Between Groups	.007	2	.003	96862.887	.000
	Within Groups	.000	6	.000		
	Total	.007	8			

Multiple Comparisons (Post Hoc Test: Scheffe)

Dependent Variable		(I) Compound	(J) Compound	Mean Difference (I-J)	Std. Error	Sig.	99% Confidence Interval Lower Bound	99% Confidence Interval Upper Bound
$t_{1/2}$	Scheffe	DOX	P-A-DOX	-275.983695*	29.422475	.000	-413.51459	-138.45280
			P-DOX	-356.634730*	29.422475	.000	-494.16563	-219.10383
		P-A-DOX	DOX	275.983695*	29.422475	.000	138.45280	413.51459
			P-DOX	-80.651035	29.422475	.088	-218.18193	56.87986
		P-DOX	DOX	356.634730*	29.422475	.000	219.10383	494.16563
			P-A-DOX	80.651035	29.422475	.088	-56.87986	218.18193
k_{obs}	Scheffe	DOX	P-A-DOX	.057667524*	.000151946	.000	.05695727	.05837777
			P-DOX	.058165333*	.000151946	.000	.05745508	.05887558
		P-A-DOX	DOX	-.057667524*	.000151946	.000	-.05837777	-.05695727
			P-DOX	.000497810	.000151946	.046	-.00021244	.00120806
		P-DOX	DOX	-.058165333*	.000151946	.000	-.05887558	-.05745508
			P-A-DOX	-.000497810	.000151946	.046	-.00120806	.00021244

*. The mean difference is significant at the 0.01 level.

4. **Statistical analysis of *cytotoxicity results* of P-A-DOX conjugate, P-DOX conjugate and DOX**

   4.1. **MDA-MB-231 cell line (significant level = 0.01)**

One-Way ANOVA

IC_{50}

	Sum of Squares	df	Mean Square	F	Sig.
Between Groups	.015	2	.007	101.397	.000
Within Groups	.001	9	.000		
Total	.016	11			

Multiple Comparisons (Post Hoc Test: Scheffe)

Dependent Variable: IC_{50}

	(I) Treatment	(J) Treatment	Mean Difference (I-J)	Std. Error	Sig.	99% Confidence Interval	
						Lower Bound	Upper Bound
Scheffe	DOX	P-A-DOX	.083612000[*]	.006051242	.000	.05937450	.10784950
		P-DOX	.059865750[*]	.006051242	.000	.03562825	.08410325
	P-A-DOX	DOX	-.083612000[*]	.006051242	.000	-.10784950	-.05937450
		P-DOX	-.023746250	.006051242	.011	-.04798375	.00049125
	P-DOX	DOX	-.059865750[*]	.006051242	.000	-.08410325	-.03562825
		P-A-DOX	.023746250	.006051242	.011	-.00049125	.04798375

*. The mean difference is significant at the 0.01 level.

4.2. MCF-7 cell line (significant level = 0.01)

One-Way ANOVA

IC_{50}

	Sum of Squares	df	Mean Square	F	Sig.
Between Groups	.003	2	.002	37.895	.000
Within Groups	.000	9	.000		
Total	.003	11			

Multiple Comparisons (Post Hoc Test: Scheffe)

Dependent Variable: IC_{50}

	(I) Treatment	(J) Treatment	Mean Difference (I-J)	Std. Error	Sig.	99% Confidence Interval	
						Lower Bound	Upper Bound
Scheffe	DOX	P-A-DOX	.038414750[*]	.004465073	.000	.02053045	.05629905
		P-DOX	.024355500[*]	.004465073	.001	.00647120	.04223980
	P-A-DOX	DOX	-.038414750[*]	.004465073	.000	-.05629905	-.02053045
		P-DOX	-.014059250	.004465073	.035	-.03194355	.00382505
	P-DOX	DOX	-.024355500[*]	.004465073	.001	-.04223980	-.00647120
		P-A-DOX	.014059250	.004465073	.035	-.00382505	.03194355

[*]. The mean difference is significant at the 0.01 level.

จุฬาลงกรณ์มหาวิทยาลัย

CHULALONGKORN UNIVERSITY

4.3. MCF-10A cell line (significant level = 0.01)

One-Way ANOVA

IC_{50}

	Sum of Squares	df	Mean Square	F	Sig.
Between Groups	.023	2	.011	81.245	.000
Within Groups	.001	9	.000		
Total	.024	11			

Multiple Comparisons (Post Hoc Test: Scheffe)

Dependent Variable: IC_{50}

						99% Confidence Interval	
	(I) Treatment	(J) Treatment	Mean Difference (I-J)	Std. Error	Sig.	Lower Bound	Upper Bound
Scheffe	DOX	P-A-DOX	-.106004250[*]	.008331630	.000	-.13937556	-.07263294
		P-DOX	-.047354000[*]	.008331630	.001	-.08072531	-.01398269
	P-A-DOX	DOX	.106004250[*]	.008331630	.000	.07263294	.13937556
		P-DOX	.058650250[*]	.008331630	.000	.02527894	.09202156
	P-DOX	DOX	.047354000[*]	.008331630	.001	.01398269	.08072531
		P-A-DOX	-.058650250[*]	.008331630	.000	-.09202156	-.02527894

*. The mean difference is significant at the 0.01 level.

จุฬาลงกรณ์มหาวิทยาลัย

CHULALONGKORN UNIVERSITY

APPENDIX E

Culture media

1. **Reagents**

    1.1. Dulbecco's modified Eagle's medium (DMEM) (Gibco 12800)

    1.2. Fetal bovine serum (FBS) (Gibco, 16000044)

    1.3. Ham's F-12 Nutrient Mixture (Gibco, 11765054)

    1.4. Horse serum (Lonza, 14-403E)

    1.5. L-Glutamine 200 mM (100x) (Gibco, 25030081)

    1.6. Nonessential amino acids (Gibco, 11140050)

    1.7. Penicilin-Streptomycin (Gibco, 15140122)

    1.8. Fungizone (Gibco, 15290081)

    1.9. Sodium bicarbonate ($NaHCO_3$) (MW 84.01) (Sigma Co. S5761)

2. **Heat-inactivated fetal bovine serum (ΔFBS)**

    FBS was thawed in water bath at 37°C and then FBS was incubated in water bath at 56.7°C for 30 minute and mix every 10 minutes.

3. **Basal Dulbecco's Modified Minimum Essential Medium (D7777) (1 L)** (Basal DMEM or serum free media)

    3.1. 850 mL deionized H_2O.

    3.2. Slowly add contents from 1 pack of powdered DMEM (12800, Gibco) into the beaker with stir bar at moderate speed.

    3.3. Stir at moderate rate to dissolve for 30 min at room temp.

    3.4. Add 3.7 g $NaHCO_3$/L (44 mM) and stir until solubilized.

    3.5. Adjust pH to 7.2-7.3 with 1M HCl or 1M NaOH.

    3.6. Transfer medium to volumetric flask and adjust volume to 1L. Filter sterilize, label indicating contents, your initials and date, and store at 4°C.

4. **Complete media (cDMEM + 15% of 100 mL-sterile** Δ**FBS) for MDA-MB-231 and MCF-7 cell lines**

   4.1. Pipette 15 mL of FBS heat inactivate.

   4.2. Pipette 1 mL of penicilin-streptomycin.

   4.3. Pipette 1 mL of L-glutamine 200 mM.

   4.4. Pipette 1 mL of nonessential amino acids.

   4.5. Pipette 0.2 mL of fungizone.

   4.6. Adjust total volume to 100 mL by basal DMEM.

5. **Complete media (cDMEM/Ham's F12 Medium + 15% of 100 mL-horse serum) for MCF-10A cell line**

   5.1. Pipette 15 mL of horse serum.

   5.2. Pipette 1 mL of penicilin-streptomycin.

   5.3. Pipette 1 mL of L-glutamine 200 mM

   5.4. Pipette 1 mL of nonessential amino acids.

   5.5. Pipette 0.2 mL of fungizone.

   5.6. Adjust total volume to 100 mL by basal DMEM.

APPENDIX F

Cell culture and cytotoxicity assay procedure

1. **Resuscitation of frozen cells**

   1.1. Warm complete media in a 37°C water bath for 30 min before removing cryogenic tube from liquid nitrogen.

   1.2. Add 12 mL of cDMEM in 75 cm^2 flask and incubated in incubator.

   1.3. Add 9 mL of cDMEM in 15 mL plastic tubes.

   1.4. Transfer cryogenic tube to a 37°C water bath for 1-2 min until fully thawed. Quickly thawing the cryogenic tube will minimise any damage to the cell membranes. Be careful not to totally immerse the cryogenic tube – this may increase contamination risk.

   1.5. Wipe cryogenic tube with a tissue soaked in 70% alcohol prior to opening.

   1.6. Transfer total cell stock solution from cryogenic tube (about 1 mL) into 15 mL plastic tubes containing 4 mL of cDMEM.

   1.7. Centrifuge at 800 rpm for 5 min.

   1.8. Discard supernate and resuspend with 1 mL of cDMEM.

   1.9. Transfer total cell solution into 75 cm^2 flask containing 12 mL of cDMEM and incubate in CO$_2$ incubator.

2. **Growth and maintenance of live cell cultures**

   2.1. Place media in water bath (37°C) for 15-20 min.

   2.2. Take dish of cells out of CO$_2$ incubator.

   2.3. Examine cells under microscope to determine health/condition.

   2.4. In hood, label the appropriate number of a new dish with the cell line name, the passage number, the date and initial name. Cells will be subculture or split when it showed 70-80% confluence (about 4-5 days after seeding the cells on the flask).

2.5.   Remove old media from flask by aspiration. Wash cell with 5 mL pre-warmed DMEM.

2.6.   Add 5 mL 1X trypsin-EDTA and then incubate 37°C for 5-10 min.

2.7.   Add 5 mL of cDMEM -.

2.8.   Transfer total solution to 15 mL tube.

2.9.   Centrifuge at 800 rpm for 5 min.

2.10.   Discard supernate and resuspend with 2-3 ml of cDMEM +15% FBS for count cell in hemacytometer.

2.11.   Seed cells on a new 75 cm^2 flask at 0.4 x 10^6/flask with 12 mL cDMEM +15% FBS/flask and return the plate to the CO_2 incubator.

3. **Cell Quantification**

3.1.   Clean the haemocytometer.

3.2.   Under sterile pipette remove 30 µL of cell suspension into 30 µL trypan blue (dilution factor =2) by gentle pipetting.

3.3.   Fill both sides of the chamber (approx. 10 µL) with cell suspension and view under a light microscope using x20 magnification.

3.4.   Count the number of viable (seen as bright cells) and non-viable cells (stained blue).

3.5.   Calculate the concentration of viable and non-viable cells and the percentage of viable cells.

Calculate total cell number as follows:

a.   Mean of 16 square x 2)dilution into trypan blue (x 10^4)volume of cell suspension per 16 squares is 0.1 µL = (number of cells per mL.

b.   For example, if 111 and 97 cells in two sets of 16 squares,

)   111+97/(2   = 104

            10^4 x 2)dilution factor (x 10^4 =   2.08 x 10^6 cells/mL

Also count cells that accumulate trypan blue)dead cells(.

in each set of 16 squares, viable cells) /viable cells +dead cells (x 100 = %viability)routinely > 95% viability.(

Calculate cell numbers needed for new T-75 flasks and new 6 or 12 well plates.

Seeding number at   3.0-4.0 x 10^5 cells per T75-flask)vol.12 mL/flask(.

2.5-3.5 x 10^5 cells per well of a 6 well-dish)vol. 2 mL/well(.

2.0-2.5 x 10^5 cells per well of insert)vol .1.5 mL/insert(.

c.   When preparing cells for seeding new dish or flasks, always make 1.2 flask or for an extra well to account for pipetting errors.

4. Cytotoxicity assay

4.1.   Cultured cells were transferred in 96-well plates at a density of 5,000 – 10,000 cells in 200 µL of complete medium per well and then incubated at 5% CO_2 in 37°C incubator for   24 h.

4.2.   The cultured cells were treated with medium containing varies concentration of compounds or DMSO (solvent for solubilized samples) and incubated at 5% CO_2 in 37°C incubator.

4.3.   After 24 and 72 h, they were added with 10 µL of 3-(4,5-dimethythiazol-2-yl)-2,5-diphenyl tetrazolium bromide (MTT) solution (concentration 5 mg/mL in PBS) into each well and incubated at 5% CO_2 in 37°C incubator for 4 h.

4.4.   Removed culture medium and added a mixture of DMSO (150 µL) and glycine (75 µL), mixed for cell lysis and dissolving of the formazan crystal. (some studies dissolved formazan crystal by acidic isopropanol).

4.5.   Measured the absorbance at 540 nm.

Calculation of %cell viability and IC$_{50}$

%Cell viability) = OD of sample group x /(100OD of control group)DMSO or solvent for solubilized samples(.

IC$_{50}$ derived from standard curve between varies concentration of compounds and % cell viability.

จุฬาลงกรณ์มหาวิทยาลัย
CHULALONGKORN UNIVERSITY

VITA

NAME   Wiwat Supasena

DATE OF BIRTH   5 Aug 1984

PLACE OF BIRTH   Bangkok, Thailand

INSTITUTIONS ATTENDED King Mongkut's Institute of Technology North Bangkok

HOME ADDRESS   133/328 Pruksaville 33, Atchariya pattana, Kanchanaphisek
                       road, Plai bang, Bang kruai, Nonthaburi, Thailand, 11130

PUBLICATION   1. Wiwat Supasena, Chawanphat Muangnoi, Wuttinont
                       Thaweesest, Chalermkiat Songkram, Keisuke Ueda,
                       Kenjirou Higashi, Kunikazu Moribe, Somboon Tanasupawat,
                       Pornchai Rojsitthisak, Enhanced Antipsoriatic Activity of
                       Mycophenolic Acid Against the TNF-α-Induced HaCaT Cell
                       Proliferation by Conjugated Poloxamer Micelles. Journal of
                       Pharmaseutical Sciences, (2020) 109(2), 1153-1160

                       2. Chawanphat Muangnoi, Ponsiree Jithavech, Pahweenvaj
                       Ratnatilaka Na Bhuket, Wiwat Supasena, Wisut
                       Wichitnithad, Pasarapa Towiwat, Nuansri Niwattisaiwong,
                       Ian S. Haworth & Pornchai Rojsitthisak, A Curcumin-
                       Diglutaric Acid Conjugated Prodrug With Improved Water
                       Solubility and Antinociceptive Properties Compared To
                       Curcumin. Bioscience, Biotechnology, and Biochemistry,
                       (2018) 1-8.

                       3. Pahweenvaj Ratnatilaka Na Bhuket, Polsak
                       Teerawonganan, Ekawan Yoosakul, Wiwat Supasena,
                       Chotika Watananikorn, Bancha Chuasuwan, Piengthong
                       Narakorn, Isariya Techatanawat, P. Pitisuttithum. Validation
                       of Liquid Chromatography–Tandem Mass Spectrometric
                       Method for Simultaneous Determination of Lopinavir and

Ritonavir in Human Plasma, and Its Application in a Bioequivalence Study in Thai Volunteers. Journal of Health Research, 29 (2015) 417-424.

4. Isariya Techatanawat, Chutima Manamuti, Jaturavit Vattanarongkup, Polsak Teerawonganan, Ekawan Yoosakul, Wiwat Supasena, Bancha Chuasuwan, Piengthong Narakorn, Porranee Puranaoti. Bioequivalence Study of Abacavir 300 mg Tablets in Healthy Thai Male Volunteers under Fasting Conditions, Thai Journal of Pharmaceutical Sciences, 38 (2014) 164-167.

5. Bancha Chuasuwan, Pahweenvaj Ratnatilaka Na Bhuket, Wiwat Supasena, Chutima Manamuti, Isariya Techatanawat, Piengthong Narakorn, Archawin Rojanawiwat, A. Eksaengsri, Bioequivalence Study of Sildenafil 20 mg Tablets in Healthy Thai Male Volunteers, Mahidol University Journal of Pharmaceutical Sciences, 41 (2014) 1-6.